



*Nebraska Department of Transportation
Research Project Number: SPR FY21(004) SG-01*

APPROACH GUARDRAIL TRANSITION RETROFIT TO EXISTING BUTTRESSES & BRIDGE RAILS

Submitted by

Scott K. Rosenbaugh, M.S.C.E.
Research Engineer

Robert W. Bielenberg, M.S.M.E.
Research Engineer

Chen Fang, Ph.D.
Post-Doctoral Research Associate

Ronald K. Faller, Ph.D., P.E.
Research Professor & MwRSF Director

Cody S. Stolle, Ph.D.
Research Assistant Professor

MIDWEST ROADSIDE SAFETY FACILITY

Nebraska Transportation Center
University of Nebraska-Lincoln

Main Office

Prem S. Paul Research Center at Whittier School
Room 130, 2200 Vine Street
Lincoln, Nebraska 68583-0853
(402) 472-0965

Outdoor Test Site

4630 N.W. 36th Street
Lincoln, Nebraska 68524

Submitted to

NEBRASKA DEPARTMENT OF TRANSPORTATION

1500 Nebraska Parkway
Lincoln, Nebraska 68502

MwRSF Research Report No. TRP-03-480-24

May 15, 2024

TECHNICAL REPORT DOCUMENTATION PAGE

1. Report No. TRP-03-480-24	2. Government Accession No.	3. Recipient's Catalog No.	
4. Title and Subtitle Approach Guardrail Transition Retrofit to Existing Buttresses & Bridge Rails		5. Report Date May 15, 2024	
		6. Performing Organization Code	
7. Author(s) Rosenbaugh, S.K., Bielenberg, R.W., Fang, C., Faller, R.K., and Stolle, C.S.		8. Performing Organization Report No. TRP-03-480-24	
9. Performing Organization Name and Address Midwest Roadside Safety Facility (MwRSF) Nebraska Transportation Center University of Nebraska-Lincoln Main Office: Prem S. Paul Research Center at Whittier School Room 130, 2200 Vine Street Lincoln, Nebraska 68583-0853		10. Work Unit No.	
		11. Contract SPR FY21(004) SG-01	
12. Sponsoring Agency Name and Address Nebraska Department of Transportation 1500 Nebraska Highway 2 Lincoln, Nebraska 68502		13. Type of Report and Period Covered Draft Report: 2021 – 2024	
		14. Sponsoring Agency Code SPR FY21(004) SG-01	
15. Supplementary Notes Prepared in cooperation with U.S. Department of Transportation, Federal Highway Administration.			
16. Abstract <p>The Nebraska Department of Transportation (NDOT) frequently applies roadway overlays to the surface of bridges to extend the bridge's lifespan. To minimize repair costs, NDOT does not desire to replace or alter any bridge rails with adequate structural capacity and height. Bridge rails installed to NCHRP Report 350 or MASH standards are likely to remain in place, though their effective heights would be reduced by the overlay. This creates a problem of attaching new, 31-in. tall approach guardrail transitions (AGTs) to existing concrete bridge rails and buttresses (after an overlay) that were not designed for such connections and the resulting system may not be crashworthy to current safety standards.</p> <p>The objective of this project was to develop retrofit options for attachment of thrie-beam AGT systems to existing NDOT bridge railings and buttresses. The project began with a review of existing bridge railings and end buttresses used by NDOT to identify issues related to connection hardware alignment and crash safety performance. Retrofit options were then developed to address these issues while adhering to established design criteria. A new connector plate assembly was designed to facilitate the attachment of the thrie-beam terminal connector to these bridge railings and buttresses. Additionally, three retrofit concepts, including concrete fill, a steel assembly, and a curb, were considered to mitigate concerns related to vehicle snag below the thrie beam. These selected retrofit concepts were evaluated through a combination of structural analysis and computer simulated crash tests. All simulations of the AGT attached to these buttresses through these retrofit concepts met MASH TL-3 safety performance criteria.</p>			
17. Key Words Highway Safety, Crash Test, Roadside Appurtenances, MASH 2016, Test Level 3, Approach Guardrail Transition, Retrofit Design, Computer Simulation		18. Distribution Statement No restrictions. This document is available through the National Technical Information Service. 5285 Port Royal Road Springfield, VA 22161	
19. Security Classification (of this report) Unclassified	20. Security Classification (of this page) Unclassified	21. No. of Pages 124	22. Price

DISCLAIMER STATEMENT

This report was completed with funding from the Nebraska Department of Transportation. The contents of this report reflect the views and opinions of the authors who are responsible for the facts and the accuracy of the data presented herein. The contents do not necessarily reflect the official views or policies of the University of Nebraska-Lincoln, Nebraska Department of Transportation, the Federal Highway Administration, nor U.S. Department of Transportation. This report does not constitute a standard, specification, regulation, product endorsement, or an endorsement of manufacturers.

ACKNOWLEDGEMENTS

The authors wish to acknowledge several sources that made a contribution to this project: (1) the Nebraska Department of Transportation for sponsoring this project; and (2) the Holland Computing Center at the University of Nebraska, which receives support from the Nebraska Research Initiative, for providing computational resources. Acknowledgement is also given to the following individuals who contributed to the completion of this research project.

Midwest Roadside Safety Facility

K.A. Lechtenberg, M.S.M.E., Research Engineer
J.S. Steelman, Ph.D., P.E., Associate Professor
M. Asadollahi Pajouh, Ph.D., P.E., Research Assistant Professor
B.J. Perry, M.E.M.E., Research Engineer
E.L. Urbank, B.A., Research Communication Specialist
Z.Z. Jabr, Engineering Technician
Undergraduate and Graduate Research Assistants

Nebraska Department of Transportation

Phil TenHulzen, P.E., Design Standards Engineer
Jim Knott, P.E., Construction Engineer
Mick Syslo, P.E., State Roadway Design Engineer
Fouad Jaber, Assistant State Bridge Engineer
Brandon Varilek, P.E., Materials and Research Engineer & Division Head
Mark Fischer, P.E., PMP, Research Program Manager
Lieska Halsey, Former Research Project Manager
Angela Andersen, Research Coordinator
David T. Hansen, Internal Research Coordinator
Jodi Gibson, Former Research Coordinator

TABLE OF CONTENTS

TECHNICAL REPORT DOCUMENTATION PAGE i

DISCLAIMER STATEMENT ii

ACKNOWLEDGEMENTS ii

LIST OF FIGURES v

LIST OF TABLES viii

1 INTRODUCTION 1

 1.1 Introduction 1

 1.2 Objective 1

 1.3 Scope 2

2 REVIEW OF NDOT STANDARD PLANS 3

 2.1 NDOT Approach Guardrail Transition 3

 2.2 Review of NDOT Bridge Railings and End Buttresses 5

 2.2.1 Buttress 1 6

 2.2.2 Buttress 2 6

 2.2.3 Buttress 3 7

 2.2.4 Buttress 4 8

 2.2.5 Buttress 5 8

 2.2.6 Buttress 6 9

 2.2.7 Buttress 7 9

 2.2.8 Buttress 8 10

 2.2.9 Buttress 9 10

 2.2.10 Buttress 10 11

3 IDENTIFICATION OF ATTACHMENT ISSUES AND CONCERNS 12

 3.1 Vertical Bolt Hole Positions 12

 3.2 Increased Unsupported Span Length in Thrie Beam Guardrail 13

 3.3 Wheel Snag below the Thrie Beam 14

 3.4 Vehicle Snag on Buttresses 16

 3.5 Reverse Direction Snag 17

 3.6 Buttress Priority and Selection Methodology 17

4 DESIGN CONCEPTS 19

 4.1 Connector Plate Assembly for Rail Attachment 19

 4.2 Design Concept for Wheel Snag Prevention 24

5 LS-DYNA MODEL DEVELOPMENT 27

 5.1 AGT Model 27

 5.1.1 Upstream Anchorage 27

 5.1.2 Steel Guardrail Posts and Timber Blockouts 28

 5.1.3 Soil Model 28

- 5.1.4 Guardrail 29
- 5.2 Concrete Buttress 30
- 5.3 Overlay..... 31
- 5.4 Options for Wheel Snag Prevention 32
- 5.5 Options for Reverse Direction Snag – Buttress 2 33
- 5.6 Vehicle Models 34
- 5.7 Model Validation 35

- 6 LS-DYNA SIMULATION RESULTS..... 38
 - 6.1 AGT Model Variations and Evaluation Metrics 38
 - 6.2 Buttress 5 Simulation Results 42
 - 6.2.1 Vehicle Behavior 42
 - 6.2.2 Barrier Damage 49
 - 6.2.3 Occupant Risk 50
 - 6.2.4 Damage to Connector Plate 50
 - 6.3 Buttress 6 Simulation Results 52
 - 6.3.1 Vehicle Behavior 52
 - 6.3.2 Barrier Damage 59
 - 6.3.3 Occupant Risk 60
 - 6.4 Buttress 8 Simulation Results 61
 - 6.4.1 Vehicle Behavior 61
 - 6.4.2 Barrier Damage 72
 - 6.4.3 Occupant Risk 74
 - 6.4.4 MASH Test Designation No. 3-20 Evaluation 75
 - 6.5 Buttress 10 Simulation Results 80
 - 6.5.1 Vehicle Behavior 80
 - 6.5.2 Barrier Damage 83
 - 6.5.3 Occupant Risk 83
 - 6.6 Buttress 2 Simulation Results 85
 - 6.6.1 Vehicle Behavior 86
 - 6.6.2 Barrier Damage 92
 - 6.6.3 Occupant Risk 93
 - 6.6.4 Reverse Impact Evaluation 93

- 7 SUMMARY, CONCLUSIONS, AND RECOMMENDATIONS 101
 - 7.1 Retrofit AGT Recommendations 107
 - 7.2 Future Research 109

- 8 REFERENCES 110

- 9 APPENDICES 112
 - Appendix A. NDOT Standard Drawings for Bridge Railings and Buttresses 113

LIST OF FIGURES

Figure 1. 34-in. Tall AGT Initial Installation, No Overlay.....	3
Figure 2. 34-in. Tall AGT After a 3-in. Roadway Overlay	3
Figure 3. System Cross-Sections both Before and After a 3-in. Roadway Overlay.....	4
Figure 4. Geometry of the Modified Standardized Transition Buttress [2].....	5
Figure 5. Isometric Picture of Buttress 1	6
Figure 6. Isometric Picture of Buttress 2	7
Figure 7. Isometric Picture of Buttress 3	7
Figure 8. Isometric Picture of Buttress 4	8
Figure 9. Isometric Picture of Buttress 5	8
Figure 10. Isometric Picture of Buttress 6	9
Figure 11. Isometric Picture of Buttress 7	9
Figure 12. Isometric Picture of Buttress 8	10
Figure 13. Isometric Picture of Buttress 9	10
Figure 14. Isometric Picture of Buttress 10	11
Figure 15. Top Bolt Position with a 32-in. Tall Buttress.....	12
Figure 16. Top Bolt Position with a 29-in. Tall Buttress.....	13
Figure 17. Unsupported Span Length from the As-Tested 34-in. Tall AGT	13
Figure 18. Location of Existing Bolt Holes on Buttress 6.....	14
Figure 19. Location of Potential Wheel Snag below Thrie Beam	15
Figure 20. Wheel Snag on 34-in. AGT during MASH Crash Testing [2].....	15
Figure 21. Wheel Snag Concern for Buttress 9	16
Figure 22. Typical Shape Transition to Mitigate Wheel Snag on New Jersey Shaped Buttresses	16
Figure 23. Vehicle Snag at Connection Blockout or Buttress Recess	17
Figure 24. Reverse Direction Snag Concerns	17
Figure 25. Rail Position on Buttress 5, Adjusted for Height and Unsupported Span Length	19
Figure 26. Connector Plate Assembly	20
Figure 27. AGT with Connector Plate Assembly with Buttress 5.....	20
Figure 28. Trimming of Original Assembly for Buttresses 8, 4, and 2	21
Figure 29. Connector Plate Assembly Corners Cut at 2:1 Slopes for Buttresses 2 and 4	22
Figure 30. Block Design for Recessed Buttress: Block (left) and AGT assembly (right).....	23
Figure 31. Risk of Vehicle Snag during Reverse-Direction Impact	23
Figure 32. Design Concepts for Reverse-Direction Snag: (a) Concrete Fill; (b) Modified Attachment Spacer	24
Figure 33. Retrofit Option 1, Concrete Fill.....	25
Figure 34. Option 2, Steel Assembly – Backside View.....	25
Figure 35. Option 2, Steel Assembly Placed on Buttress 8	26
Figure 36. Option 3, Addition of 6-in. Tall Curb.....	26
Figure 37. AGT Guardrail Installation.....	27
Figure 38. Upstream AGT Anchorage.....	27
Figure 39. AGT Post Spacing	28
Figure 40. Guardrail Post with Soil Tube and Soil Springs.....	29
Figure 41. Connector Plate Assembly Model	30
Figure 42. Attachment Spacer Model	30
Figure 43. End Terminal Bolted Connection: (a) Traffic-Side Face; (b) Back Face.....	31

Figure 44. 3-in. Tall Overlay Model.....32

Figure 45. Options for Wheel Snag: (a) Concrete Fill; (b) Steel Assembly; (c) Curb33

Figure 46. Options for Reverse Direction Snag on Buttress 2: (a) Concrete Fill; (b) Modified Attachment Spacer34

Figure 47. 2018 Dodge Ram Finite Element Model.....35

Figure 48. 2010 Toyota Yaris Finite Element Model35

Figure 49. Ram Pickup Truck Impact Point38

Figure 50. Ram Vehicle Model Right-Front Suspension Joints39

Figure 51. Design Options for Bolted Connection40

Figure 52. Tire-Buttress Overlap Measurement41

Figure 53. Sequential Images, Simulation No. B5-CP-5N-WA44

Figure 54. Sequential Images, Simulation No. B5-CP-5N-WD45

Figure 55. Sequential Images, Simulation No. B5-CP-3N-WA46

Figure 56. Sequential Images, Simulation No. B5-CP-3N-WD47

Figure 57. Tire-Buttress Overlap, Buttress 548

Figure 58. System Damage, Buttress 549

Figure 59. Effective Plastic Strain Distribution in Connector Plate, Buttress 551

Figure 60. Sequential Images, Simulation No. B6-CP-5N-WA54

Figure 61. Sequential Images, Simulation No. B6-CP-5N-WD55

Figure 62. Sequential Images, Simulation No. B6-CP-3N-WA56

Figure 63. Sequential Images, Simulation No. B6-CP-3N-WD57

Figure 64. Tire-Buttress Overlap, Buttress 658

Figure 65. System Damage, Buttress 659

Figure 66. Sequential Images, Simulation No. B8-CP-3N-WA63

Figure 67. Sequential Images, Simulation No. B8-CP-3N-WD64

Figure 68. Sequential Images, Simulation No. B8-CP+CF-3N-WA65

Figure 69. Sequential Images, Simulation No. B8-CP+CF-3N-WD66

Figure 70. Sequential Images, Simulation No. B8-CP+SA-3N-WA67

Figure 71. Sequential Images, Simulation No. B8-CP+SA-3N-WD68

Figure 72. Sequential Images, Simulation No. B8-CP+CB-3N-WA69

Figure 73. Sequential Images, Simulation No. B8-CP+CB-3N-WD70

Figure 74. Tire-Buttress Overlap, Buttress 8 without Wheel Snag Retrofits72

Figure 75. Tire-Buttress Overlap, Buttress 8 with Wheel Snag Retrofit Options72

Figure 76. System Damage, Buttress 873

Figure 77. 1100C Vehicle Impact Point75

Figure 78. Sequential Images, Simulation No. B8-CP-3N-3-2077

Figure 79. Sequential Images, Simulation No. B8-CP+CF-3N-3-2078

Figure 80. System Damage under MASH 3-20, Buttress 879

Figure 81. Sequential Images, Simulation No. B10-CP+CF-3N-WA81

Figure 82. Sequential Images, Simulation No. B10-CP+CF-3N-WD82

Figure 83. System Damage, Buttress 1083

Figure 84. Concrete Fill (red) Placed above Connection Blockout, Buttress 285

Figure 85. Redesigned Connection Spacer (teal), Buttress 2.....85

Figure 86. Sequential Images, Simulation No. B2-CP+CF-3N-WA-CFA88

Figure 87. Sequential Images, Simulation No. B2-CP+CF-3N-WD-CFA89

Figure 88. Sequential Images, Simulation No. B2-CP+CF-3N-WA-RBA90

Figure 89. Sequential Images, Simulation No. B2-CP+CF-3N-WD-RBA91

Figure 90. System Damage, Buttress 292
Figure 91. Sequential Images, Simulation No. B2-CP+CF-3N-WA-CFA-REV.....95
Figure 92. Sequential Images, Simulation No. B2-CP+CF-3N-WD-CFA-REV96
Figure 93. Sequential Images, Simulation No. B2-CP+CF-3N-WA- RBA-REV97
Figure 94. Sequential Images, Simulation No. B2-CP+CF-3N-WD- RBA-REV98
Figure 95. System Damage for Reverse-Direction Impacts, Buttress 2100
Figure 96. NDOT’s 34-in. Tall AGT Shown with 3-in. Overlay101
Figure 97. Connector Plate Assembly, Design Details.....103
Figure 98. Connector Plate Assembly, Back Plate Design Details.....104
Figure 99. Connector Plate Assembly, Trim Lines for Thrie Beam Terminal Connector.....105
Figure 100. Connector Plate Assembly, Bill of Materials106
Figure 101. Connection Spacer Dimensions.....107
Figure A-1. NDOT Design Details, Buttress 1114
Figure A-2. NDOT Design Details, Buttress 2115
Figure A-3. NDOT Design Details, Buttress 3116
Figure A-4. NDOT Design Details, Buttress 4117
Figure A-5. NDOT Design Details, Buttress 5118
Figure A-6. NDOT Design Details, Buttress 6119
Figure A-7. NDOT Design Details, Buttress 7120
Figure A-8. NDOT Design Details, Buttress 8121
Figure A-9. NDOT Design Details, Buttress 9122
Figure A-10. NDOT Design Details, Buttress 10123

LIST OF TABLES

Table 1. Characteristics of Existing NDOT Railings/Buttresses 5
Table 2. Issues and Concerns by Buttress..... 18
Table 3. Comparison of MASH Test Designation No. 3-21 Results..... 36
Table 4. Comparison of MASH Test Designation No. 3-20 Results..... 37
Table 5. Simulations on Retrofit AGT with Buttress 5 42
Table 6. Vehicle Angular Displacements Results, Buttress 5 43
Table 7. Tire-Buttress Overlap, Buttress 5 48
Table 8. Summary of OIV, ORA, and Lateral Deflection, Buttress No. 5 50
Table 9. Simulations on Retrofit AGT with Buttress 6 52
Table 10. Vehicle Angular Displacements Results, Buttress 6 53
Table 11. Tire-Buttress Overlap, Buttress 6 58
Table 12. Summary of OIV, ORA, and Lateral Deflection, Buttress 6..... 60
Table 13. Simulations on Retrofit AGT with Buttress 8 61
Table 14. Vehicle Angular Displacements Results, Buttress 8 62
Table 15. Tire-Buttress Overlap, Buttress 8 71
Table 16. Summary of OIV, ORA, and Lateral Deflection, Buttress 8..... 74
Table 17. MASH 3-20 Simulations on AGT with Buttress No. 8 75
Table 18. Vehicle Behavior Results under MASH Test Designation No. 3-60 Impacts, Buttress
No. 8..... 76
Table 19. Summary of OIV, ORA, and Lateral Deflection, Buttress No. 8 under MASH Test
Designation No. 3-20 79
Table 20. Simulations on AGT with Buttress No. 10..... 80
Table 21. Vehicle Behavior Results, Buttress 10 80
Table 22. Summary of OIV, ORA, and Lateral Deflection, Buttress 10 84
Table 23. Normal-Direction Simulations on Retrofit AGT with Buttress 2..... 86
Table 24. Vehicle Angular Displacements Results, Buttress 2 87
Table 25. Summary of OIV, ORA, and Lateral Deflection, Buttress 2 93
Table 26. Vehicle Angular Displacements for Reverse-Direction Impacts, Buttress 2..... 99
Table 27. Summary of OIV and ORA for Reverse-Direction Impacts, Buttress 2 99

1 INTRODUCTION

1.1 Introduction

Approach guardrail transitions (AGTs) are commonly used to shield the ends of bridge rails and concrete buttresses as well as provide a safe transition in lateral stiffness between semi-rigid approach guardrail and rigid bridge rail. However, AGTs are sensitive systems, meaning that small changes to an otherwise crashworthy AGT (e.g., shape of railing end buttress or rail height alterations) can, and have, led to an inadequate design and failed crash tests. Recently, there have been multiple advancements in the design of thrie beam AGTs, including the development of the standardized transition buttress [1] and the 34-in. tall thrie beam AGT designed to accommodate future overlays [2]. When used together, the effective height of the 34-in. tall AGT will be reduced to the nominal thrie beam AGT height of 31 in. after a 3-in. thick overlay is applied to the roadway.

Unfortunately, these new AGT systems can only be implemented in new construction applications where the concrete end buttress can be formed with the correct geometry (e.g., height, end tapers, attachment bolt locations, etc...). Nebraska Department of Transportation (NDOT) has many existing bridges that will be resurfaced with an overlay, and most of these existing structures will not have end buttress configurations compatible with crashworthy AGTs. Concrete barriers as low as 29 in. have been shown to adequately perform to Test Level 3 (TL-3) standards of the American Association of State Highway and Transportation Officials' (AASHTO's) *Manual for Assessing Safety Hardware (MASH)* [3], so bridge rails with an original height of 32 in. or greater will still satisfy current safety standards. However, AGTs with rail heights below 31 in. have resulted in vehicle rollovers and inadequate safety performance [4]. Additionally, many of these existing AGTs were designed to satisfy the safety standards of National Cooperative Highway Research Program (NCHRP) Report 350 [5] and may not satisfy MASH criteria, which incorporates heavier passenger vehicles, a taller pickup truck, and a higher impact angle for the small car test vehicle.

Accordingly, NDOT Roadway Design has a policy to update/replace existing AGTs adjacent to bridges receiving an overlay with a MASH TL-3 crashworthy design. To minimize repair costs, NDOT does not desire to replace or alter any bridge rails with adequate structural capacity and height. Bridge rails installed under NCHRP Report 230 [6] or earlier standards are likely too short for current standards and need to be replaced, but bridge rails installed to NCHRP Report 350 TL-4 standards should meet MASH TL-3 criteria and could remain in place. However, this creates a problem of attaching new, 31-in. tall AGTs to existing concrete bridge rails and buttresses (after an overlay) that were not designed for such connections and the resulting system may not be crashworthy to current safety standards. Therefore, the development of cost-effective retrofit options is desired for attaching 31-in. tall AGTs to existing NDOT bridge rail and buttress designs following a roadway overlay.

1.2 Objective

The objective of this project was to develop retrofit options for the attachment of 31-in. tall thrie beam AGT systems to existing NDOT concrete bridge rails and end buttresses following a bridge and roadway overlay up to 3 in. thick. The retrofits could involve the addition of connection plates to attach the 31-in. thrie beam to the end buttresses, the addition of deflector plates to prevent

vehicle snag, and overlapping the AGT onto the bridge railing to prevent contact with the end of the buttress. However, the existing concrete bridge railings and end buttresses were not to be modified except for the installation of anchorage hardware. The new retrofit designs will improve the overall safety of the barrier systems by creating systems that satisfy MASH TL-3 performance criteria while preventing costly replacements of concrete structures.

1.3 Scope

The project began with a review of existing bridge rails and end buttresses to identify issues related to connection hardware alignment and crash safety performance. Retrofit options were then developed to address these issues while adhering to established design criteria. The steel connector plate assembly was designed to facilitate the attachment of the three beam terminal connector to the bridge railings and buttresses. Additionally, three retrofit design concepts, including concrete fill, a steel assembly, and a curb, were evaluated to mitigate concerns related to vehicle snagging. The selected retrofit designs were evaluated through a combination of structural analysis and computer simulation, which conformed to MASH TL-3 criteria. Finally, the project concluded with the formulation and summarization of results and conclusions in a comprehensive summary report.

2 REVIEW OF NDOT STANDARD PLANS

2.1 NDOT Approach Guardrail Transition

NDOT currently utilizes an AGT system comprising of nested thrie beam, a W-to-thrie connection segment, W-beam guardrail, W6x15 posts spaced at 37.5 in. on-center, and W6x8.5 posts at various spacings. This AGT was designed with an original top rail height of 34 in. so that it would remain crashworthy after roadway overlays up to 3 in. thick. After an overlay, the symmetric W-to-thrie transition segment would be replaced with an asymmetric W-to-thrie segment and the W-beam would be raised 3 in. on the standard guardrail posts. These minor changes created an effective height of 31 in. for the entire AGT and upstream Midwest Guardrail System (MGS) without having to remove/reinstall the guardrail posts. Sketches of NDOT's 34-in. AGT both before and after an overlay are shown in Figures 1 through 3. Since this AGT was already designed for roadway overlays, it made sense to utilize this AGT configuration in the development of AGT retrofits to existing buttresses after bridge overlays.

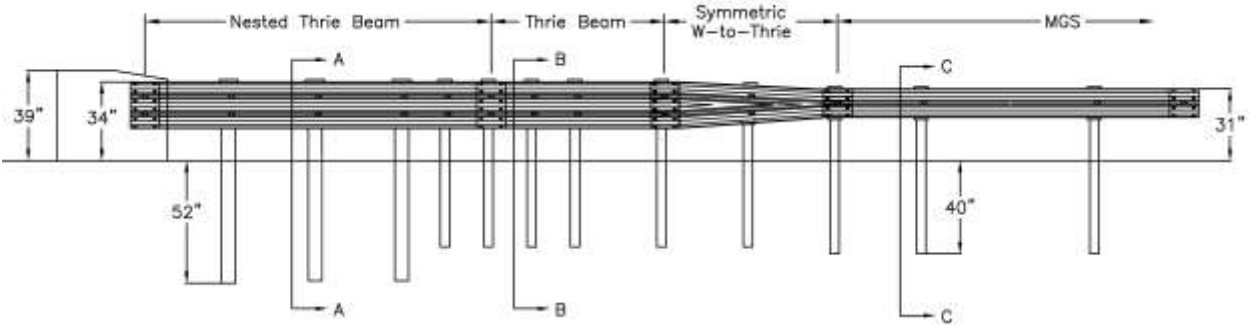


Figure 1. 34-in. Tall AGT Initial Installation, No Overlay

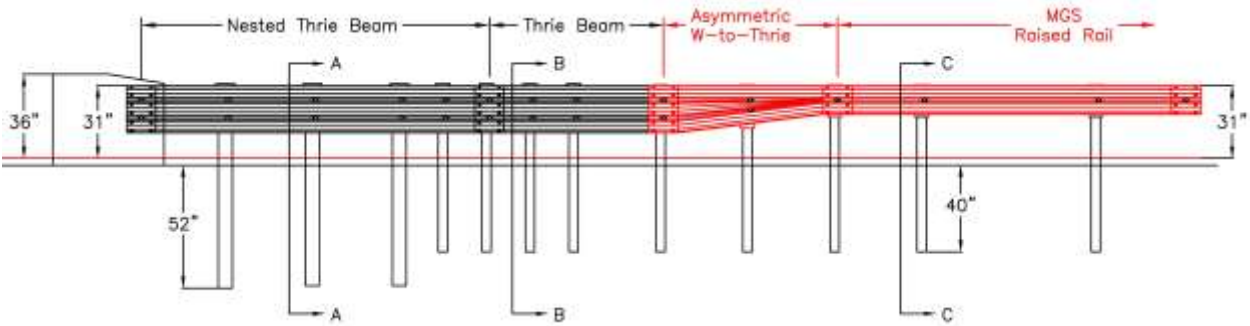


Figure 2. 34-in. Tall AGT After a 3-in. Roadway Overlay

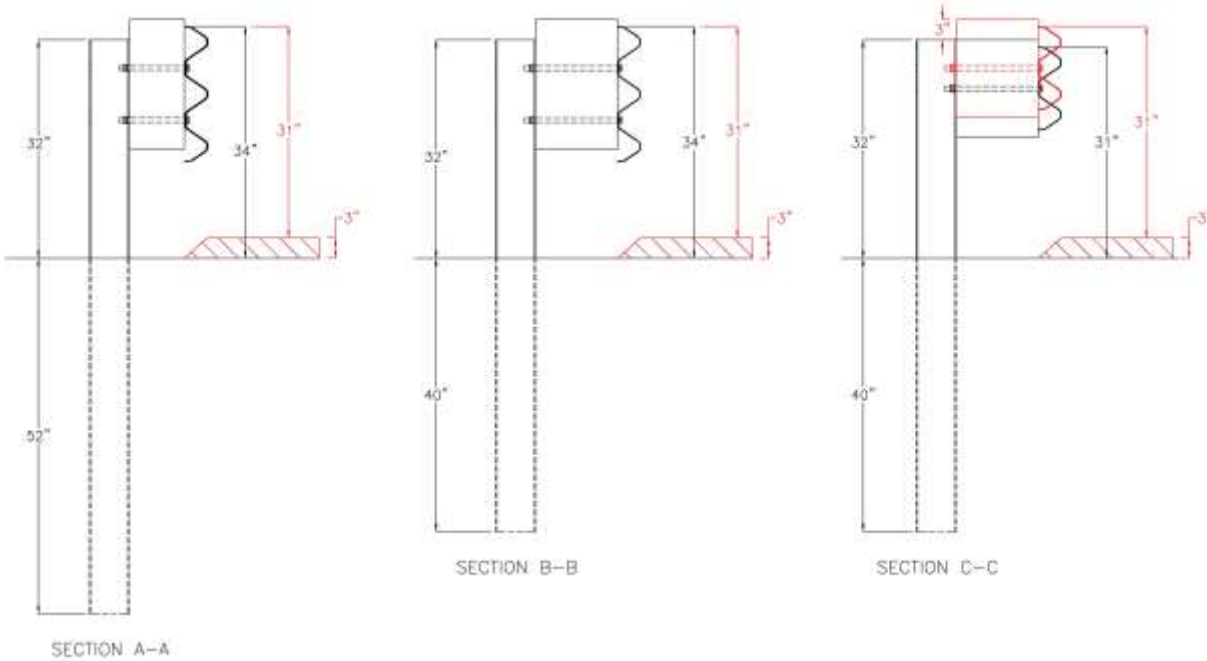


Figure 3. System Cross-Sections both Before and After a 3-in. Roadway Overlay

NDOT's 34-in. tall AGT was previously evaluated through crash testing, and the AGT satisfied all MASH TL-3 safety performance criteria [2]. The test article evaluated according to MASH was connected to a modified version of the standardized transition buttress (i.e., the height of the buttress was increased by 3 in. to match the rail height increase). This buttress utilized a dual taper design along its upstream edge to mitigate vehicle snag [1]. The lower chamfer measured 4.5 in. laterally by 18 in. longitudinally and was designed to limit wheel snag. The upper chamfer measured 3 in. laterally by 4 in. longitudinally and was designed to mitigate vehicle bumper and frame snag on the buttress while limiting the unsupported span length of the rail between the buttress and adjacent guardrail post to 30¹/₄-in. The transition point between the two chamfers was located 17 in. above the roadway surface. A sketch of the modified standardized transition buttress is shown in Figure 4.

The shape of the standardized concrete buttress was thought to be critical to the performance of the AGT during crash testing. Thus, the retrofits developed herein needed to consider details like the taper of the buttress below the thrie beam and the unsupported span length between the concrete buttress and the adjacent guardrail post.

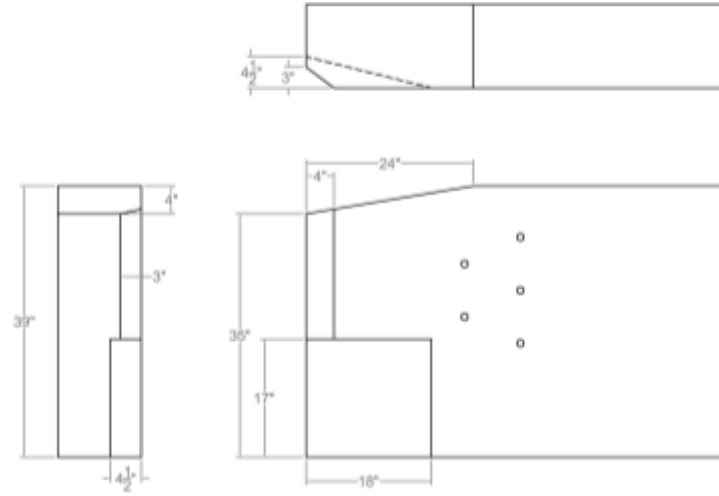


Figure 4. Geometry of the Modified Standardized Transition Buttruss [2]

2.2 Review of NDOT Bridge Railings and End Buttrusses

At the beginning of this study, researchers requested the standard plans for the existing bridge railings and end buttrusses that were to be considered as part of the AGT retrofit attachment design. NDOT submitted ten different bridge railing/buttruss configurations. These structures differed in cross section shape, height, adjacent bridge rail, and adjacent guardrail. Table 1 provides a summary of these existing railings/buttrusses and allows for easier comparison between buttrusses. Note, the assigned buttruss numbers were based on the order they were submitted for review. Thus, the buttruss numbers do not represent a priority or level of importance.

Table 1. Characteristics of Existing NDOT Railings/Buttrusses

Buttruss No.	Buttruss Shape	Buttruss Height	Adjacent Guardrail	Guardrail Height	Bridge Rail Description	Plan Date
1	Vertical	29"	W-beam	27"	29" Open Concrete Rail 11" × 11" Post, 12" × 14" Rail	1985
2	Vertical	32.5"	Thrie Beam	32"	29" Open Concrete Rail 11" × 11" Post, 16" × 14" Rail	1986
3	Vertical	29"	W-beam	27"	29" Open Concrete Rail 11" × 11" Post, 16" × 14" Rail	1987
4	Vertical	32"	Thrie Beam	31"	29" Open Concrete Rail 24" × 11" Post, 16" × 14" Rail	1991
5	Vertical	32"	Thrie Beam	31"	29" Open Concrete Rail 24" × 11" Post, 16" × 14" Rail	2019
6	Vertical	34"	Thrie Beam	31"	34" Open Concrete Rail 30" × 10.5" Post, 23" × 14" Rail	2019
7	Vertical	36"	Thrie Beam	34"	36" Open Concrete Rail 30" × 10.5" Post, 24" × 14" Rail	2019
8	Vertical – New Jersey	32" - 42"	Thrie Beam	31"	42" New Jersey	1990
9	New Jersey	32"	Thrie Beam	32"	32" New Jersey	N/A
10	Vertical	32"	Thrie Beam	31"	42" New Jersey	1997

The following sections provide a brief description of each railing/buttruss and an isometric picture of models created for each buttruss. The models were originally created for use in the computer simulation tasks of this project, but are used here as a 3D representation of the buttrusses. The original NDOT standard plans for each buttruss are contained in Appendix A.

2.2.1 Buttruss 1

Buttruss 1 was an end post for an open concrete bridge rail. The end post had a vertical front face and measured 3 ft long, 29 in. tall, and 14 in. wide. The adjacent guardrail was originally W-beam, and a 3½-in. deep recess was placed in the upper corner of the end post where the W-beam terminal connector attached to the end post. The recess measured 16 in. long by 14½ in. tall. The W-beam was mounted at a height of 27 in., and the front of the guardrail would be on the same vertical plane as the face of the railing. A 3D model of Buttruss 1 is shown in Figure 5.

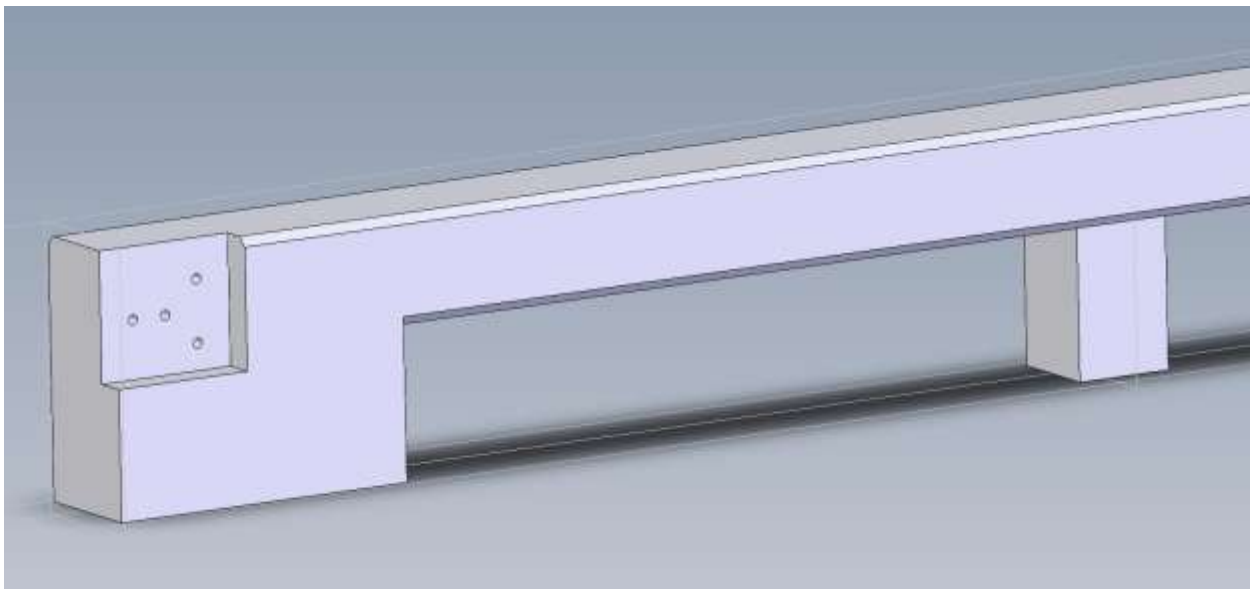


Figure 5. Isometric Picture of Buttruss 1

2.2.2 Buttruss 2

Buttruss 2 was a standalone buttruss placed adjacent to an open concrete bridge railing. The buttruss had a height of 32½ in. and tapered down to match the bridge railing's height of 29 in. over a distance of 40 in. The total length of the buttruss was 7 ft – 1 in. An 18-in. long cantilevered segment extended from the upstream end of the buttruss. The cantilevered segment was tapered back from the face of the buttruss 4½ in. over its length. The width of the buttruss was 12 in. at the base and 10½ in. where the thrie beam terminal connector attached to the buttruss. The downstream end of the buttruss contained a 3½-in. thick by 16 in. tall guardrail connection blockout, which brought the width of the buttruss at its downstream end to 14 in. to match the width of the adjacent bridge railing. When assembled, the front of the 32-in. tall thrie beam would be on the same vertical plane as the connection blockout and the face of the railing. A 3D model of Buttruss 2 is shown in Figure 6.

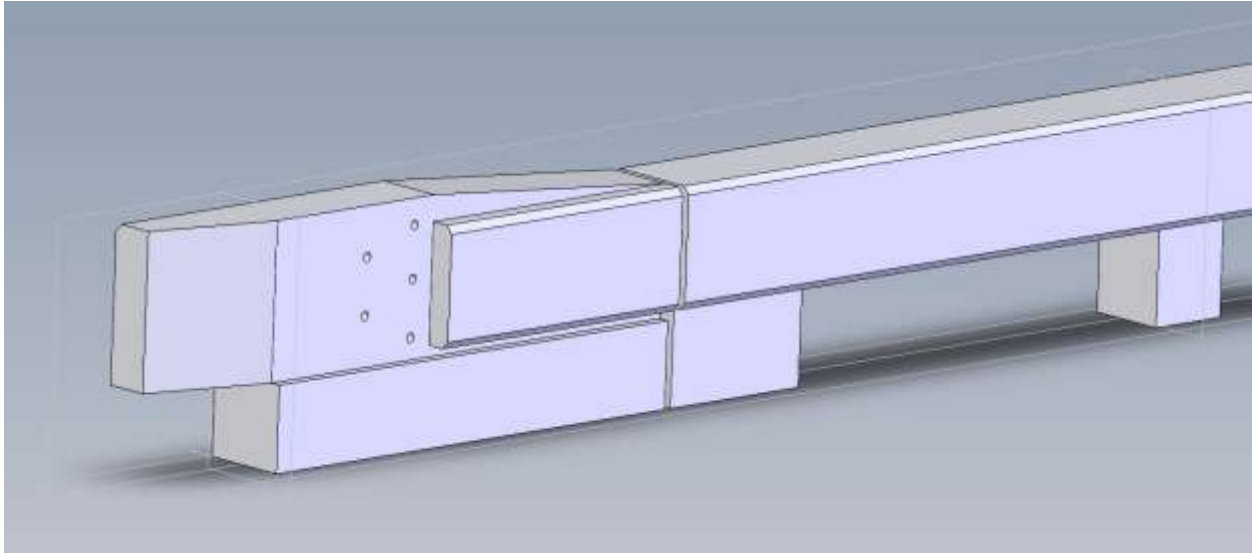


Figure 6. Isometric Picture of Buttriss 2

2.2.3 Buttriss 3

Buttriss 3 was similar to Buttriss 2, but stood only 29 in. tall and had a total length of 6 ft. Additionally, Buttriss 3 was an end post of the bridge railing, not a stand-alone buttress. The upstream end of the buttress contained an 18-in. long cantilevered segment that tapered back 4½ in. Buttriss 3 also had the same base width, top width, and connection blockout width as Buttriss 2. However, Buttriss 3 was originally connected to W-beam guardrail with a mounting height of 27 in. A 3D model of Buttriss 3 is shown in Figure 7.

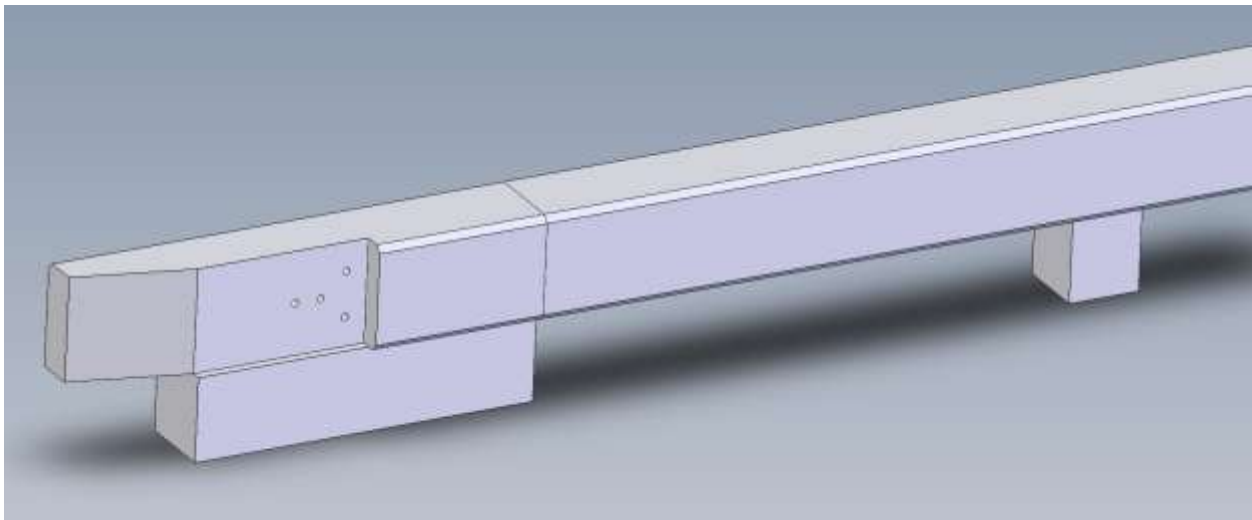


Figure 7. Isometric Picture of Buttriss 3

2.2.4 Buttress 4

Buttress 4 was unique as it was a standalone buttress consisting of two “support posts” instead of a continual base. Buttress 4 had a height of 32 in. and tapered down to 29 in. prior to the second support post. The upstream end of the buttress contained an 18-in. long cantilevered segment that tapered back 4½ in. The upstream portion of the buttress had a width of 12 in. However, starting at the height transition, the buttress width increased to 14 in. to match the width of the bridge rail. A 3D model of Buttress 4 is shown in Figure 8.

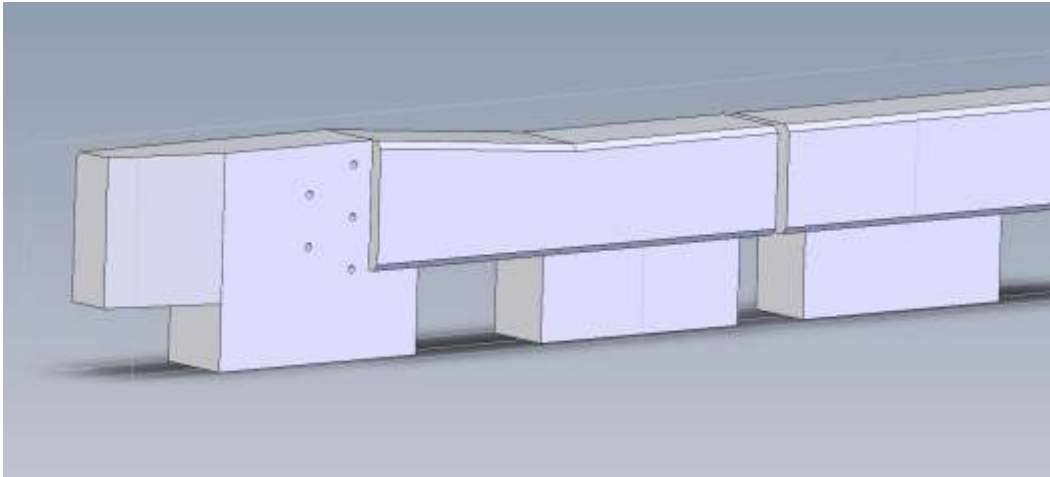


Figure 8. Isometric Picture of Buttress 4

2.2.5 Buttress 5

Buttress 5 was a stand-alone buttress with a vertical face. The buttress was 32 in. tall and 14 in. wide. The upstream end of Buttress 5 was tapered back 4½ in. over a distance of 18 in. The buttress was originally designed to be connected to 31-in. tall thrie beam guardrail. The end post of the bridge rail was designed with the same cross section as Buttress 5, but transitioned to a 29-in. tall open concrete bridge railing prior to the second post. A 3D model of Buttress 5 is shown in Figure 9.

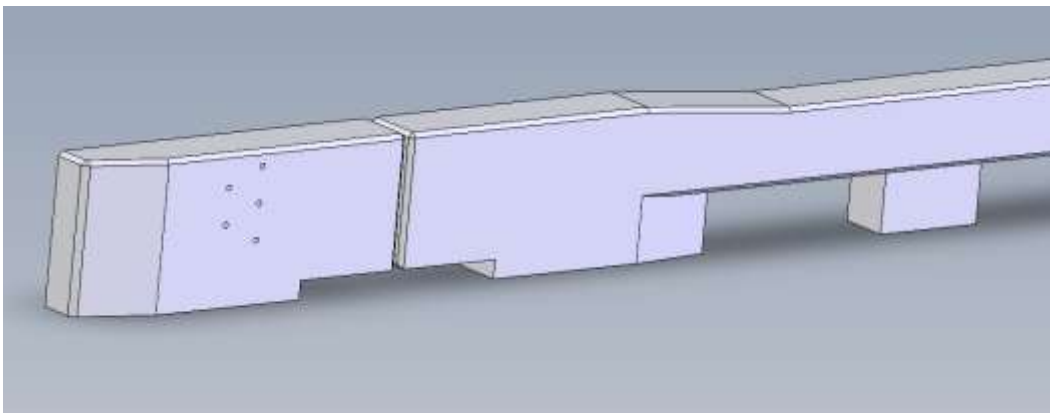


Figure 9. Isometric Picture of Buttress 5

2.2.6 Buttress 6

Buttress 6 was a 14-in. wide stand-alone buttress with a vertical face. The upstream end of Buttress 6 was 32 in. tall but the height was increased to 34 in. over the first 18 in. of length. Additionally, the upstream end of the buttress was tapered back 4½ in. over a distance of 18 in. The top edge of Buttress 6 had a 2-in. tall by 4½-in. lateral chamfer. The buttress was originally designed to be connected to 31-in. tall thrie beam guardrail. A 3D model of Buttress 6 is shown in Figure 10.

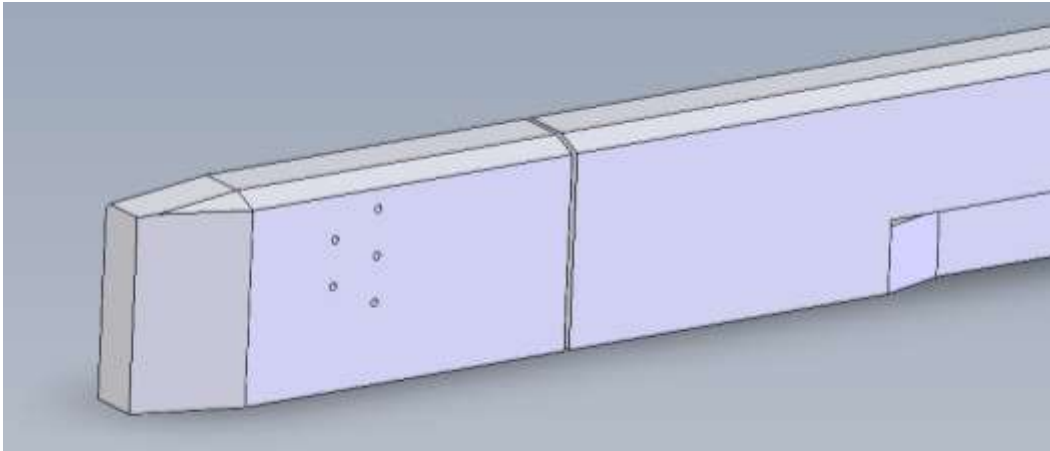


Figure 10. Isometric Picture of Buttress 6

2.2.7 Buttress 7

Buttress 7 was a 35-in. tall, stand-alone buttress with a vertical face. The buttress was 14 in. wide, and the front face was tapered back 4½ in. over 18 in. in length at the upstream end of the barrier. Buttress 7 was originally designed to be attached to NDOT's 34-in. tall AGT. After a 3-in. overlay, both the bridge railing and the AGT would remain crashworthy without the need for any retrofits. Thus, Buttress 7 was removed from consideration for the remainder of this study. A 3D model of Buttress 7 is shown in Figure 11.

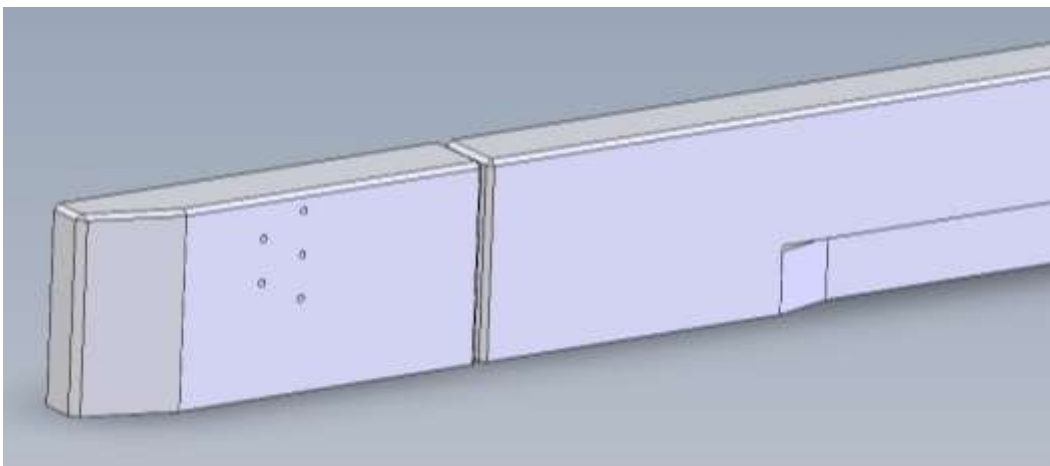


Figure 11. Isometric Picture of Buttress 7

2.2.8 Buttress 8

Buttress 8 was a 12-ft long, stand-alone buttress that transitioned from a 32-in. tall vertical shape to a 42-in. tall New Jersey shape. An 18-in. long cantilevered segment extended from the upstream end of the buttress and was tapered back 4½ in. Buttress 8 was originally designed to be attached to 31-in. tall thrie beam guardrail. The shape transition began just downstream from the location of the thrie-beam terminal connector. A 3D model of Buttress 8 is shown in Figure 12.

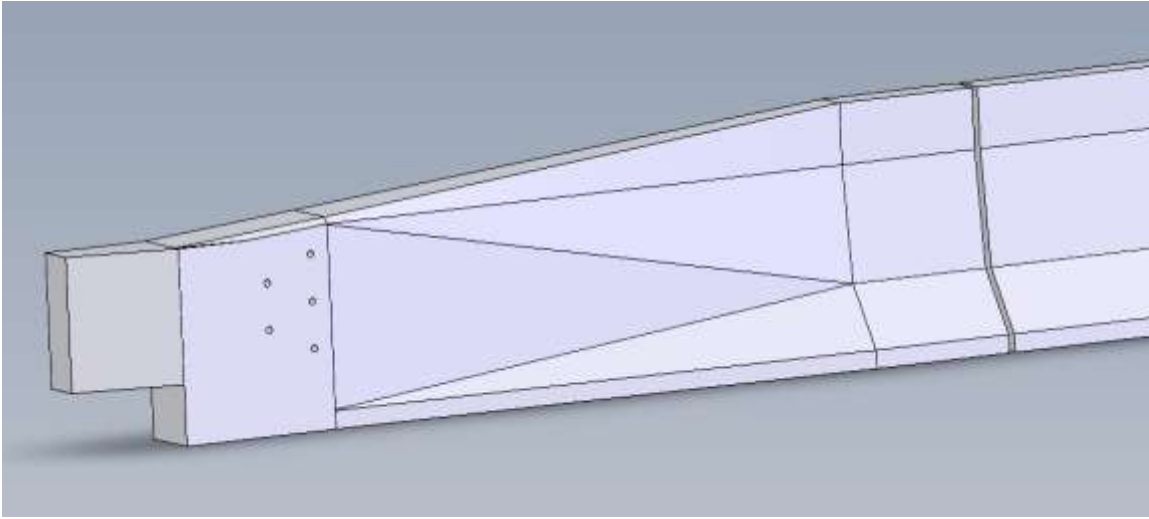


Figure 12. Isometric Picture of Buttress 8

2.2.9 Buttress 9

Buttress 9 was the end section of a 32-in. tall New Jersey shaped bridge rail. The upstream 18 in. of the barrier was flared back at a 30-degree angle. Buttress 9 was originally designed for attachment to 31-in. tall thrie beam guardrail. A 3D model of Buttress 9 is shown in Figure 13.

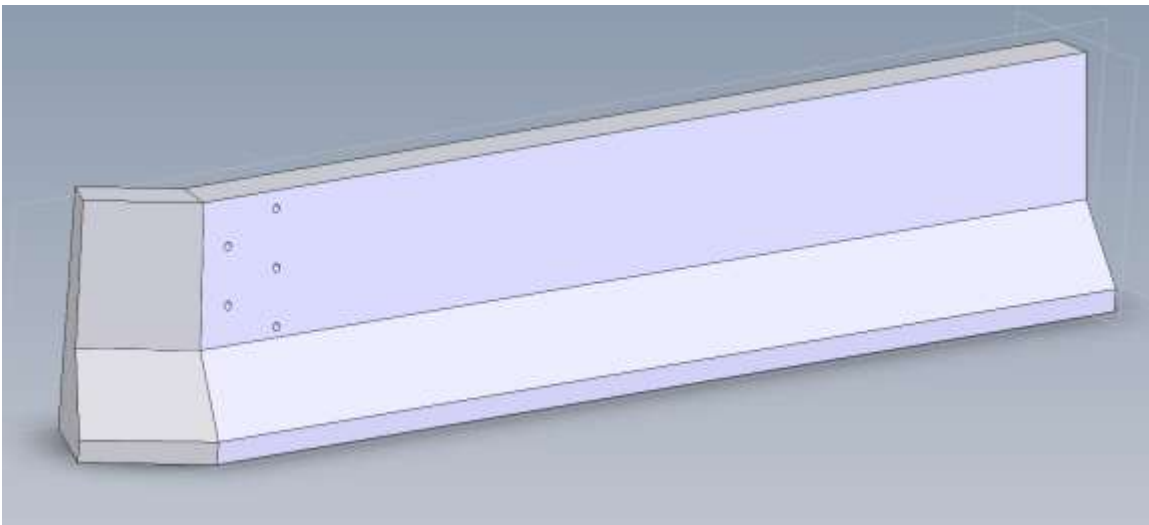


Figure 13. Isometric Picture of Buttress 9

2.2.10 Buttress 10

Buttress 10 was similar to Buttress 8, but the shape transition from vertical to New Jersey occurred within the bridge rail, not within the stand-alone buttress. Thus, Buttress 10 was 32 in. tall and 16 in. wide. An 18-in. long cantilevered segment extended from the upstream end of the buttress and was tapered back 4½ in. Buttress 10 was originally designed to be attached to 31-in. tall thrie beam guardrail. A 3D model of Buttress 10 is shown in Figure 14.

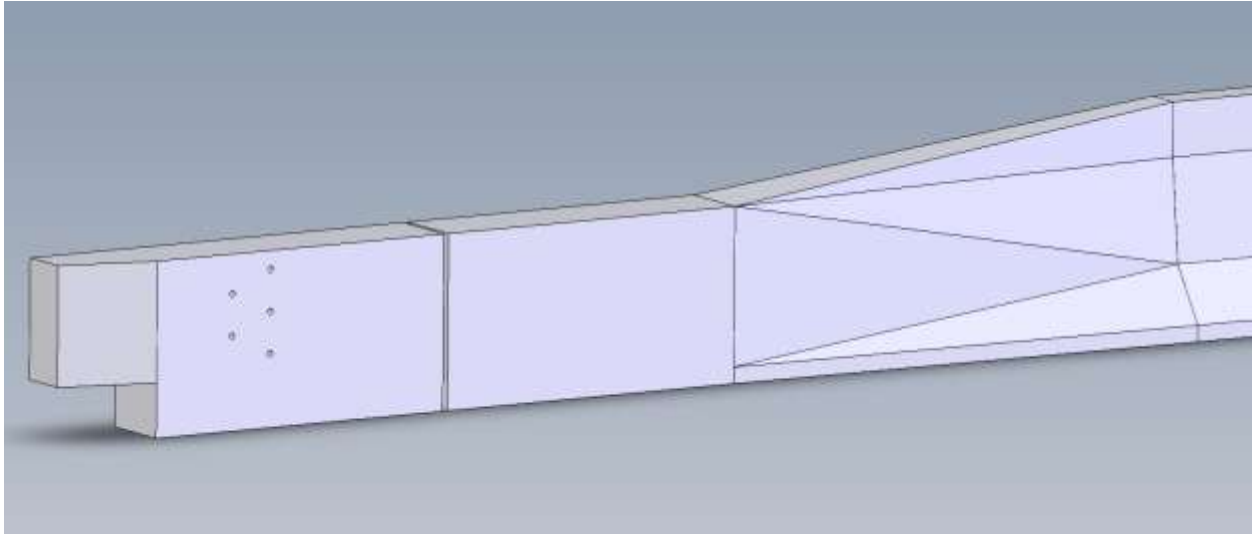


Figure 14. Isometric Picture of Buttress 10

3 IDENTIFICATION OF ATTACHMENT ISSUES AND CONCERNS

After 3D models were created for all ten existing buttress configurations, a thrie beam terminal connector was placed on the front face of the buttresses to identify attachment issues and possible safety concerns. The thrie beam terminal connector was prescribed a height of 34 in. relative to the original ground line. This height corresponds to a 31-in. mounting height relative to the new roadway surface after a 3-in. overlay is applied. Issues were identified with the alignment of the thrie beam in both vertical and longitudinal directions. Further, vehicle snag hazards were identified for impacts in both the nominal and reverse directions. These issues are discussed in the following sections.

3.1 Vertical Bolt Hole Positions

Nearly all of the buttresses were not tall enough to utilize standard attachment hardware (i.e., a thrie beam terminal connector and attachment bolts). The desired 34-in. guardrail height relative to the original ground resulted in the terminal connector extending above the top of the buttresses. For the existing 32-in. tall buttresses, the terminal connector extended 2 in. above the buttresses and the top bolt hole for standard 5-hole terminal connectors was located at the top surface of the buttresses, as shown in Figure 15. New holes could not be drilled at these locations as the bolt would not have enough concrete cover. Additionally, the terminal connector was now located above the position of the original lower bolt, which made using the existing bolts/holes very difficult.

This vertical alignment issue was worse for the 29-in. tall buttress, where the terminal connector extended 5 in. above the buttresses. As shown in Figure 16, the top bolt hole was well above the buttresses and the second highest bolt hole was located at the top surface. Retrofit designs were needed that could account for this vertical shift in bolt/hole locations.

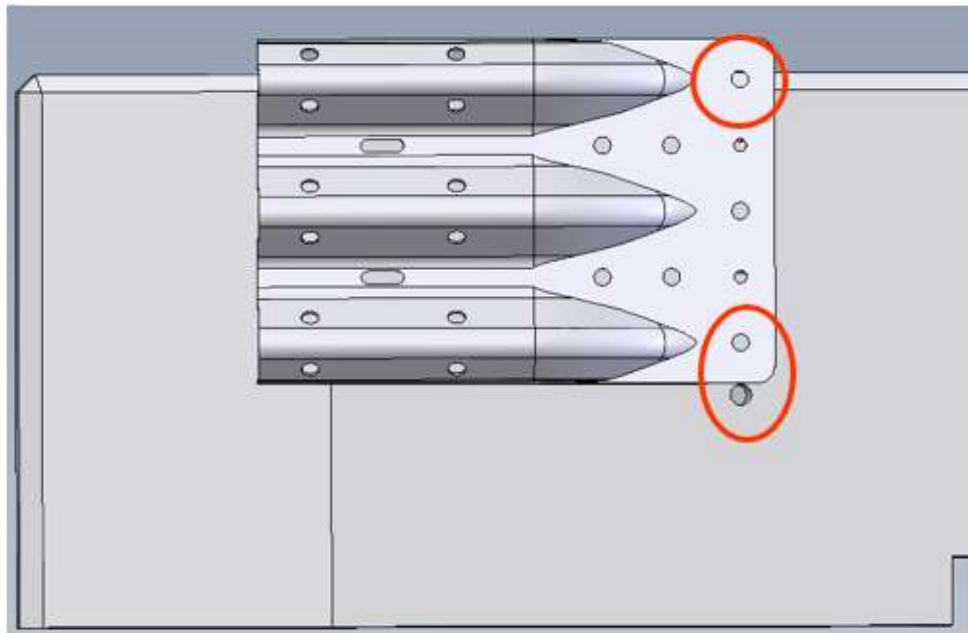


Figure 15. Top Bolt Position with a 32-in. Tall Buttress

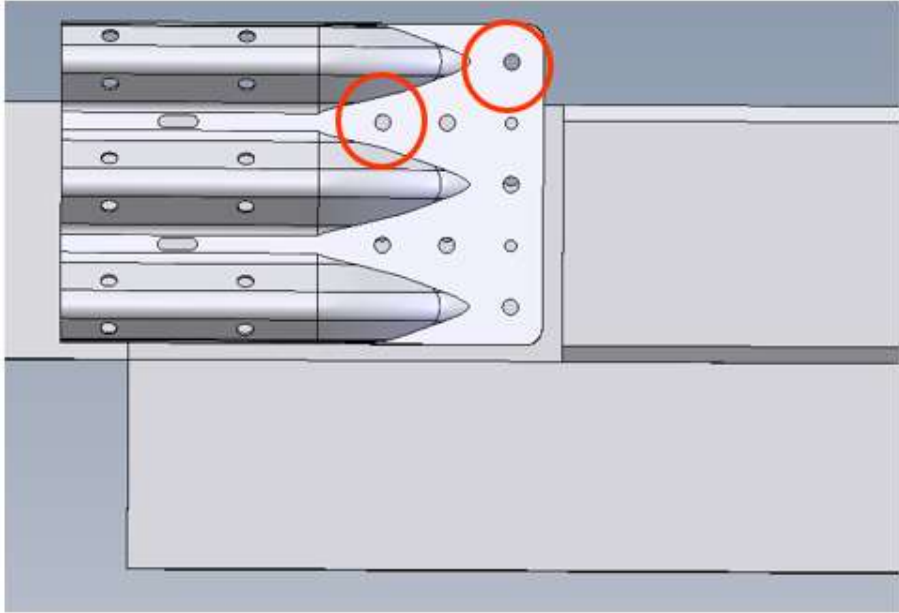


Figure 16. Top Bolt Position with a 29-in. Tall Buttress

3.2 Increased Unsupported Span Length in Thrie Beam Guardrail

Unsupported span length for AGTs refers to the distance between the location in which the buttress is laterally supporting the guardrail and the first transition post. Large unsupported span lengths result in decreased system stiffness, increased deflections, and increased snag on the buttress. Thus, it was important to maintain the unsupported span length from the as-tested 34-in. tall AGT when attaching to the existing buttresses. The as-tested unsupported span length was 30¼ in., which resulted in the upstream pair of attachment bolts being located 18¾ in. downstream from where the guardrail is laterally supported by the buttress, as shown in Figure 17.

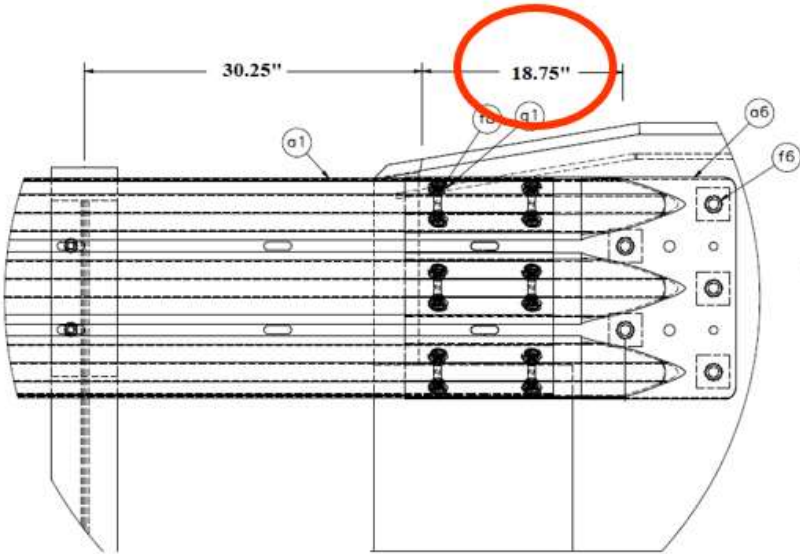


Figure 17. Unsupported Span Length from the As-Tested 34-in. Tall AGT

A review of the drawings for NDOT's existing buttresses led to the discovery that all nine of the buttresses utilized bolt locations closer to the lateral support point than the desired minimum distance of 18³/₄ in. For most of the thrie beam attached buttresses, this distance was 15³/₄ in., or 3 in. less than desired, as illustrated in Figure 18. For the remaining buttresses, this distance was even shorter with a minimum of only 3³/₄ in. Therefore, the location of the terminal connectors on each of the existing buttresses would need to shift downstream in order to maintain the unsupported span length for the AGT and prevent the risk of increased vehicle snag on the concrete buttresses.

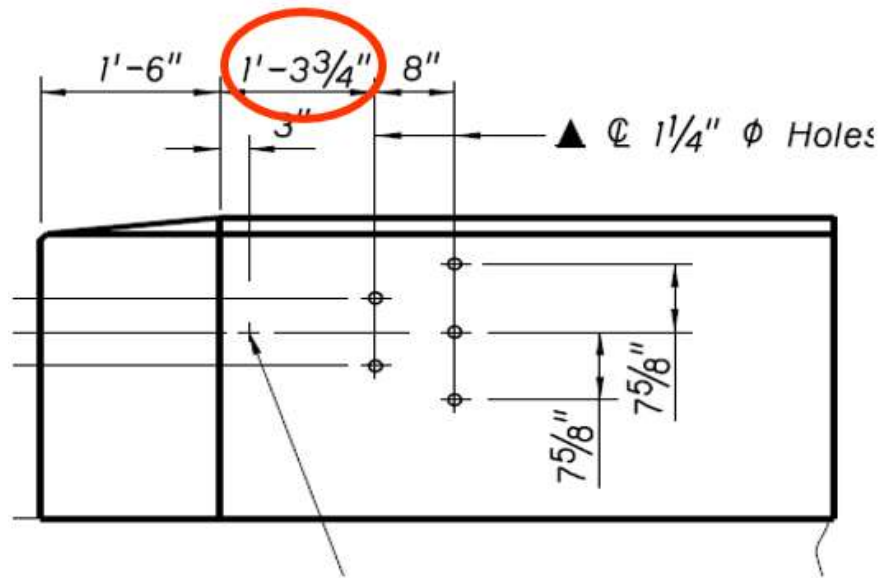


Figure 18. Location of Existing Bolt Holes on Buttress 6

3.3 Wheel Snag below the Thrie Beam

Five of NDOT's existing buttress configurations have a cantilevered segment extending from the upstream end of the buttresses. The cantilevered segment is tapered laterally to mitigate vehicle snag on the buttress. However, the cantilevered portion only exists behind the guardrail and stops 10 in. to 13 in. from the ground line. This leaves an opening for an impacting wheel to extend under the thrie beam and impact the upstream faces of the buttresses, as shown in Figure 19.

Previous MASH testing has shown that wheels can and will extend underneath AGT rails and contact the concrete buttress. As shown in Figure 20, tire marks on the buttress from the MASH testing of NDOT's 34-in. AGT can be seen extending nearly 10 in. past the front face of the buttress. The 4¹/₂-in. x 18-in. tapered face of the standardized buttress greatly reduced the magnitude of the wheel snag as compared to the perpendicular surface circled in Figure 19.

Buttress 9 poses a unique wheel snag situation. Although the barrier is flared back, the toe of the New Jersey shape barrier still extends in front of the thrie beam. Subsequently, wheel interaction with the toe of the barrier, as circled in Figure 21, is likely. Most AGTs attached to New Jersey shaped barriers incorporate tapers to eliminate the barrier toe under the rail, as illustrated in Figure 22. Previous crash testing of a similar AGT buttress design could not be found,

so the crashworthiness of this design is unknown. Thus, additional retrofits to mitigate wheel snag may be necessary when attaching new AGTs to these existing systems with either exposed perpendicular faces or exposed barrier toes beneath the thrie beam.

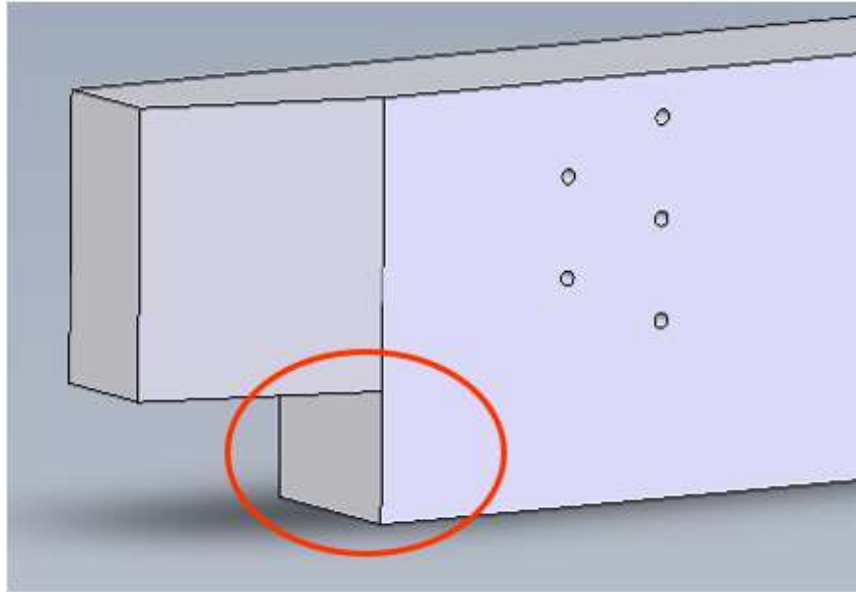


Figure 19. Location of Potential Wheel Snag below Thrie Beam



Figure 20. Wheel Snag on 34-in. AGT during MASH Crash Testing [2]

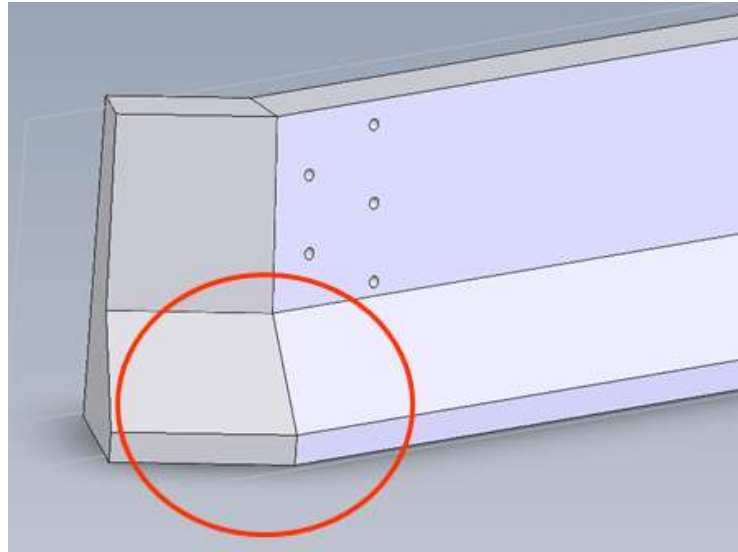


Figure 21. Wheel Snag Concern for Buttress 9

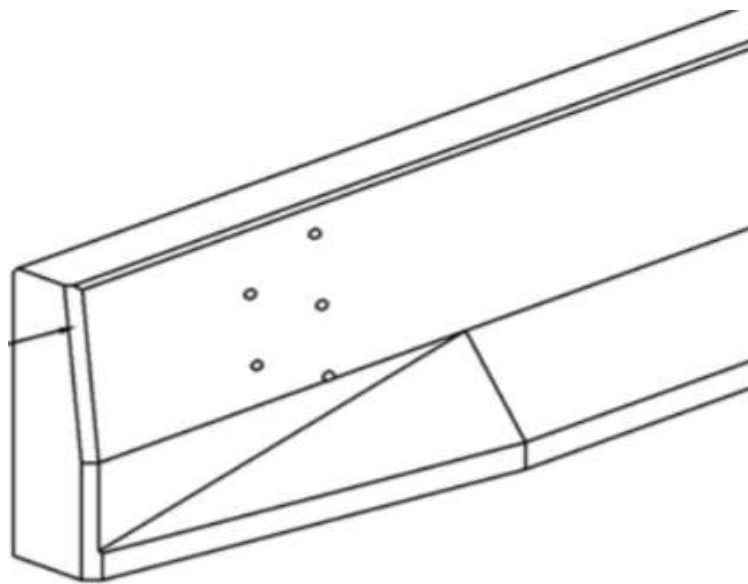


Figure 22. Typical Shape Transition to Mitigate Wheel Snag on New Jersey Shaped Buttresses

3.4 Vehicle Snag on Buttresses

Four of the existing NDOT buttresses incorporated recesses or guardrail connection blockouts just downstream from the terminal connectors. This geometry was likely designed to keep the face of the guardrail flush with the face of the buttress and bridge rail. However, this geometry also results in a vehicle snag hazard downstream from the terminal connector, as shown in Figure 23. Exposed edges of this size can easily result in excessive vehicle decelerations and/or vehicle instabilities as a result of vehicle snag. Thus, retrofit designs were needed that addressed these snag hazards.

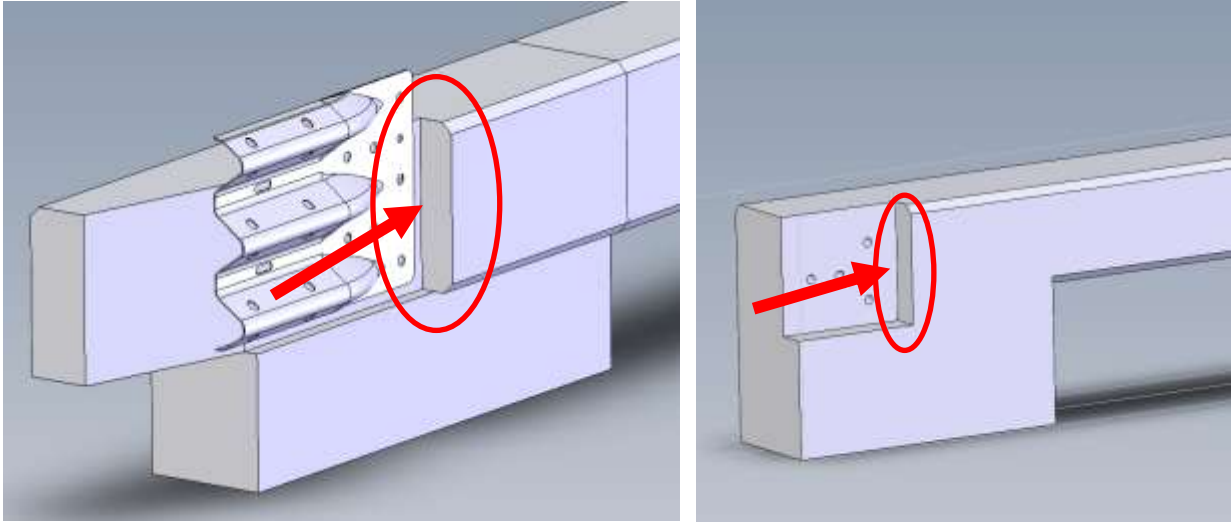


Figure 23. Vehicle Snag at Connection Blockout or Buttress Recess

3.5 Reverse Direction Snag

As discussed in Section 3.1, attaching the AGT at height of 34 in. (31 in. relative to the new roadway surface after a 3-in. overlay) resulted in the thrie beam terminal connector extending above the tops of most of the buttresses. This could lead to vehicle snag on the guardrail during reverse direction impacts, as illustrated in Figure 24. Vehicle snag on guardrail components can negatively affect barrier performance and result in excessive decelerations, occupant compartment crush, or vehicle instabilities. Consequently, retrofit designs were needed that could mitigate this snag issue for reverse direction impacts.

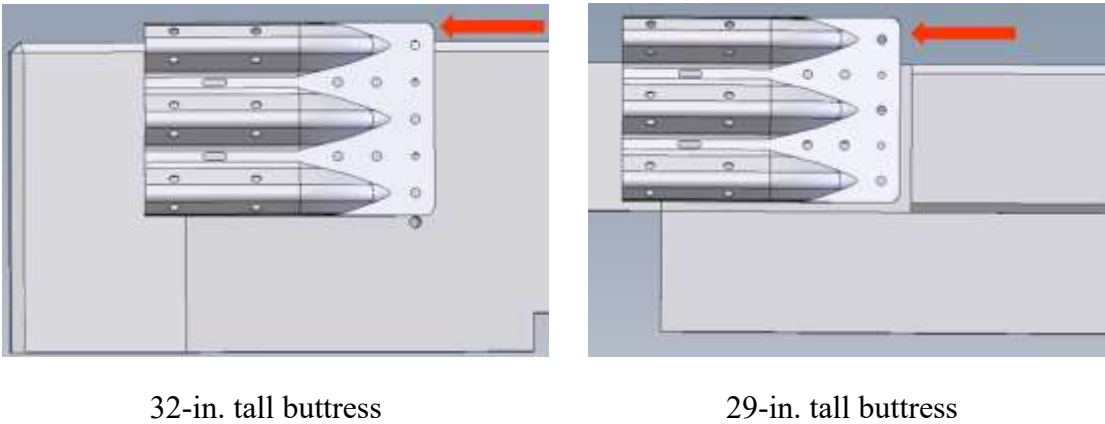


Figure 24. Reverse Direction Snag Concerns

3.6 Buttress Priority and Selection Methodology

As detailed in Chapter 2, the existing NDOT transition buttresses had a wide variety of geometric characteristics. Subsequently, the issues and concerns that were identified for each buttress differed greatly. Table 2 was created to summarize the issues associated with each buttress

as well as indicate the complexity that attachment retrofits may require. First, the various issues and concerns were listed in the left column. Issues that were considered easier to overcome were placed at the top of the column, while those thought to be more difficult to address were placed at the bottom. The individual buttresses were listed across the top of the remaining columns, and an “X” was placed in the cells when a buttress contained the issue listed for that row. The buttresses, or columns, were then reorganized so show them by increasing retrofit complexity going left to right. Finally, it was observed that the buttress could be characterized into five groups based on their associated issues, as shown in Table 2. Because of the shared characteristics and associated retrofit issues, it was thought that one retrofit design may work for the buttresses in a particular group. However, different retrofits may be needed for buttresses in differing groups.

Table 2. Issues and Concerns by Buttress

Issues and Concerns	Buttress No.								
	5	6	10	8	4	2	1	3	9
Increased Unsupported Span Length (Weakened AGT Stiffness)	X	X	X	X	X	X	X	X	X
Rail 2 in. above Buttress (Top Bolt/Hole above Buttress) (Reverse Direction Snag)	X	X	X		X	X			X
Exposed Upstream Face below Rail (Wheel Snag)			X	X	X	X	X	X	
Buttress Recess or Connection Blockout (Vehicle Snag)					X	X	X	X	
Rail 5 in. above Buttress (Top Two Bolts/Holes above Buttress) (Reverse Direction Snag)							X	X	
Sloped Buttress Surface (Extra Hardware Required)									X
Toe of NJ barrier in Front of Rail (Wheel Snag)									X

During the formulation of this research and design project, it was assumed that retrofit AGT attachments would be developed for one or two buttresses. The proposal and budget were made to reflect this assumption. With ten buttresses submitted at the beginning of the project, it was unlikely that the available funds could cover the development and evaluation of AGT attachment retrofits for all the buttresses. Thus, the buttresses had to be prioritized.

Through discussions with the project’s technical advisory committee, it was decided to prioritize the buttress starting with the simpler AGT attachment retrofits and working toward the more complicated retrofits (going from left to right across Table 2), beginning with Buttress 5. This approach allowed the research team to address as many buttresses as possible with the available funds. Note, solutions were developed for the first six buttresses shown in Table 2 before funding ran out. Retrofit AGT attachments for Buttresses 1, 3, and 9 were not developed as part of this project due to budget and time limitations.

4 DESIGN CONCEPTS

4.1 Connector Plate Assembly for Rail Attachment

As discussed in Chapter 2, NDOT's 34-in. tall AGT was to be attached to existing buttresses so that the guardrail would be at a nominal height of 31 in. after a 3-in. thick overlay was applied to the bridge surface, and as described in Chapter 3, design of the AGT attachment hardware began with Buttress 5. In comparison to the original position of the thrie beam attachment on Buttress 5, the new AGT rail height of 34 in. would be 3 in. higher. Also, in order to maintain the as-tested unsupported span length of $30\frac{1}{4}$ in. (or a minimum distance of $18\frac{3}{4}$ in. between the upstream bolt holes in the terminal connector and the location of first contact with the buttress), the AGT had to be shifted 3 in. downstream. The resulting guardrail position on Buttress 5 is shown in Figure 25.

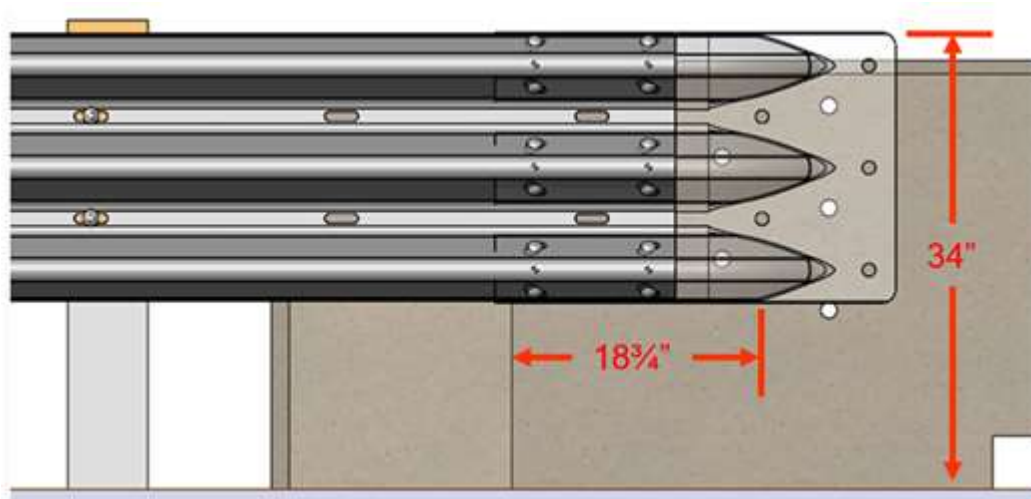


Figure 25. Rail Position on Buttress 5, Adjusted for Height and Unsupported Span Length

New bolt holes could not simply be drilled into Buttress 5 corresponding to the location of the holes in the terminal connector as the top hole was located on the top surface of the buttress. Similarly, new holes could not simply be drilled into the terminal connector at the locations of the existing bolts as the upstream bolts were within the middle and lower guardrail corrugations and the lower bolt was below the terminal connector. Thus, a connector plate assembly was created to allow for the attachment of the thrie beam to the buttress using the existing bolts.

The connector plate assembly consisted of a standard thrie beam terminal connector, a $\frac{3}{16}$ -in. thick steel plate, and two nuts. The plate was welded to the back of the terminal connector and extended far enough below the terminal connector such that the assembly reached the lower bolt. The downstream edge of the plate was beveled, and the top corner of the steel plate was tapered with a 2:1 slope to mitigate vehicle snag for reverse direction impacts. Five holes were drilled in the plate at the locations of the original bolts, and two holes were drilled into the terminal connector. Finally, the nuts were welded to the plate over the bolt holes inside the middle and lower guardrail corrugations. This allowed the two upstream bolts to be installed from the back of

the buttress and threaded into the nuts. The other three bolts could be installed from the front as they would normally be. A model of the connector plate assembly concept is shown in Figure 26, while Figure 27 shows the connector plate assembly placed on Buttress 5.

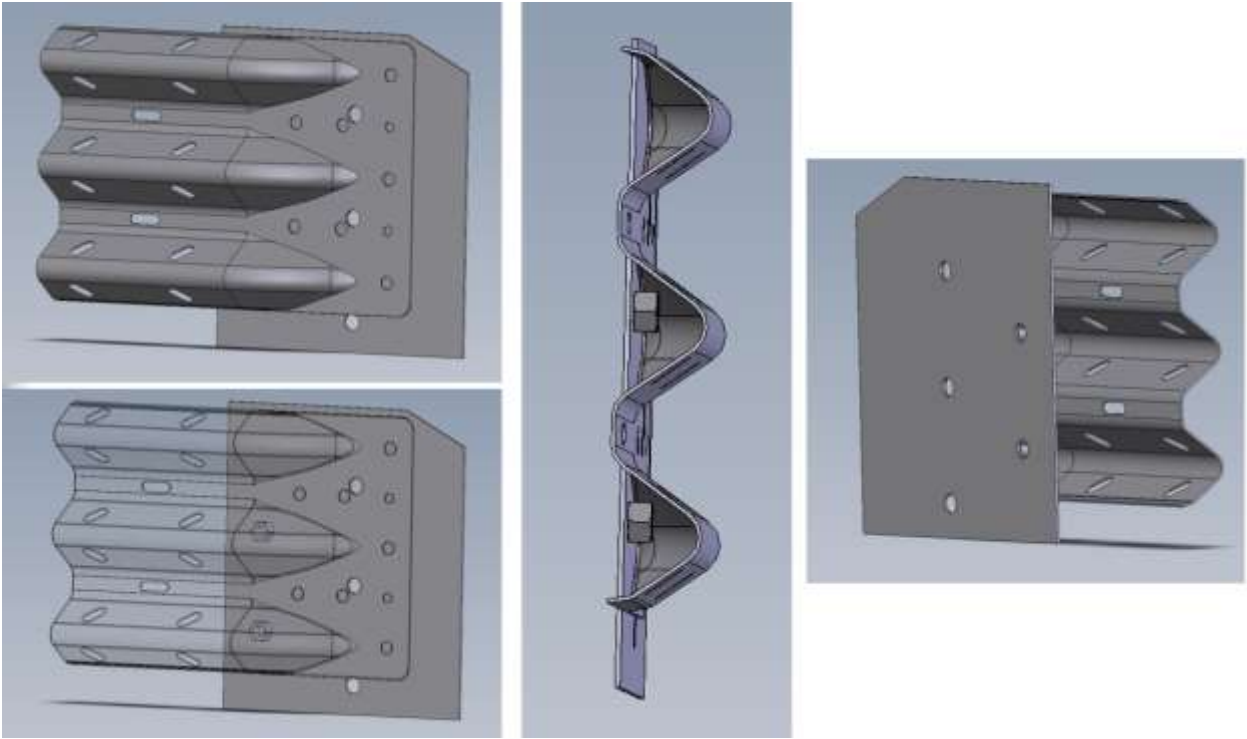


Figure 26. Connector Plate Assembly

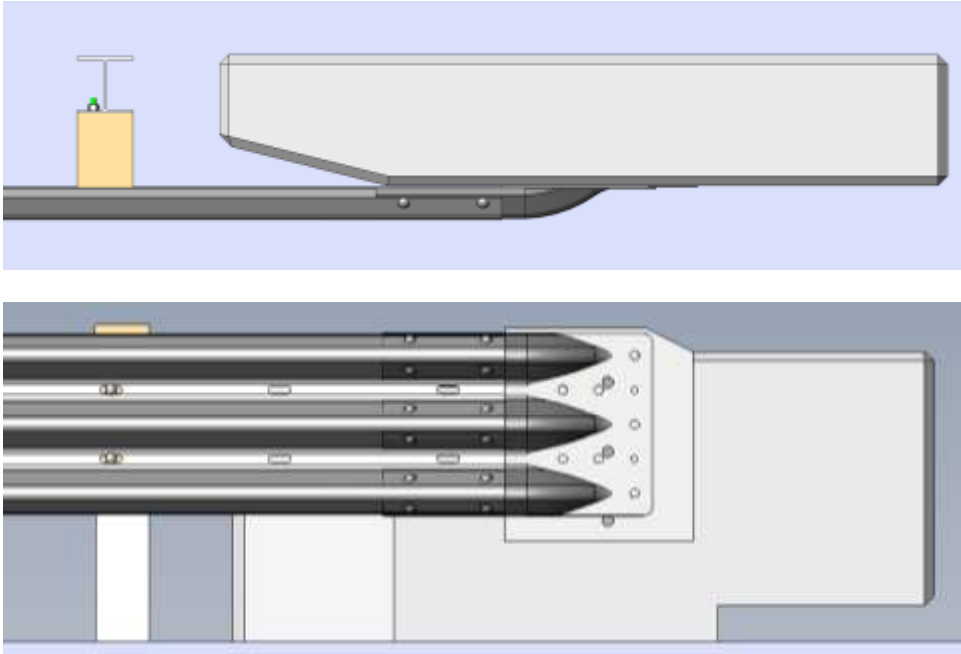


Figure 27. AGT with Connector Plate Assembly with Buttress 5

Buttresses 6 and 10 have similar geometries to Buttress 5. All three had the same bolt pattern that required a 3-in. vertical and a 3-in. longitudinal shift for the guardrail. Buttress 6 was 2 in. taller than Buttress 5, which did not affect the connector plate assembly. Buttress 10 had the same height as Buttress 5, but incorporated a cantilevered tapered segment on its upstream end instead of the continuous height tapered end of Buttresses 5 and 6. The cantilevered end of Buttress 10 increased the risk of wheel snag below the rail, but that issue was dealt with separately from the guardrail attachment to the buttress. Thus, the connector plate assembly shown in Figures 26 and 27 would work to attach the thrie beam guardrail to Buttresses 5, 6, and 10.

Buttress 8 contained a shape transition from a vertical face to a New Jersey shape. This shape transition began 27 in. downstream from the tapered end segment, or $3\frac{1}{4}$ in. downstream from the original bolt holes. The original connector plate assembly, shown in Figure 26, extended into the transition region and would not lay flat against the front face of Buttress 8. Buttresses 2 and 4 had concrete recesses or connection blockouts that would also prevent the connector plate assembly from extending past the beginning of these features. Coincidentally, these blockout features also started $3\frac{1}{4}$ in. downstream from the original attachment bolt locations on Buttresses 2 and 4. Therefore, it was decided to trim the downstream end of the connector plate assembly such that it remained on the flat, vertical face of Buttresses 8, 2, and 4. Note, this cut through both the thrie beam terminal connector and the $\frac{3}{16}$ -in. thick plate, as shown in Figure 28.

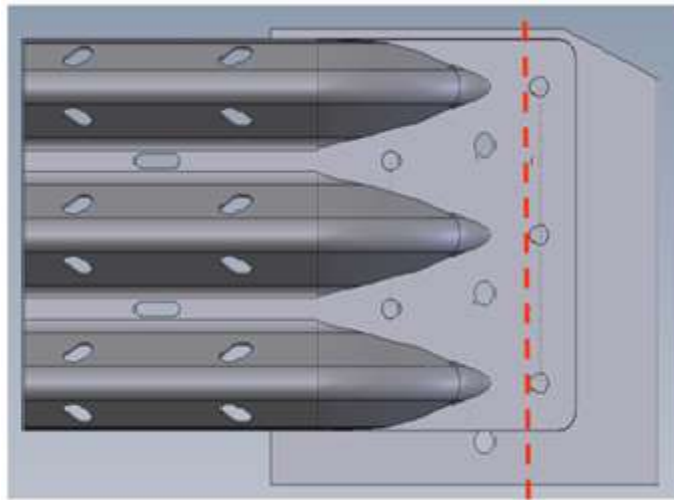


Figure 28. Trimming of Original Assembly for Buttresses 8, 4, and 2

Similar to how the top corner of the connector plate assembly was originally tapered, both downstream corners of the connector plate assembly were cut at 2:1 slopes to prevent reverse direction snag. The bottom corner was also tapered because the bottom of the connector plate assembly extended below the connection blockout on the Buttresses 2 and 4, as shown in Figure 29. Note, none of the cuts shown in Figures 28 and 29 to fit the connector plate assembly on various buttresses affected its attachment to any of the previous buttresses. Thus, the final shape of the connector plate should work for six of the buttresses, specifically Buttresses 2, 4, 5, 6, 8, and 10.

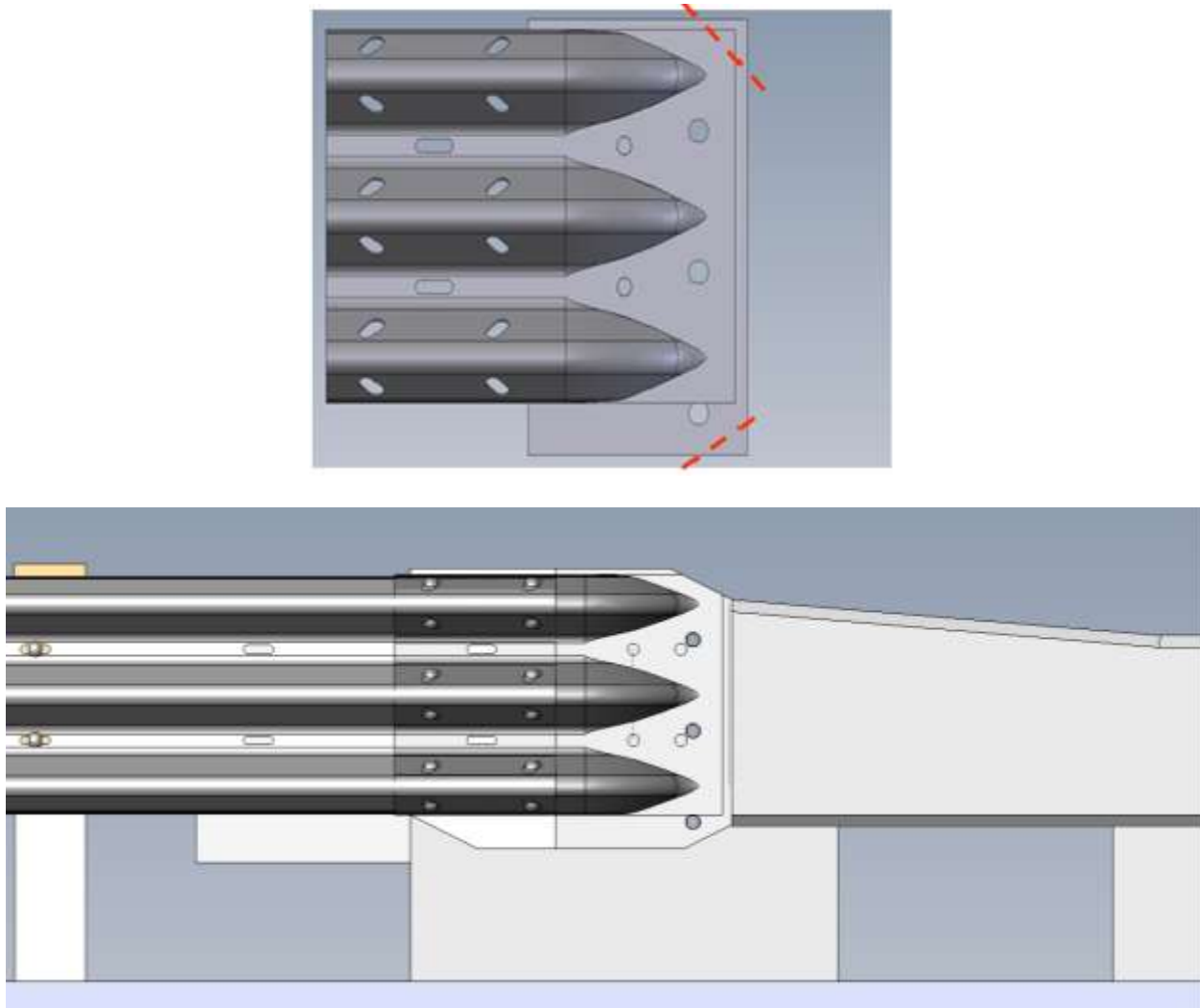


Figure 29. Connector Plate Assembly Corners Cut at 2:1 Slopes for Buttresses 2 and 4

Recall, Buttresses 2 and 4 contained a guardrail connection blockout downstream from the guardrail attachment bolts that protruded from the flat, vertical face of the buttresses. These connection blockouts posed a significant vehicle snag risk that needed to be addressed. Thus, an attachment spacer was placed behind the rail such that the downstream end of the connector plate assembly was flush with the concrete connection block (i.e., the face of the buttresses downstream from the attachment location). The attachment spacer block would be held in place by the five AGT bolts that passed through it, similar to guardrail blockout attachments to guardrail posts.

Since the buttresses had different connection blockout depths, the attachment spacer would be 3½ in. thick for Buttress 2 or 2 in. thick for Buttress 4. The attachment spacer was placed directly behind the connector plate assembly and had the same shape (height and 2:1 sloped corners) as the connection plate assembly. The attachment spacer extended upstream to the beginning of the buttress taper in order to maintain the unsupported span length for the three beam AGT. Finally, the attachment spacer could be fabricated from steel, timber, or any other material that would not compress under crash loads. The attachment spacer is shown in Figure 30.

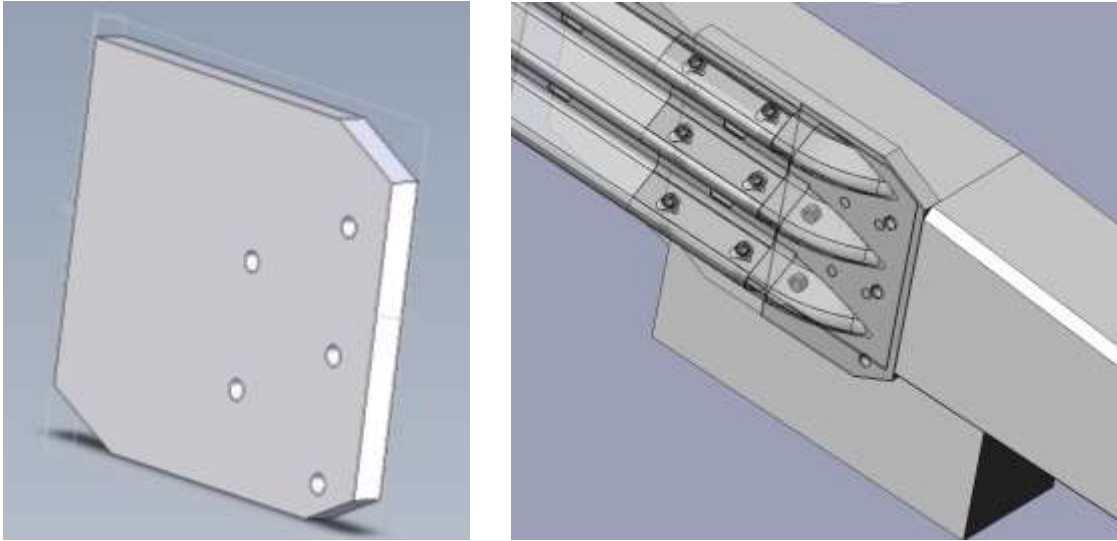


Figure 30. Attachment Spacer Design for Recessed Buttresses

The concrete connection breakout on Buttress 2 was not as tall as the connector plate assembly and attachment spacer, as illustrated in Figure 31. This created potential for vehicle snag during reverse-direction impacts. Vehicle components snagging on the exposed ends of the connector could result in excessive decelerations, occupant compartment crush, or vehicle instabilities. Subsequently, two concepts were designed to provide a smooth transition and mitigate vehicle snag in this region. The first concept involved filling concrete in the void above the buttress at the downstream end of the connector, as depicted in Figure 32(a). In the second concept, the connector block was modified to extend its 2:1 slope down to the top of the concrete connection breakout, as shown in Figure 32(b).

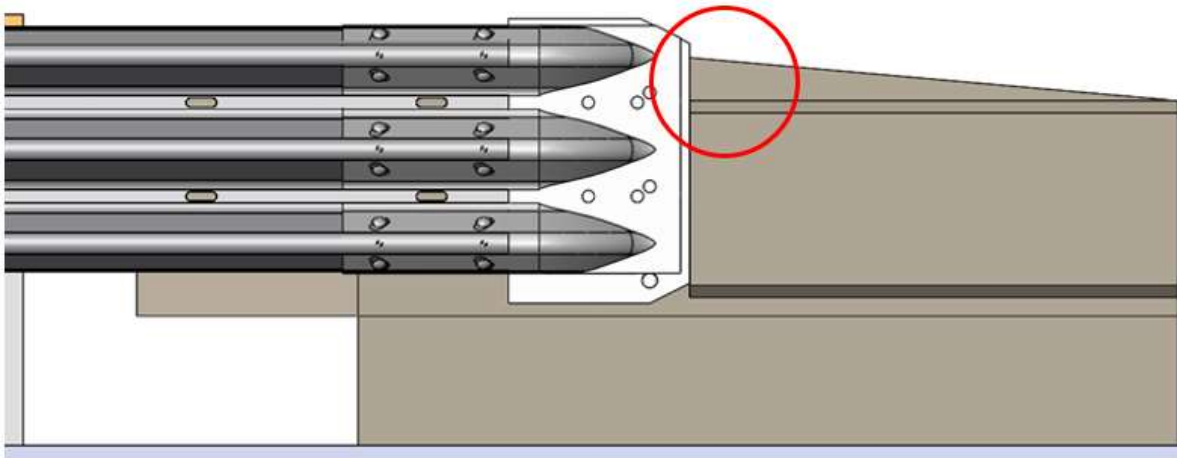


Figure 31. Risk of Vehicle Snag during Reverse-Direction Impact

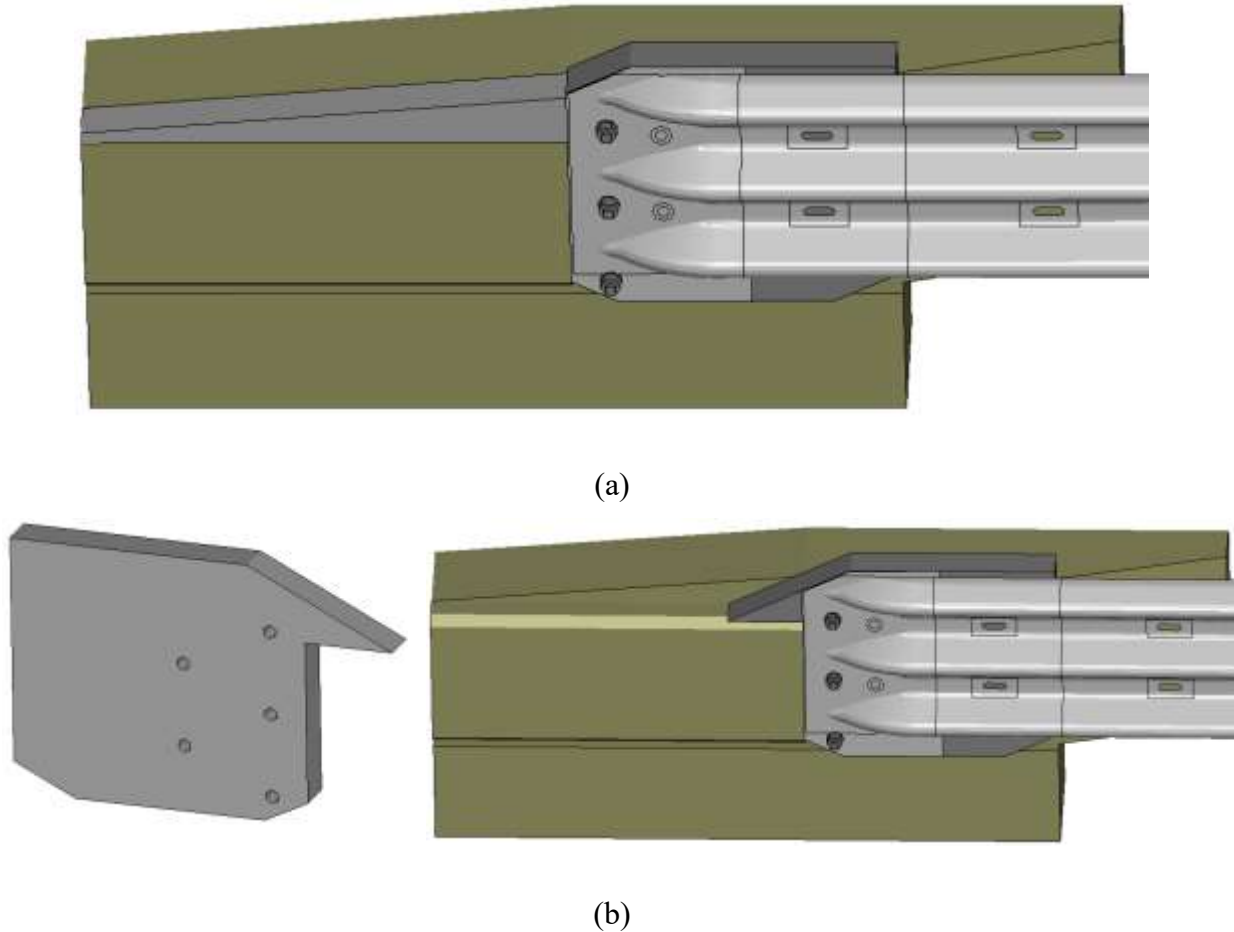


Figure 32. Design Concepts for Reverse-Direction Snag: (a) Concrete Fill; (b) Modified Attachment Spacer

4.2 Design Concept for Wheel Snag Prevention

As discussed in Section 3.3, an increased potential for wheel snag arises when the tapered end of the buttress is cantilevered and exposes the upstream face of the buttress below the thrie beam. Vehicle wheel snagging on the exposed ends could result in excessive decelerations and vehicle instabilities. Therefore, retrofit design concepts were needed to mitigate wheel snag at the buttress recess. Three design options were developed for the NDOT bridge railings and buttresses with a cantilevered end (i.e., Buttresses 2, 4, 8, and 10). The first option was to fill the void below the cantilevered portion of the buttress with concrete, as shown in Figure 33 for Buttress 8. The concrete fill would maintain the 4½-in. × 18-in. taper of the cantilevered segment and matched previously tested MASH crashworthy AGTs [1-2].

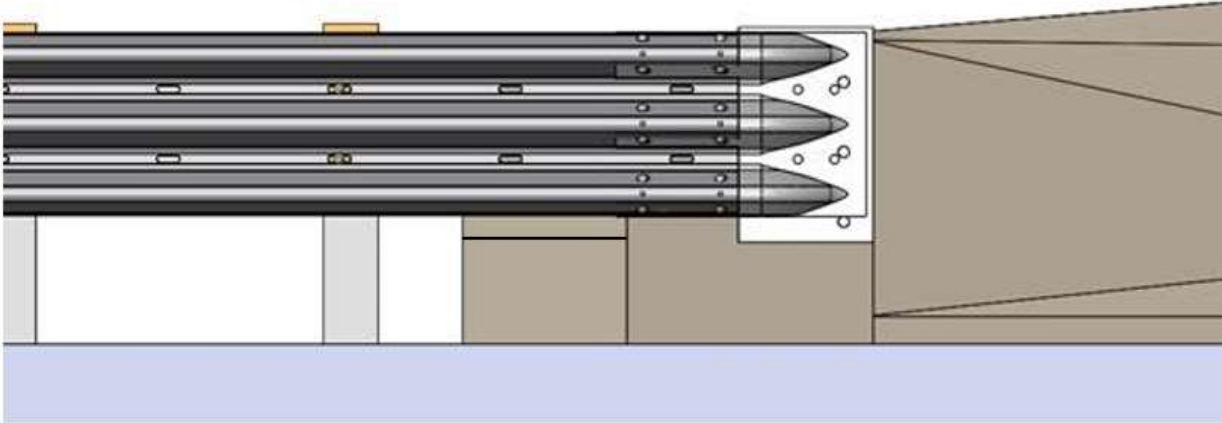


Figure 33. Retrofit Option 1, Concrete Fill

The second option consisted of a steel assembly designed to be installed below the cantilevered segment of the buttress. The steel assembly was fabricated using ¼-in. thick plates and held the same 4½-in. x 18-in. taper. Two gussets were placed behind the front plate to provide strength against deformation, as illustrated in Figure 34. The steel assembly can be bolted onto the front side of the buttress using a single anchor, as shown in Figure 35.

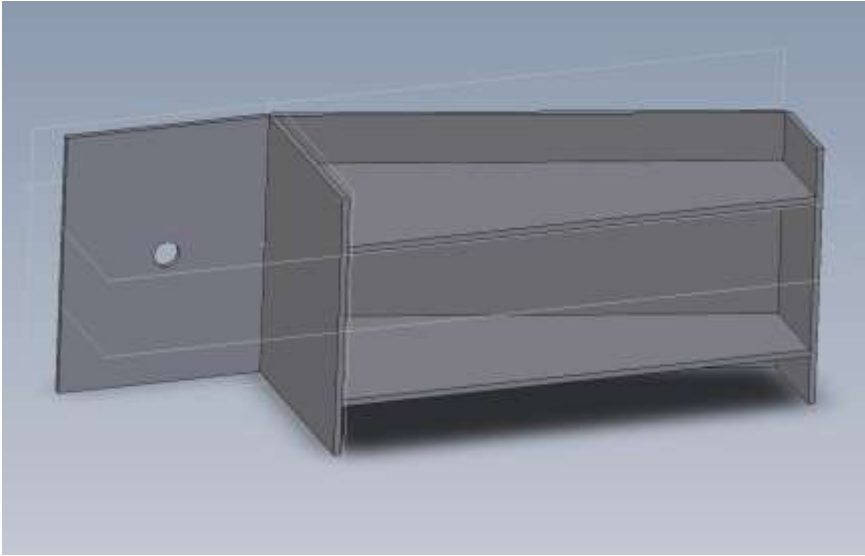


Figure 34. Option 2, Steel Assembly – Backside View

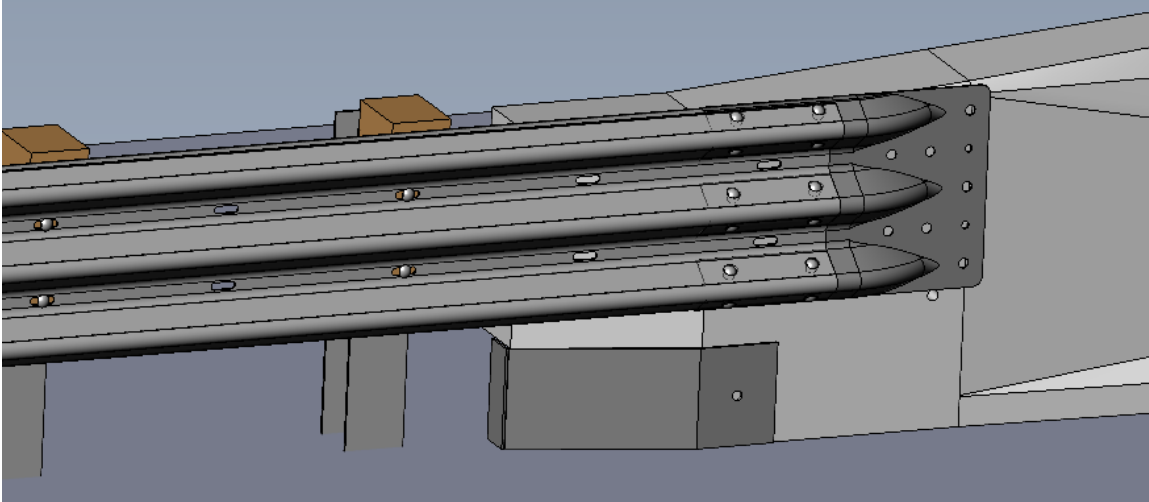


Figure 35. Option 2, Steel Assembly Placed on Buttress 8

The third retrofit option included a 6-in. tall curb placed below the thrie beam to mitigate vehicle snagging on the cantilevered portion of the buttress, as shown in Figure 36. A 6-in. tall curb has been successfully implemented into multiple MASH crashworthy AGTs to help reduce wheel snag [7-8]. The face of the curb should be placed flush with the face of the buttress (i.e., flush with the back of the guardrail). According to previous recommendations, the curb should be terminated prior to the W-to-thrie transition segment to prevent wheel snag.

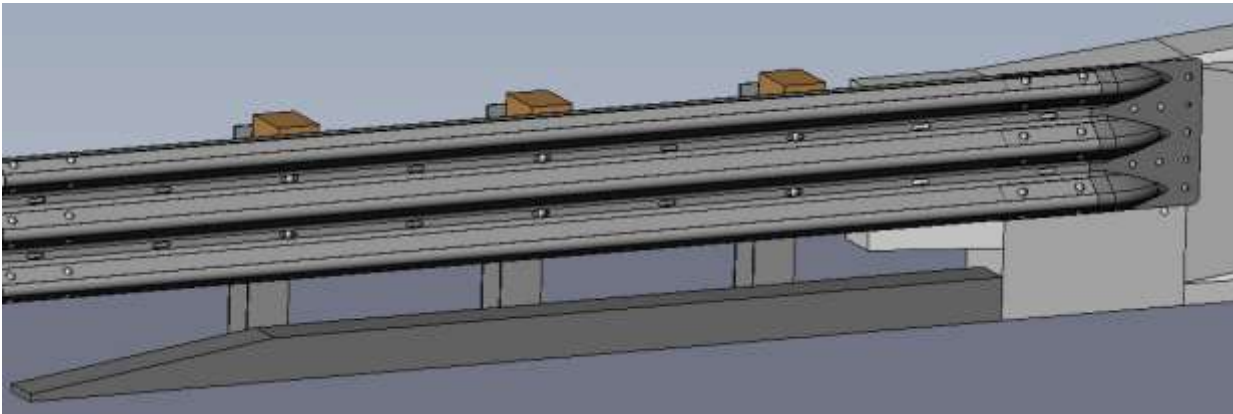


Figure 36. Option 3, Addition of 6-in. Tall Curb

5 LS-DYNA MODEL DEVELOPMENT

The retrofit concepts were evaluated using LS-DYNA computer simulation to examine crashworthiness, assist in design modifications, and provide application suggestions.

5.1 AGT Model

An LS-DYNA finite element analysis model of the NDOT 34-in. tall AGT was previously developed and validated at MwRSF [9]. This model was modified to incorporate a 3-in. thick overlay and attached to the various buttress models. The models were developed using LS-DYNA Version 10.1 [10]. The AGT model consisted of several components, including the upstream system anchorage, soil model, guardrail posts, W-beam guardrail, thrie-beam guardrail, concrete buttress, and overlay. The model AGT attached to Buttress 5 is shown in Figure 37.

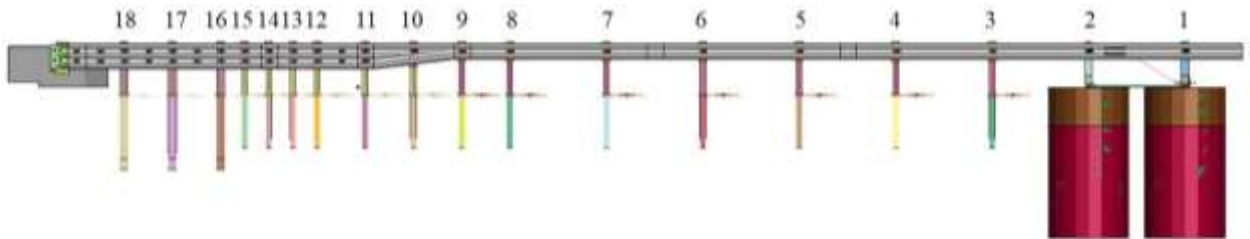


Figure 37. AGT Guardrail Installation

5.1.1 Upstream Anchorage

The upstream anchorage consisted of two timber breakaway cable terminal (BCT) posts embedded in solid Drucker-Prager soil elements, a groundline strut spanning post nos. 1 and 2, a cable anchor bracket attached to the backside of the W-beam rail, a cable anchor spanning from the cable anchor bracket through the groundline hole in post no. 1, and an anchor bearing plate. The timber BCT posts were modeled with type 2 (fully integrated S/R) solid elements given a *MAT_PLASTIC_KINEMATIC material formulation. The upstream anchorage assembly is shown in Figure 38.

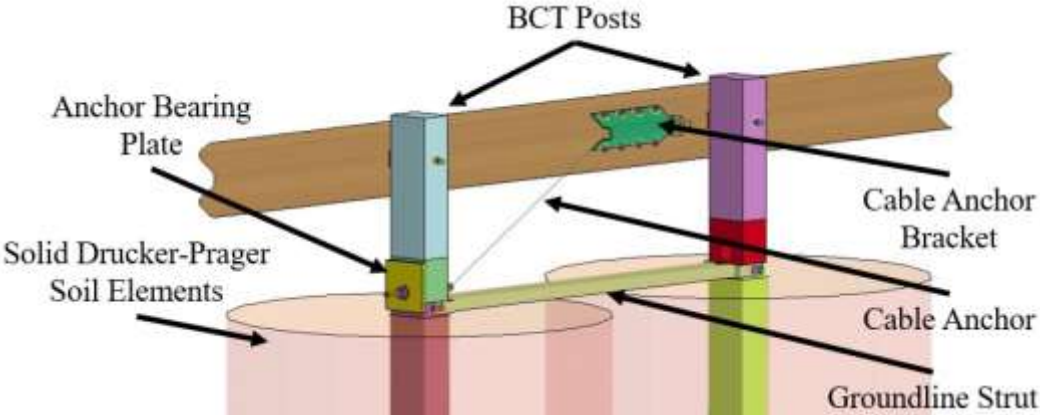


Figure 38. Upstream AGT Anchorage

5.1.2 Steel Guardrail Posts and Timber Blockouts

Steel guardrail post nos. 3 through 15 were modeled as W6×8.5 posts with a yield strength of 47 ksi. Post nos. 16 through 18 were modeled as W6×15 steel posts with a yield strength of 52 ksi. The posts were simulated using fully integrated shell element (Type 16) with the material model of *MAT_PIECEWISE_LINEAR_PLASTICITY. The spacing between posts is shown in Figure 39.

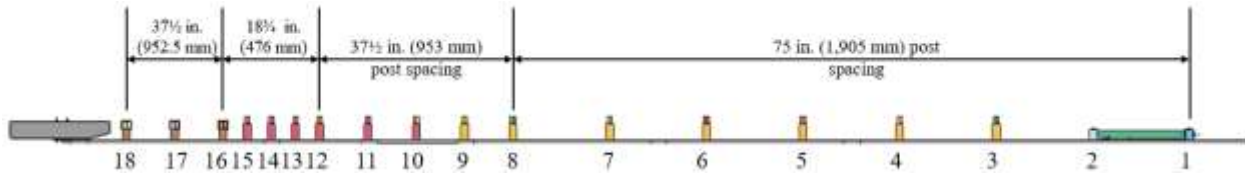


Figure 39. AGT Post Spacing

For post nos. 3 through 9, 12-in. × 6-in. × 14¼-in. timber blockouts were modeled between the W-beam guardrail and the posts. Timber blockouts with dimensions of 12 in. × 6 in. × 19 in. were used between the thrie-beam guardrail and post nos. 10 through 15. The timber blockouts were modeled using fully integrated solid elements with a *MAT_ELASTIC material model. The posts, blockouts, and guardrail were connected using bolted connections. The bolts and nuts were modeled using fully integrated solid elements with a *MAT_RIGID material property. Discrete nonlinear spring elements connected the guardrail bolts and nuts and provided preload in the bolted connection.

5.1.3 Soil Model

The soil for post nos. 3 through 18 was simulated using a rigid soil tube around the base of each post with a pair of soil springs attached to the top of the soil tube in the lateral and longitudinal directions, as shown in Figure 40. The soil tubes were pinned at the center of gravity to allow rotation. The interaction between the soil and posts was simulated using the soil spring for the improvement of computational efficiency. The soil springs were assigned a loading curve that replicated post-soil resistance during dynamic loading. Dynamic bogie tests on steel W6x8.5 and W6×16 posts embedded in MASH compliant soil were used to quantify the soil resistance and calibrate the soil spring loading curve.

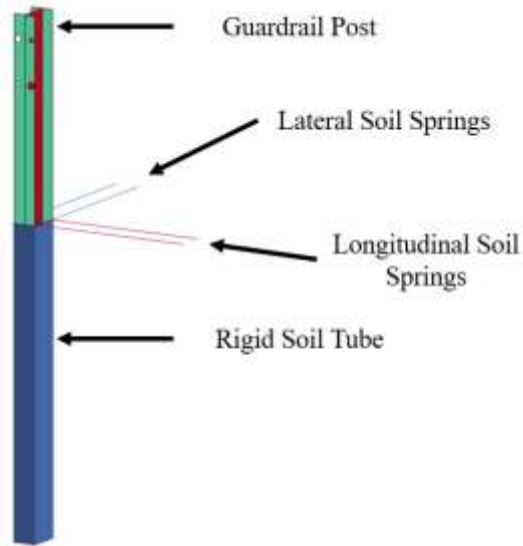


Figure 40. Guardrail Post with Soil Tube and Soil Springs

5.1.4 Guardrail

The upstream portion of the AGT consisted of 12-gauge W-beam guardrail with a top rail height of 34 in. relative to the original ground line (31 in. relative to the top of the overlay). The system transitioned from W-beam to 12-gauge thrie-beam guardrail with a 10-gauge asymmetrical W-to-thrie transition section, which maintained the top rail height. A 6-ft 3-in. long single section of 12-gauge thrie-beam was attached to the downstream end of the asymmetric W-to-thrie transition section. A 12-ft 6-in. long section of nested 12-gauge thrie-beam guardrail and a connector plate assembly comprised the downstream end of the AGT and was anchored to the concrete buttress. All guardrail sections were modeled with fully integrated (type 16) shell elements and given a *MAT_PIECEWISE_LINEAR_PLASTICITY material formulation with no failure defined.

The connector plate assembly consisted of a thrie beam terminal connector and a steel plate with dimensions of $23\frac{1}{2}$ in. \times $14\frac{3}{4}$ in. \times $\frac{3}{16}$ in. The thrie beam terminal connector was cut as described in the previous chapter to fit on the various buttresses. The two components were welded along all edges. The steel plate was modeled using fully integrated (type 16) shell element and a *MAT_PIECEWISE_LINEAR_PLASTICITY material formulation. The yield strength of the steel plate was 50 ksi. The connector plate assembly model is shown in Figure 41.

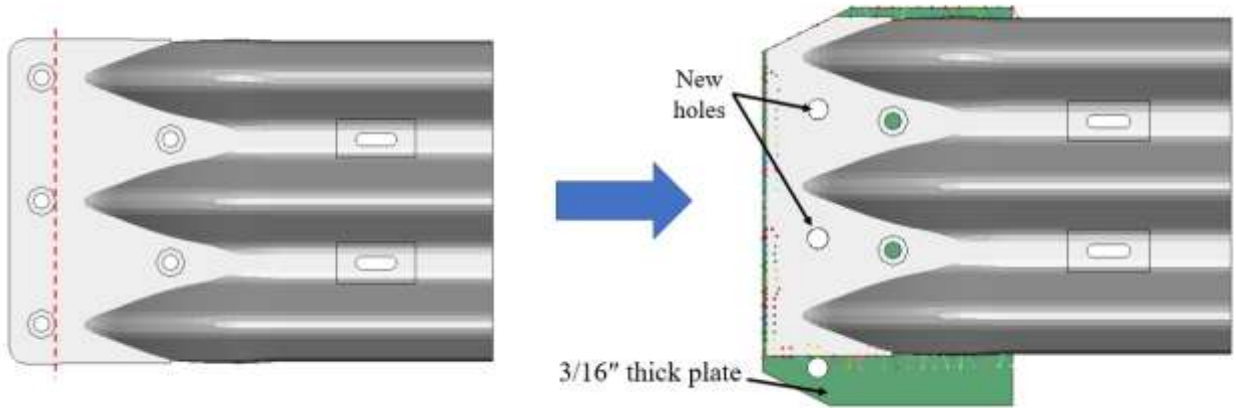


Figure 41. Connector Plate Assembly Model

To address the attachment issues identified for Buttresses 2 and 4, an attachment spacer was designed to fill the void between the AGT connector and the buttress. The attachment spacer was 27 in. long, 23.5 in. wide, and 3.5 in. thick. The attachment spacer was modeled using constant stress solid element and a *MAT_RIGID material model. The attachment spacer is shown in Figure 42.

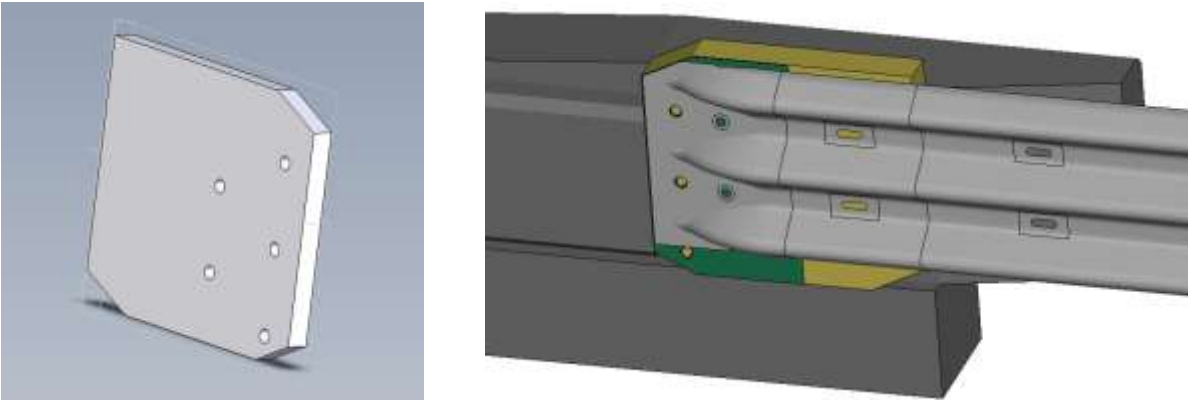
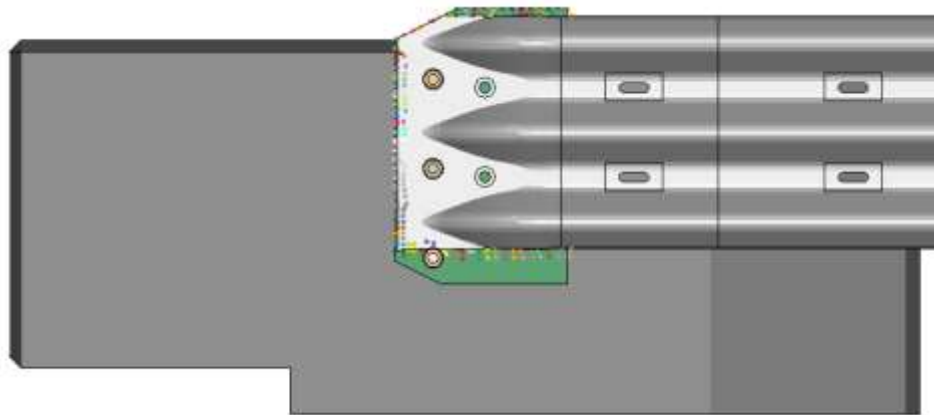


Figure 42. Attachment Spacer Model

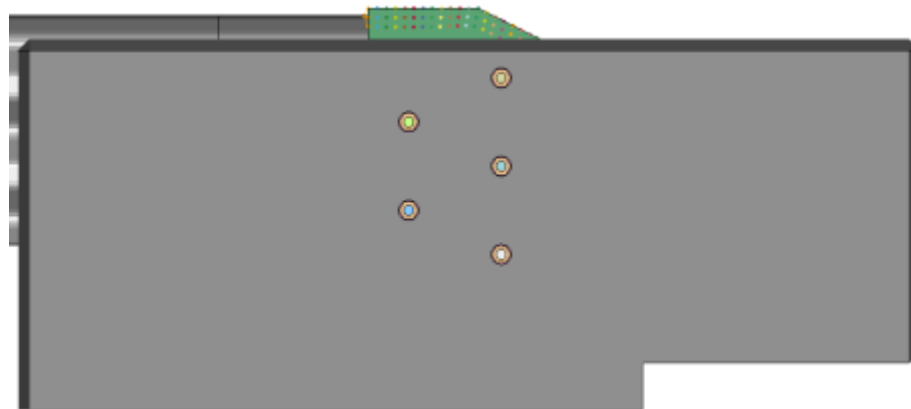
5.2 Concrete Buttress

The concrete buttresses were modeled using solid elements with a *MAT_RIGID material model. The modeled buttresses were fully constrained from displacements and rotations in the x, y, and z directions, and therefore did not experience movement during simulations. Making the buttress models rigid was a worst-case scenario for vehicle snag. Models of the concrete buttresses are shown in Section 2.2. Due to budget limitations, only Buttresses 5, 6, 8, 10, and 2 were evaluated within the simulated crash tests. Due to the similarities between Buttress 2 and Buttress 4, it was assumed conclusions from Buttress 2 simulations would also apply to Buttress 4.

The buttresses and thrie-beam terminal connector were connected using modeled bolted connections. The bolts were modeled using fully integrated solid elements with a *MAT_PIECEWISE_LINEAR_PLASTICITY material formulation. The preload to bolts was determined through field testing and applied using *INITIAL_STRESS_SECTION at a cross section near the center of each bolt. The nuts and washers were simulated using fully integrated solid elements and were given a *MAT_RIGID material model. The bolted connections are shown in Figure 43.



(a)



(b)

Figure 43. End Terminal Bolted Connection: (a) Traffic-Side Face; (b) Back Face

5.3 Overlay

The 3-in. tall overlay and ground were modeled using fully constrained rigid shell elements. As suggested by the sponsor, the overlays were aligned with the face of the guardrail posts and the front face of the buttress. Figure 44 illustrates the installation of the 3-in. tall overlay for all buttresses.

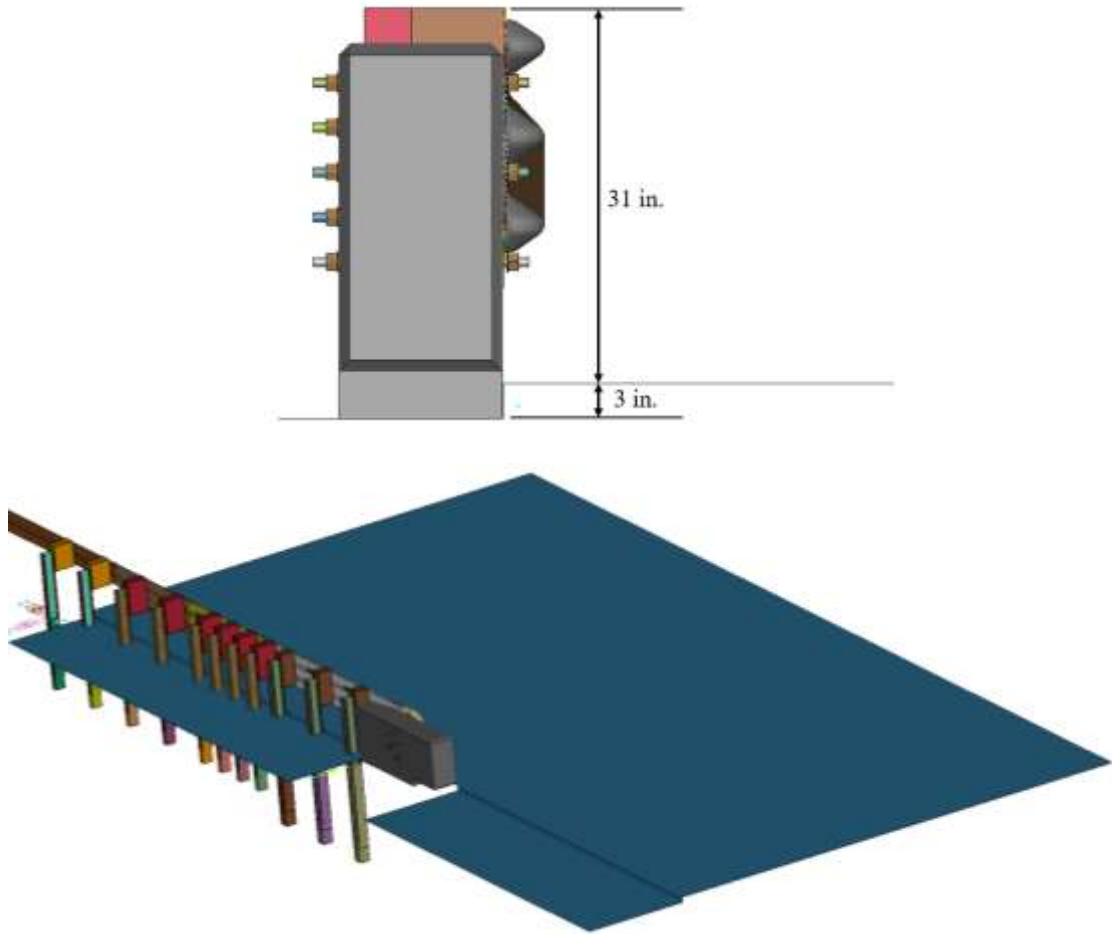
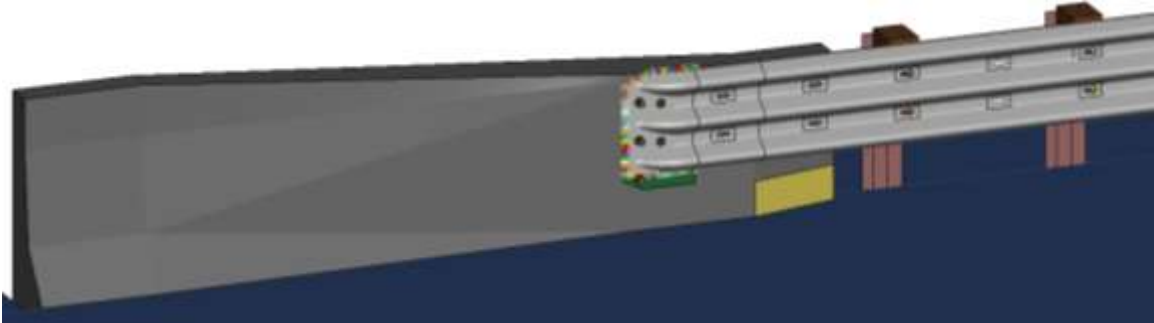


Figure 44. 3-in. Tall Overlay Model

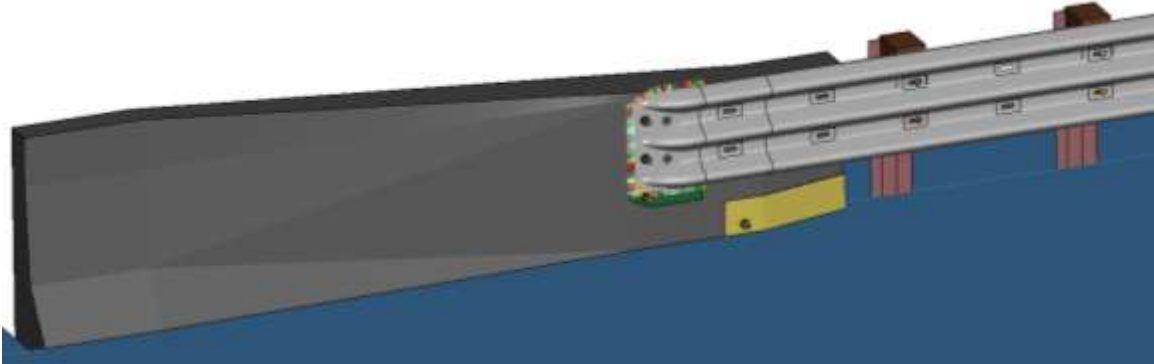
5.4 Options for Wheel Snag Prevention

Three options were evaluated for treatment of buttresses with a tapered cantilever segment to mitigate vehicle snag during a crash, including concrete fill below cantilevered segment, a steel assembly, and the addition of a 6-in. curb. The concrete fill and the curb were modeled using solid elements with a *MAT_RIGID material property. The modeled concrete fill and curb were fully constrained against displacements and rotations in the x, y, and z directions, ensuring no movement during the vehicle impact.

The steel assembly was fabricated from ¼-in. thick steel plates with a yield strength of 50 ksi. The steel assembly was modeled using fully integrated (type 16) shell elements and a *MAT_PIECEWISE_LINEAR_PLASTICITY material formulation. The steel assembly was bolted on the traffic side of the buttress through a single anchor below the cantilevered portion of the buttress. In the single anchor, the bolt, nut, and washer were modeled using fully integrated solid element with a *MAT_RIGID material property. The modeled retrofit options are shown in Figure 45.



(a)



(b)

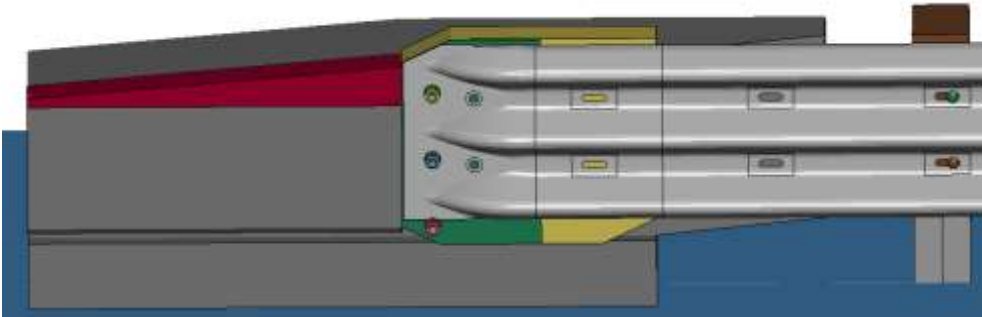


(c)

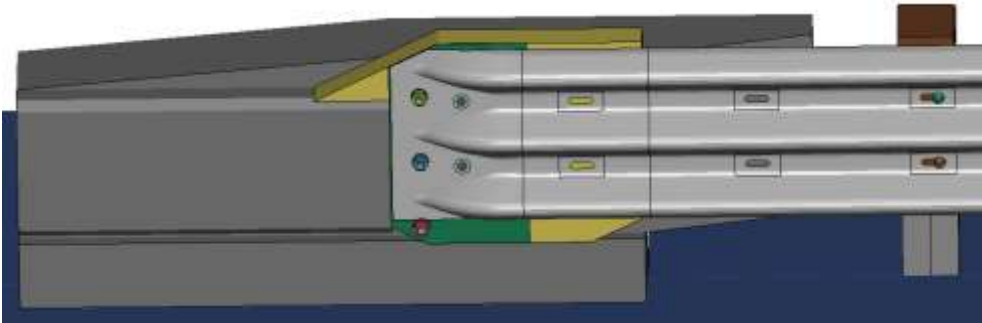
Figure 45. Options for Wheel Snag: (a) Concrete Fill; (b) Steel Assembly; (c) Curb

5.5 Options for Reverse Direction Snag – Buttress 2

Two options were developed and evaluated to mitigate reverse direction vehicle snag above the rail on Buttress 2. The first option was to fill the void with concrete downstream from the attachment spacer, as shown in Figure 46(a). The concrete fill was modeled using fully integrated solid element with a *MAT_RIGID material property. In the second option, the attachment spacer was modified to extend its 2:1 sloped top corner down until it met the top of the connection blockout, as shown in Figure 46(b).



(a)



(b)

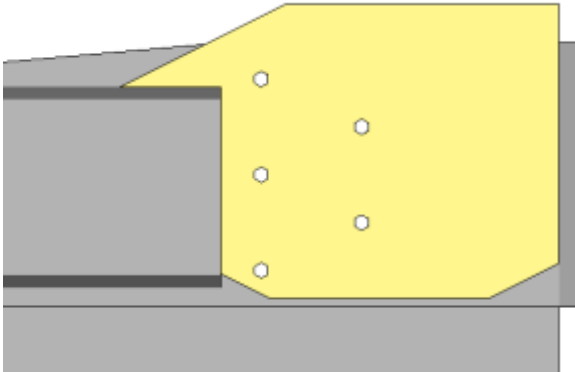


Figure 46. Options for Reverse Direction Snag on Buttress 2: (a) Concrete Fill; (b) Modified Attachment Spacer

5.6 Vehicle Models

A vehicle model of a 2018 Ram pickup truck was used for the simulation of MASH Test 3-21. The Ram vehicle model was originally developed by the Center for Collision Safety and Analysis Team at George Mason University [11] and was modified by MwRSF personnel for use in roadside safety applications. The 2018 Dodge Ram vehicle model is shown in Figure 47.

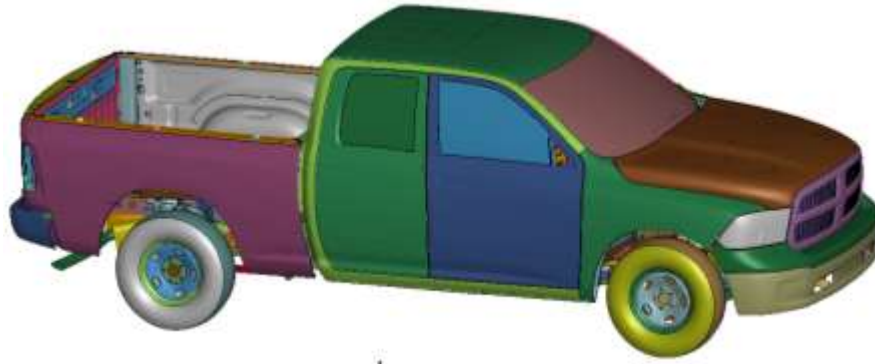


Figure 47. 2018 Dodge Ram Finite Element Model

A 2010 Toyota Yaris vehicle model was used in the simulation of MASH Test 3-20. The Yaris vehicle model was originally created by the National Crash Analysis Center [12] and later modified by MwRSF personnel for use in roadside safety applications. The Toyota Yaris vehicle model had a test inertial mass of 2,425 lb and an additional mass of 351 lb, which included the mass of two front-seated occupants, for a total mass of 2,776 lb. The 2010 Toyota Yaris vehicle model is shown in Figure 48.

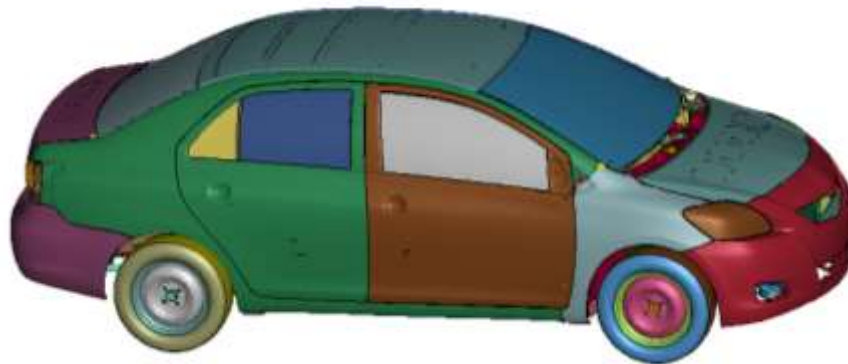


Figure 48. 2010 Toyota Yaris Finite Element Model

5.7 Model Validation

The LS-DYNA model of the AGT was validated against the two full scale crash tests conducted on NDOT's 34-in. tall AGT, test nos. 34AGT-1 and 34AGT-2 [2], which corresponded to MASH Tests 3-21 and 3-20, respectively. The total system length of the LS-DYNA model was 6.25 ft shorter than the length of the physical test installation, which was due to a shorter length of MGS being placed upstream of the AGT. Thus, 18 guardrail posts were included in the LS-DYNA model, while the physical installations had 19 posts. The shorter MGS length had negligible effects on the safety performance of the AGT. It should be noted that the overlay was not considered in the validation studies as it was not present during the crash tests.

In this project, the AGT model was validated by comparing several key parameters from the simulations to the full-scale crash test results, including occupant impact velocities (OIVs),

occupant ridedown accelerations (ORAs), angular displacements, and dynamic deflections. The comparisons of simulated and tested results for test nos. 34AGT-1 and 34AGT-2 are listed in Tables 3 and 4. The simulated results matched well with the data from test no. 34AGT-1, which used the 2270P pickup truck, though the simulation overpredicted longitudinal OIV and lateral ORA. For test no. 34AGT-2, which utilized the 1100C small car, the simulated and tested results were less aligned, with the simulation overestimating longitudinal OIV, longitudinal ORA, pitch, and dynamic deflection. However, both vehicles showed reasonable behavior in the simulation and the overestimations were considered to be a conservative analysis.

The focus of this project was on the safety performance of the AGT retrofit attached to the existing concrete buttress according to MASH Test 3-21 with the pickup truck, in which simulation compared well with test no. 34AGT-1. Simulations of MASH Test 3-20 with the small car were focused on evaluating possible wheel snag under the rail, which the small car model replicated reasonably well.

Table 3. Comparison of MASH Test 3-21 Results

Evaluation Criteria		Test No. 34AGT-1	Simulation	MASH 2016 Limits
OIV (ft/s)	Longitudinal	-20.2	-27.2	±40
	Lateral	25.9	25.4	±40
ORA (g's)	Longitudinal	-10.8	-10.2	±20.49
	Lateral	8.9	11.9	±20.49
Maximum Angular Displacement (deg.)	Roll	12.0	8.3	±75
	Pitch	4.4	5.1	±75
	Yaw	38.9	39.7	N/A
Maximum Dynamic Deflection (in.)		7.8	7.7	N/A

N/A = not applicable

Table 4. Comparison of MASH Test 3-20 Results

Evaluation Criteria		Test No. 34AGT-2	Simulation	MASH 2016 Limits
OIV (ft/s)	Longitudinal	-6.9	-10.1	±40
	Lateral	10.0	9.7	±40
ORA (g's)	Longitudinal	-10.8	-19.9	±20.49
	Lateral	14.7	11.3	±20.49
Maximum Angular Displacement (deg.)	Roll	-10.0	6.9	±75
	Pitch	-5.5	17.6	±75
	Yaw	94.9	61.0	N/A
Maximum Dynamic Deflection (in.)		2.7	5.2	N/A

N/A = not applicable

6 LS-DYNA SIMULATION RESULTS

6.1 AGT Model Variations and Evaluation Metrics

The validated AGT model was modified to incorporate the concrete buttresses submitted by the sponsor along with a 3-in. tall vertical overlay. Five concrete buttresses in combination with the AGT were evaluated according to MASH TL-3 criteria. The analysis primarily focused on MASH TL-3 impacts on concrete buttresses using a 2270P pickup truck due to its greater propensity for vehicle snag on the upstream face of the concrete buttress compared to the 1100C vehicle. However, simulations of small vehicle impacts were conducted on Buttress 8 to evaluate the interaction between the small car wheel and the three options for wheel snag prevention. The critical impact point for MASH Test 3-21 on the AGT with the pickup truck was identified as 89 in. upstream from the concrete buttress [2] and is depicted in Figure 49.

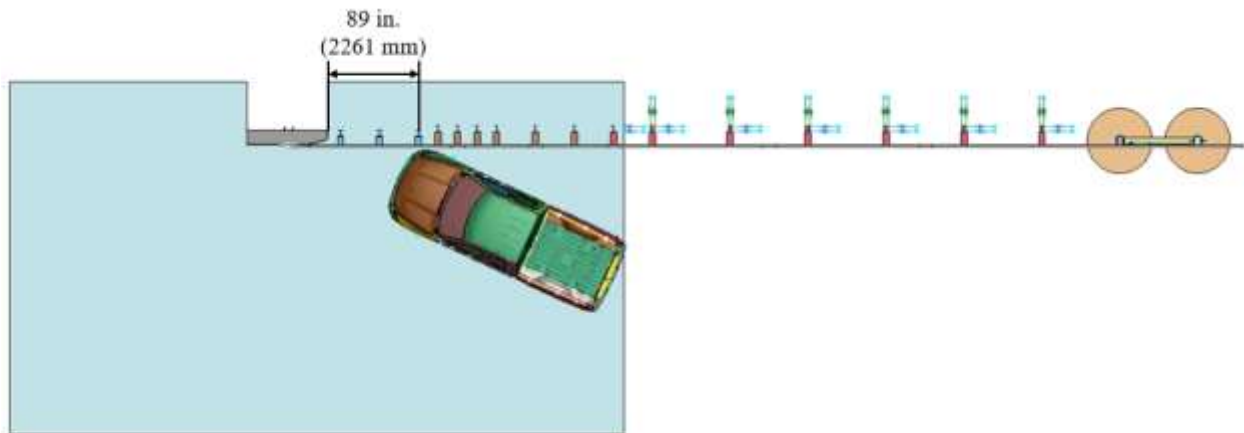


Figure 49. Ram Pickup Truck Impact Point

Previous MASH testing on AGTs has often resulted in the disengagement of the front wheel from the pickup truck. In this study, the effects of front wheel disengagement were analyzed by conducting some simulations with the front wheel remaining attached to the vehicle and others with the front wheel disengaging from the vehicle. Thus, the wheel disengagement behavior was bracketed and the critical cases for the AGT impact could be identified. To model the suspension failure and detachment of the right front wheel, the upper control arm, lower control arm, and steering arm joints, as shown in Figure 50, were separated at a specified time, which was based on when stresses in the suspension components reached a critical failure state.

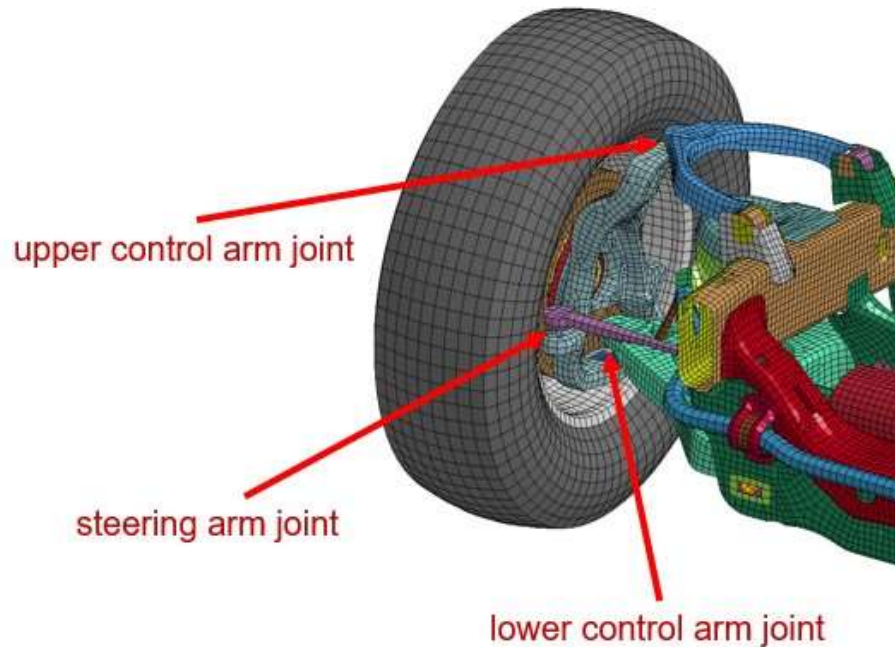
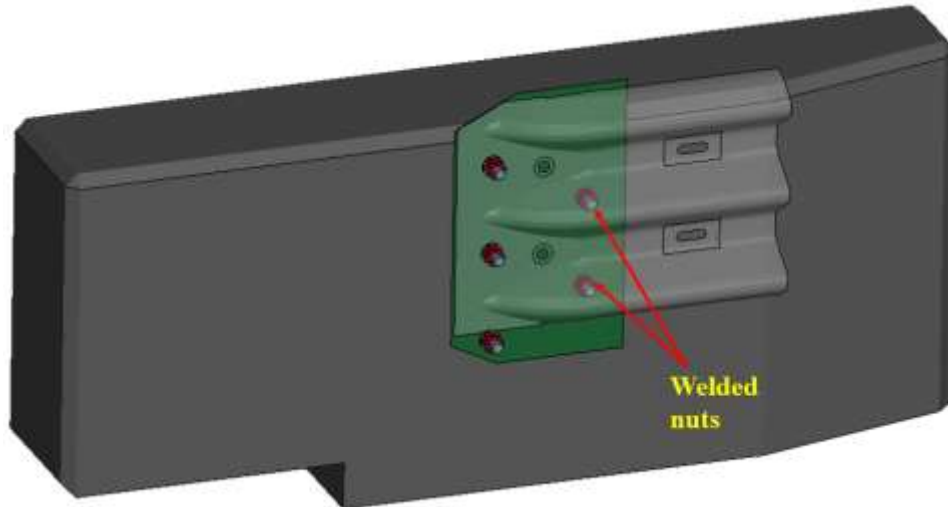
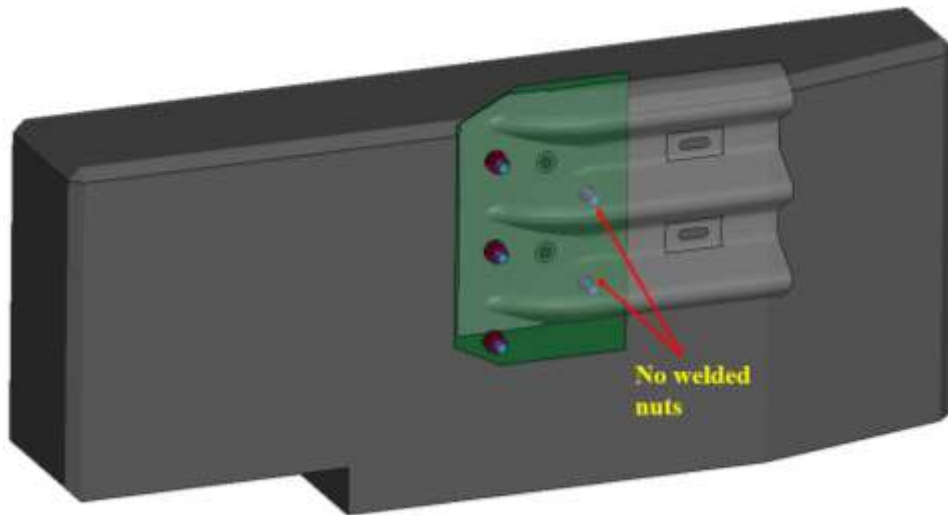


Figure 50. Ram Vehicle Model Right-Front Suspension Joints

Within the connector plate assembly, two nuts were designed to be welded to the $3/16$ -in. thick steel plate underneath the guardrail corrugations. Bolts at these locations were to be inserted from the back side of the concrete buttress and threaded into the nuts. The remaining three bolts could be inserted from the front of the buttress. However, there may be existing buttresses in which the anchor bolts were cast into the buttress and thus cannot be removed and inserted from the back of the buttress. For this situation, the welded nuts below the guardrail corrugations could be excluded, and the cast-in anchor studs would be extended through the $3/16$ -in. plate to provide shear strength for the guardrail attachment. This connection loads the bolts primarily in shear with very little tension. Thus, the three nuts on the front of the connector plate assembly were thought to be enough to hold the anchorage together. Both 5-nut and 3-nut attachment variations were analyzed herein and are shown in Figure 51.



5-Nut Anchorage



3-Nut Anchorage

Figure 51. Design Options for Bolted Connection

Computer simulations were conducted to evaluate the safety performance of the AGT retrofit designs with variations to (1) the buttress, (2) the wheel snag prevention option, (3) the number of nuts used to anchor the AGT, and (4) the front wheel disengagement. Each simulation was labeled with a reference number along with codes that identified each of these variables. The codes consisted of B# for buttress number, CP for retrofit options for wheel snag prevention, 3N/5N for design with 3 nuts or 5 nuts, and WA/WD for Ram pickup truck with right-front wheel remaining attached or disengaging during the impact events. Four options were analyzed to prevent the wheel snag under vehicle impacts: (1) CP represented no modification for vehicle wheel snag prevention; (2) CP+CF represented concrete fill below cantilevered segment of buttress; (3) CP+SA represented a steel assembly installed below the cantilevered segment of the buttress; and (4) CP+CB represented a 6-in. curb placed below the AGT. An example of simulation reference

is defined as B8-CP+SA-3N-WD, which corresponds to a simulation of Buttruss 8 retrofitted with a steel assembly, a 3-nut anchorage, and with right-front wheel disengagement during the simulated crash test.

Performance criteria were evaluated to examine each AGT model's ability to safely contain and redirect the impacting vehicle, including vehicle stability and occupant risk criteria. The vehicle stability was evaluated through the roll, pitch, and yaw of the vehicle during the impact event. MASH criteria recommends that maximum roll and pitch values be less than ± 75 degrees. The occupant risk criteria were investigated through occupant impact velocity (OIV) and occupant ridedown acceleration (ORA) in both longitudinal and lateral directions, which were calculated at the center of gravity of the vehicle model as per MASH recommendations. Post and guardrail deflections were also measured for each simulation to quantify the system deflection and assess the barrier damage. The deflections of post nos. 17 and 18 were used in this study and measured by tracking the displacement of a node at the top of each post. The guardrail deflections were measured from the nodal displacement on the upper corrugation.

The propensity for vehicle wheel snag on the upstream face of the concrete buttruss was evaluated using the lateral overlap for the impacting tire across the upstream face of the buttruss. The lateral tire overlap was measured from the traffic face of the buttruss to the wheel node that extended the farthest laterally across the upstream face of the buttruss, as shown in Figure 52. The measurement was obtained at the final plot state prior to the tire contacting the concrete buttruss. It should be noted that the Ram tire model is developed with elastic-plastic shell elements that model the tire tread and sidewalls and with plastically deformable beam elements that model steel belts and body plies of the tire. Thus, the deformed shapes of the modeled tire are not realistic. However, they can provide a general trend of the tire overlap changes with respect to the buttruss.

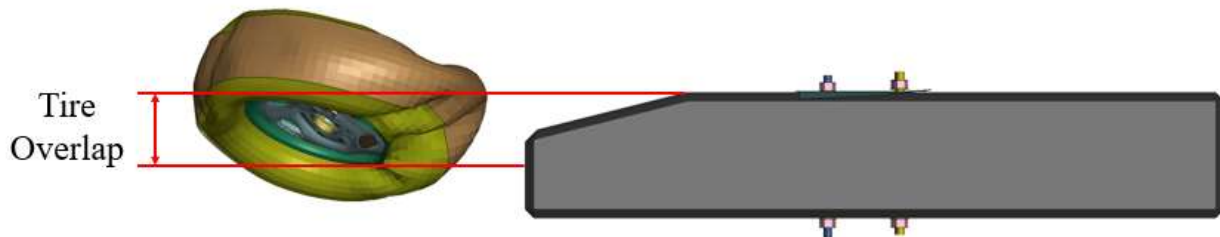


Figure 52. Tire-Buttruss Overlap Measurement

6.2 Buttress 5 Simulation Results

The simulation matrix for the evaluation of the retrofit AGT connection with Buttress 5 is shown in Table 5. Since Buttress 5 did not have a cantilevered segment on its upstream end, none of the wheel snag prevention options were necessary, and only the front wheel behavior and the number of anchorage nuts were varied.

Table 5. Simulations on Retrofit AGT with Buttress 5

Simulation No.	MASH Test No.	Test Vehicle	Impact Conditions		Wheel Behavior	Nuts
			Speed (mph)	Angle (deg.)		
B5-CP-5N-WA	3-21	2270P	62	25	Remained Attached	5
B5-CP-5N-WD	3-21	2270P	62	25	Disengaged	5
B5-CP-3N-WA	3-21	2270P	62	25	Remained Attached	3
B5-CP-3N-WD	3-21	2270P	62	25	Disengaged	3

6.2.1 Vehicle Behavior

Sequential images of the four simulations are shown in Figures 53 through 56, where $t = 0$ ms corresponds to the beginning of the impact event. In the simulations, the Ram pickup truck model impacted the AGT 89 in. upstream from Buttress 5 at a speed of 62 mph and an angle of 25 degrees. The vehicle was contained and smoothly redirected by the AGT installations. The vehicle remained stable throughout the impact events with maximum roll and pitch angular displacements within the MASH limit. The simulation results of the vehicle's behavior were compared with the results of test no. 34AGT-1 [2] and test no. AGTB-2 [1]. Comparison results indicated that the simulated vehicle behavior matched reasonably well with the tested results.

In the simulations, damage to the vehicle was moderate, with the majority of damage on the right-front corner and right side of the vehicle where the impact occurred. The right side of the front bumper was crushed inward and back. Occupant compartment deformations were observed to the right-side front panel and the toe pan where the tire was pushed backward and toward the occupant compartment. However, these deformations were similar to those observed in the physical crash tests and none of the MASH deformation limits were violated.

All maximum angular displacements of the vehicle were below MASH limits, as listed in Table 6. Based on the simulation results, simulation nos. B5-CP-5N-WD and B5-CP-3N-WD, which allowed wheel disengagement, had higher maximum roll and pitch angles than the other two simulations. Wheel disengagement diminished vehicle stability and allowed the vehicle to roll

more. For simulation nos. B5-CP-3N-WD and B5-CP-5N-WD, the maximum angular displacements were similar to those obtained from test no. AGTB-2. Note, test no. 34AGT-1 was conducted on an AGT with a 34-in. mounting height, which limited roll toward the system.

There was minimal difference between the simulations with the AGT anchored with 5 nuts compared to those anchored with only 3 nuts. As expected, the attachment bolts were loaded primarily in shear, so the reduced number of nuts did not negatively affect the system performance. Both 5-nut and 3-nut anchorage configurations provided sufficient strength for the AGT to smoothly capture and redirect the vehicle.

Table 6. Vehicle Angular Displacements Results, Buttress 5

Max. Angular Displacement	Simulation/Test No.						MASH Limits
	B5-CP-5N-WA	B5-CP-5N-WD	B5-CP-3N-WA	B5-CP-3N-WD	34AGT-1	AGTB-2	
Roll (deg.)	23.0	30.6	20.2	30.2	12.0	21.3	±75
Pitch (deg.)	5.5	7.2	5.8	6.2	4.4	6.3	±75
Yaw (deg.)	48.3	42.1	48.6	42.5	38.9	39.6	N/A

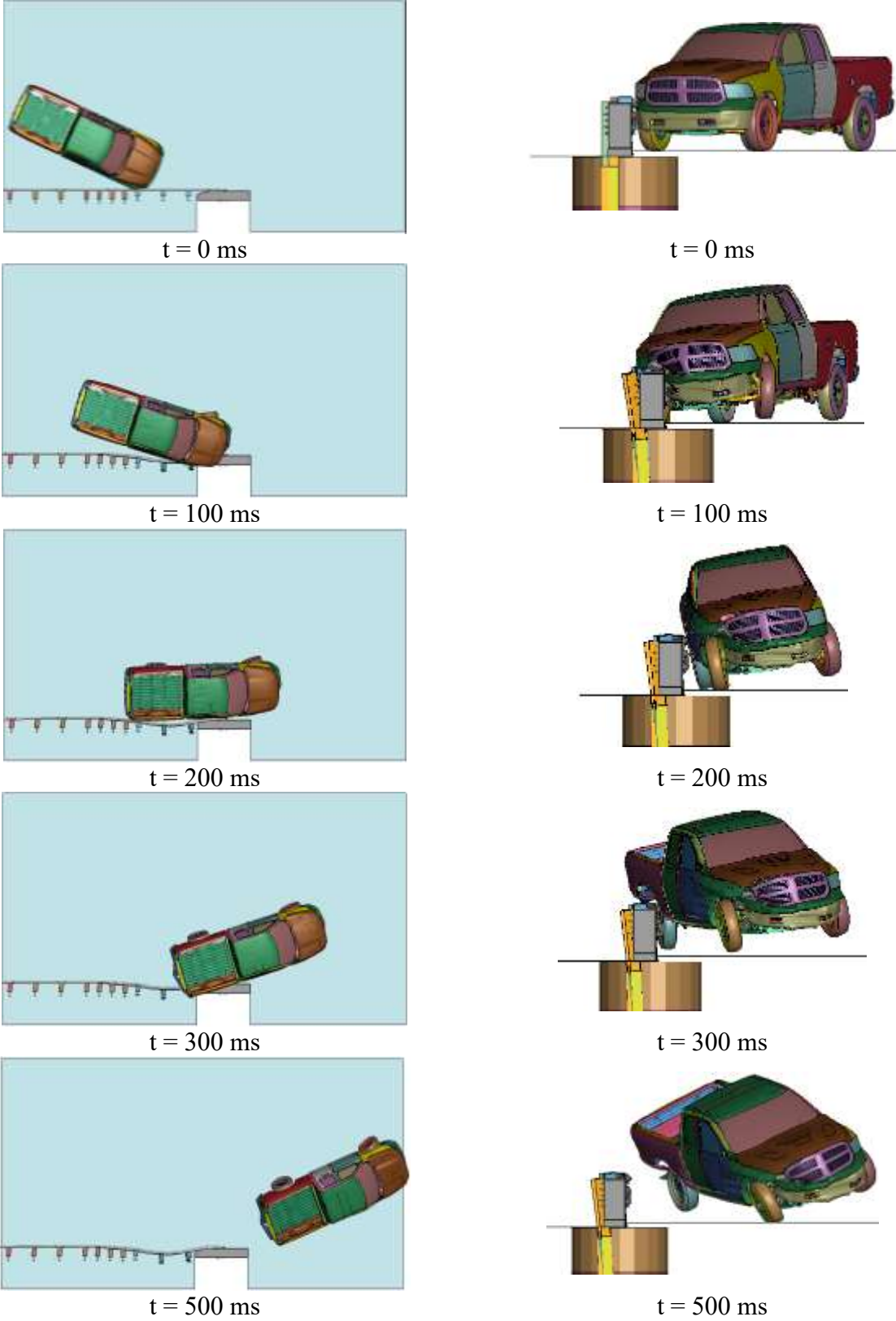


Figure 53. Sequential Images, Simulation No. B5-CP-5N-WA

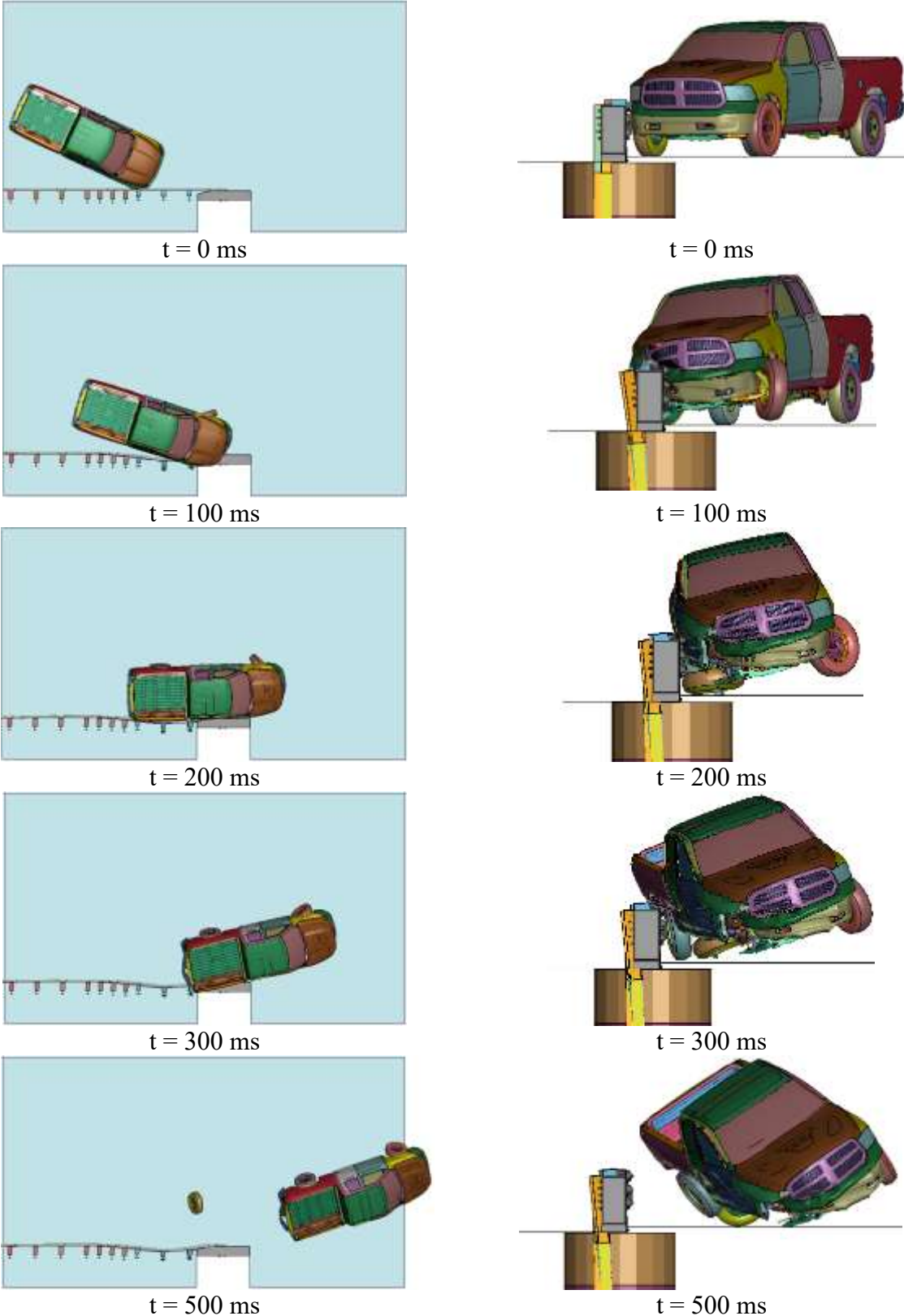


Figure 54. Sequential Images, Simulation No. B5-CP-5N-WD

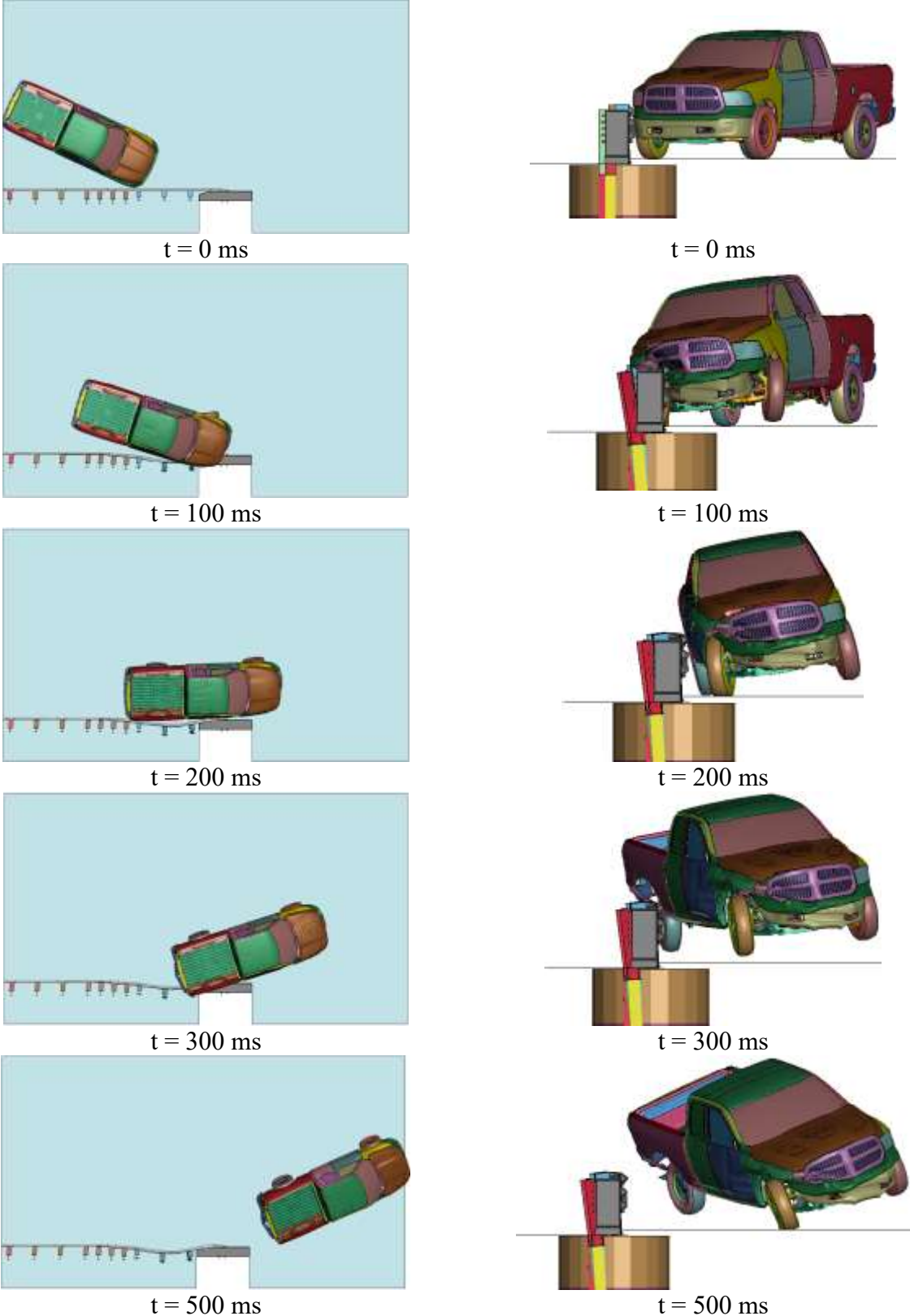


Figure 55. Sequential Images, Simulation No. B5-CP-3N-WA

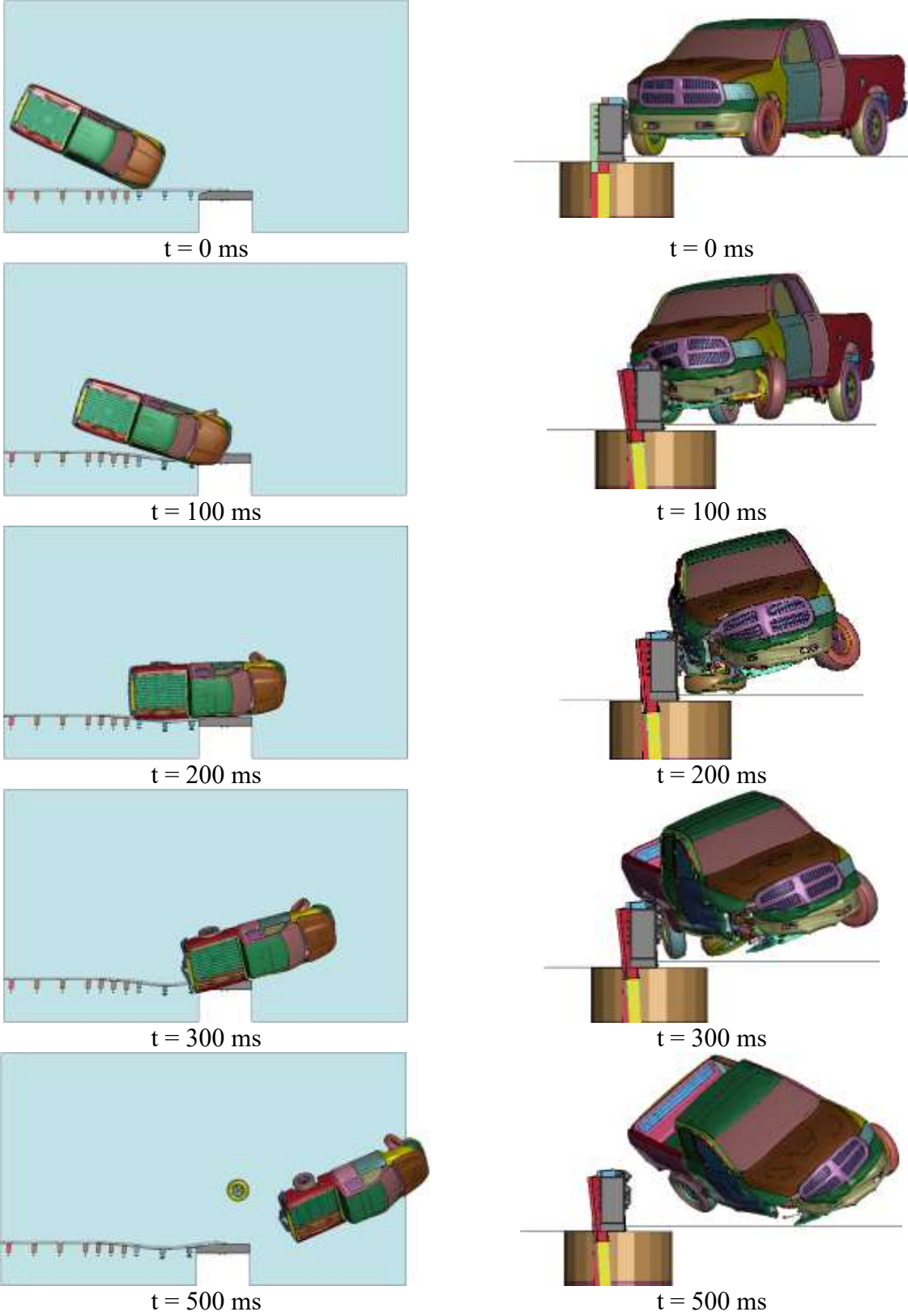


Figure 56. Sequential Images, Simulation No. B5-CP-3N-WD

The lateral overlap of the impacting tires across the upstream face of the concrete buttress are listed in Table 7 and shown in Figure 57. Simulations allowing wheel disengagement resulted in higher lateral overlap between the tire and concrete buttress. The magnitudes of these tire overlaps were less than the 10-in. overlap observed during physical testing of NDOT’s 34-in. tall AGT [2], so they did not raise concerns for excessive snag. Additionally, differences in overlap distances observed in simulations with 5-nut anchorages vs. those with 3-nut anchorages were negligible.

Table 7. Tire-Buttress Overlap, Buttress 5

Simulation No.		Overlap (in.)
Wheel Remained Attached	B5-CP-5N-WA	7.1
	B5-CP-3N-WA	6.8
Wheel Disengaged	B5-CP-5N-WD	8.6
	B5-CP-3N-WD	8.4

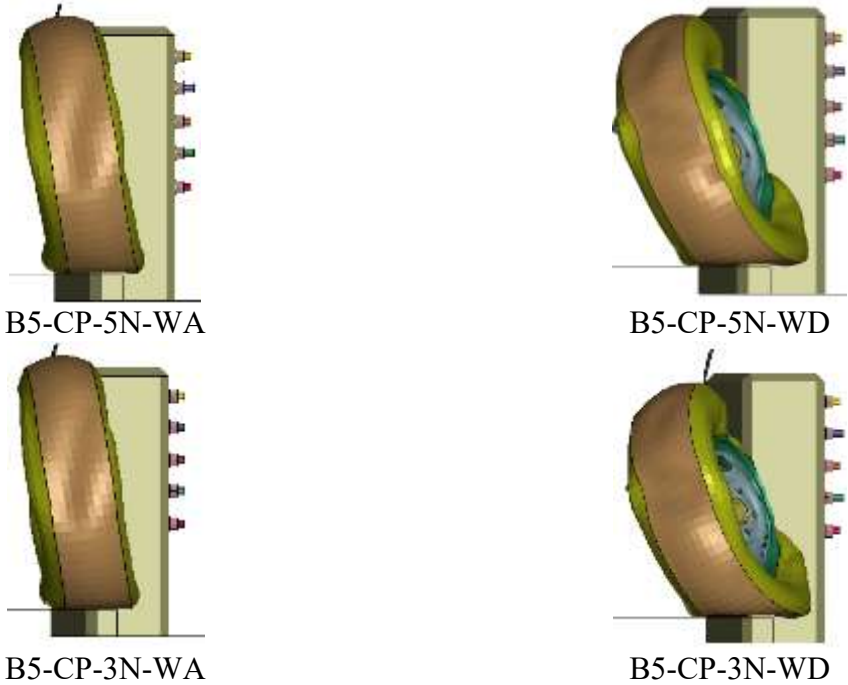


Figure 57. Tire-Buttress Overlap, Buttress 5

6.2.2 Barrier Damage

Barrier damage consisted of rail and post deformations, as shown in Figure 58. These deformations were consistent with those observed in physical crash testing. Maximum dynamic deflections were observed at the mid-span between post nos. 17 and 18 and are presented in Table 8. Deflections were slightly higher for the simulations in which the wheel remained attached to the vehicle, and all configurations showed higher deflections than those measured from the physical tests. However, the test vehicle often obstructs the overhead view of the crash test and prevents the measurement of the true maximum dynamic deflection of the system. The simulated rail deflections were similar to those measured in the validation simulations, so they were not considered to be an issue.

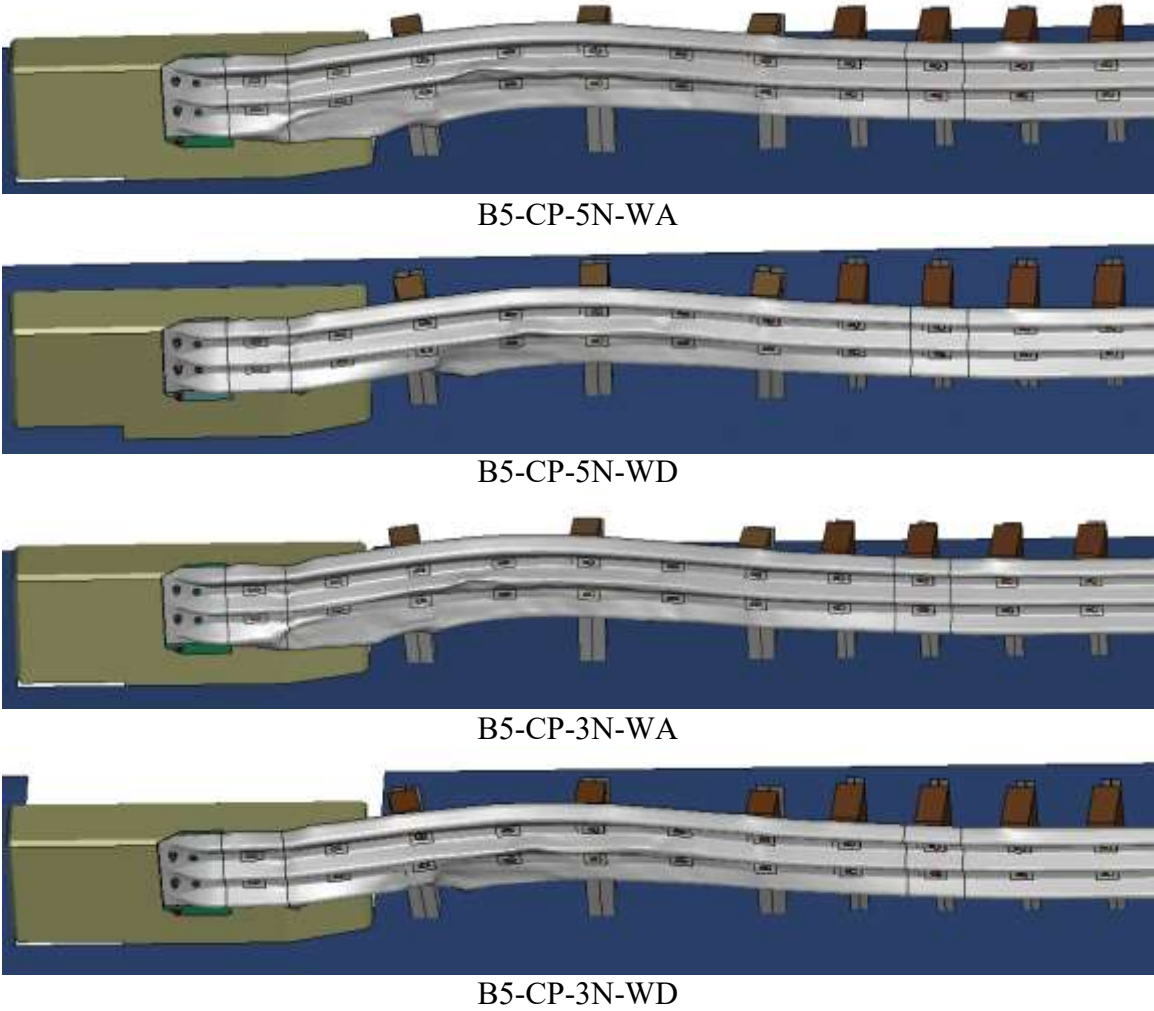


Figure 58. System Damage, Buttrass 5

6.2.3 Occupant Risk

The calculated OIV and ORA values in both the longitudinal and lateral directions are shown Table 8. These occupant risk values compared well with the results of test no. 34AGT-1 and test no. AGTB-2. All simulations resulted in occupant risk values that satisfied MASH limits. Similar to the vehicle behaviors and system deflections, there were negligible differences in occupant risk values between 5-nut and 3-nut anchorages.

Table 8. Summary of OIV, ORA, and Lateral Deflection, Buttruss No. 5

Evaluation Criteria		Simulation/Test No.						MASH Limits
		B5-CP-5N-WA	B5-CP-5N-WD	B5-CP-3N-WA	B5-CP-3N-WD	34AGT-1	AGTB-2	
OIV (ft/s)	Long.	-22.9	-23.5	-22.6	-23.9	-20.2	-20.28	±40
	Lat.	24.9	24.4	24.7	24.8	25.9	24.6	±40
ORA (g's)	Long.	-16.0	-14.4	-17.0	-13.4	-10.8	-7.06	±20.49
	Lat.	11.1	15.2	12.2	13.6	8.9	10.4	±20.49
Max. post deflection (in.)	Post no. 17	10.4	9.1	10.3	9.2	N/A	N/A	N/A
	Post no. 18	9.7	8.4	9.7	8.6	N/A	N/A	N/A
Max. dynamic deflection (in.)		11.2	10.2	11.2	10.2	7.8	5.35	N/A

6.2.4 Damage to Connector Plate

Effective plastic strain distributions in the $3/16$ -in. thick connector plate during the simulated crashes are shown in Figure 59. Blue areas represent material that remains within its elastic limits while green areas have exceeded their yield strength and have plastically deformed. The majority of the plastic deformation occurred along the top of the plate where vehicle contact bent the plate backward along the top edge of the buttruss. Minor yielding was also observed around the downstream three bolt holes, but the plastic deformation remained minimal. Thus, the new connector plate assembly demonstrated the ability to attach the AGT to the existing buttruss, adequately transfer loads to the anchor bolts, and resist significant damage during high magnitude loading.

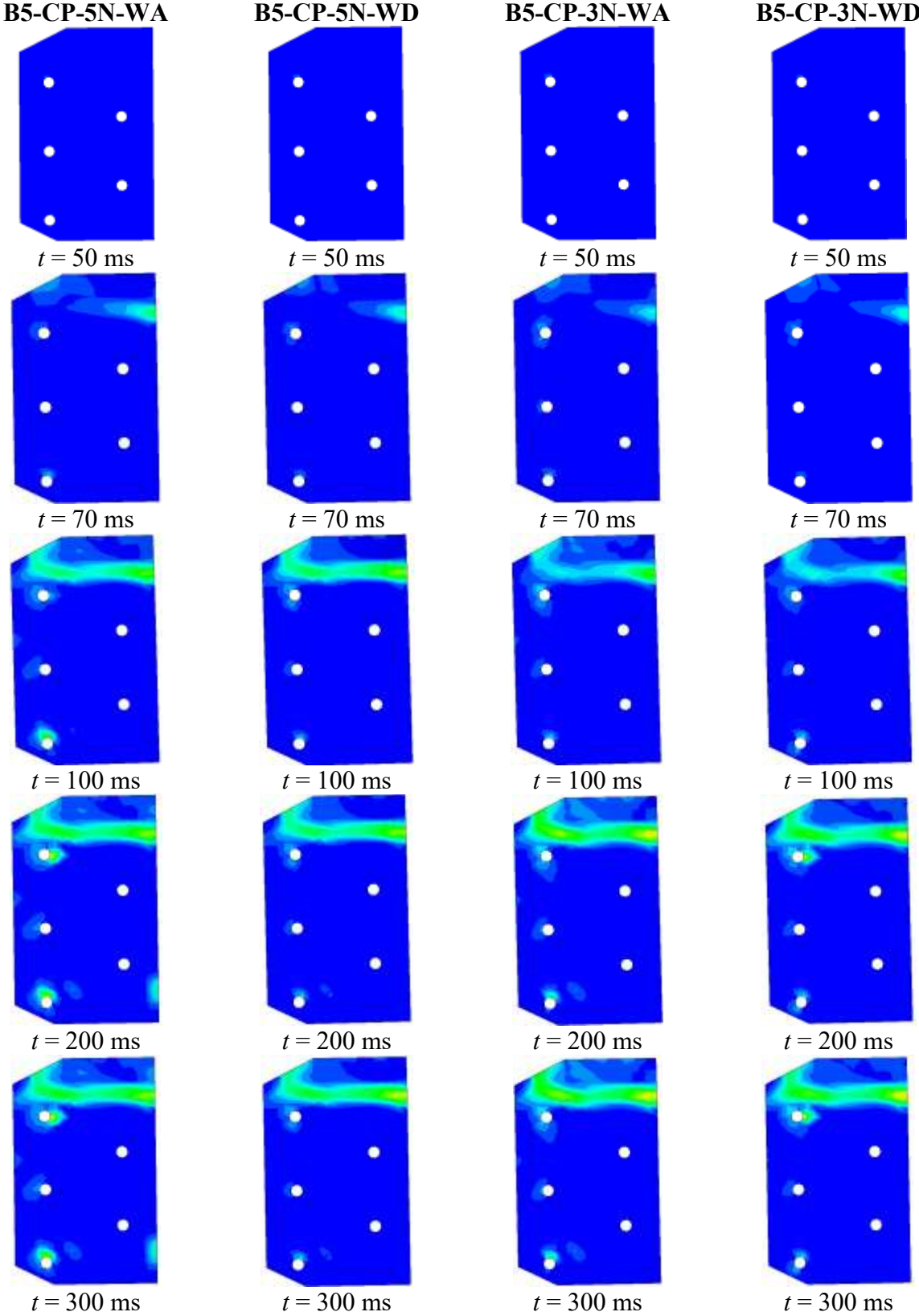


Figure 59. Effective Plastic Strain Distribution in Connector Plate, Buttress 5

6.3 Buttress 6 Simulation Results

The simulation matrix for the evaluation of the retrofit AGT connection with Buttress 6 is shown in Table 9. Since Buttress 6 did not have a cantilevered segment on its upstream end, none of the wheel snag prevention options were necessary, and only the front wheel behavior and the number of anchorage nuts were varied.

Table 9. Simulations on Retrofit AGT with Buttress 6

Simulation No.	MASH Test No.	Test Vehicle	Impact Conditions		Wheel Behavior	Nuts
			Speed (mph)	Angle (deg.)		
B6-CP-5N-WA	3-21	2270P	62	25	Remained Attached	5
B6-CP-5N-WD	3-21	2270P	62	25	Disengaged	5
B6-CP-3N-WA	3-21	2270P	62	25	Remained Attached	3
B6-CP-3N-WD	3-21	2270P	62	25	Disengaged	3

6.3.1 Vehicle Behavior

Sequential images of the four simulations are shown in Figures 60 through 63. In the simulations, the 2270P pickup model impacted the AGT 89 in. upstream from Buttress 6 at a speed of 62 mph and an angle of 25 degrees. The vehicle was contained and smoothly redirected by the AGT installations. The vehicle remained stable throughout the impact events.

Damage to the vehicles was moderate, with the majority of the damage concentrated on the right-front corner and right side of the vehicle where the impact occurred. Occupant compartment deformations were observed to the right-side front panel and the toe pan where the wheel was pushed backward and toward the occupant compartment. However, these deformations were similar to those observed in simulations with Buttress 5 and those of the physical crash tests, and none of the MASH deformation limits were violated.

All maximum angular displacements of the vehicle were below MASH limits, as listed in Table 10. Simulations incorporating wheel disengagement resulted in higher maximum roll and pitch angles as the disengagement of the wheel diminished vehicle stability. These maximum roll and pitch values were very similar to those observed for the simulations on Buttress 5 and were not a cause for concern. Additionally, the 5-nut and 3-nut anchorage configurations resulted in similar results. The difference between these anchorage configurations continued to be negligible.

Table 10. Vehicle Angular Displacements Results, Buttress 6

Simulation No.	Max. Angular Displacement (Deg.)		
	Roll	Pitch	Yaw
B6-CP-5N-WA	20.7	4.9	50.0
B6-CP-5N-WD	29.5	7.7	42.1
B6-CP-3N-WA	17.1	7.3	48.5
B6-CP-3N-WD	36.2	8.1	49.3
MASH Limits	±75	±75	N/A

N/A – Not applicable.

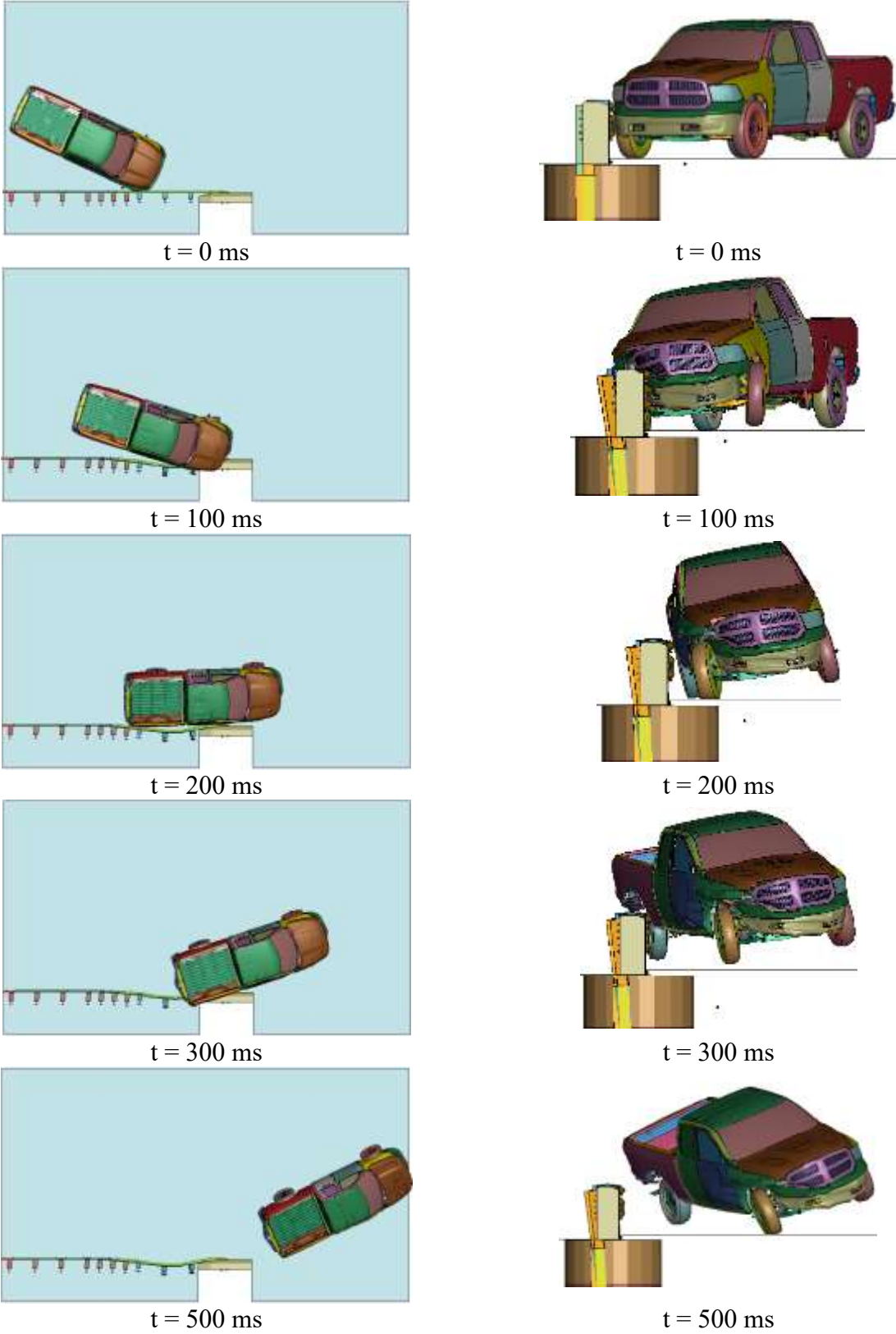


Figure 60. Sequential Images, Simulation No. B6-CP-5N-WA

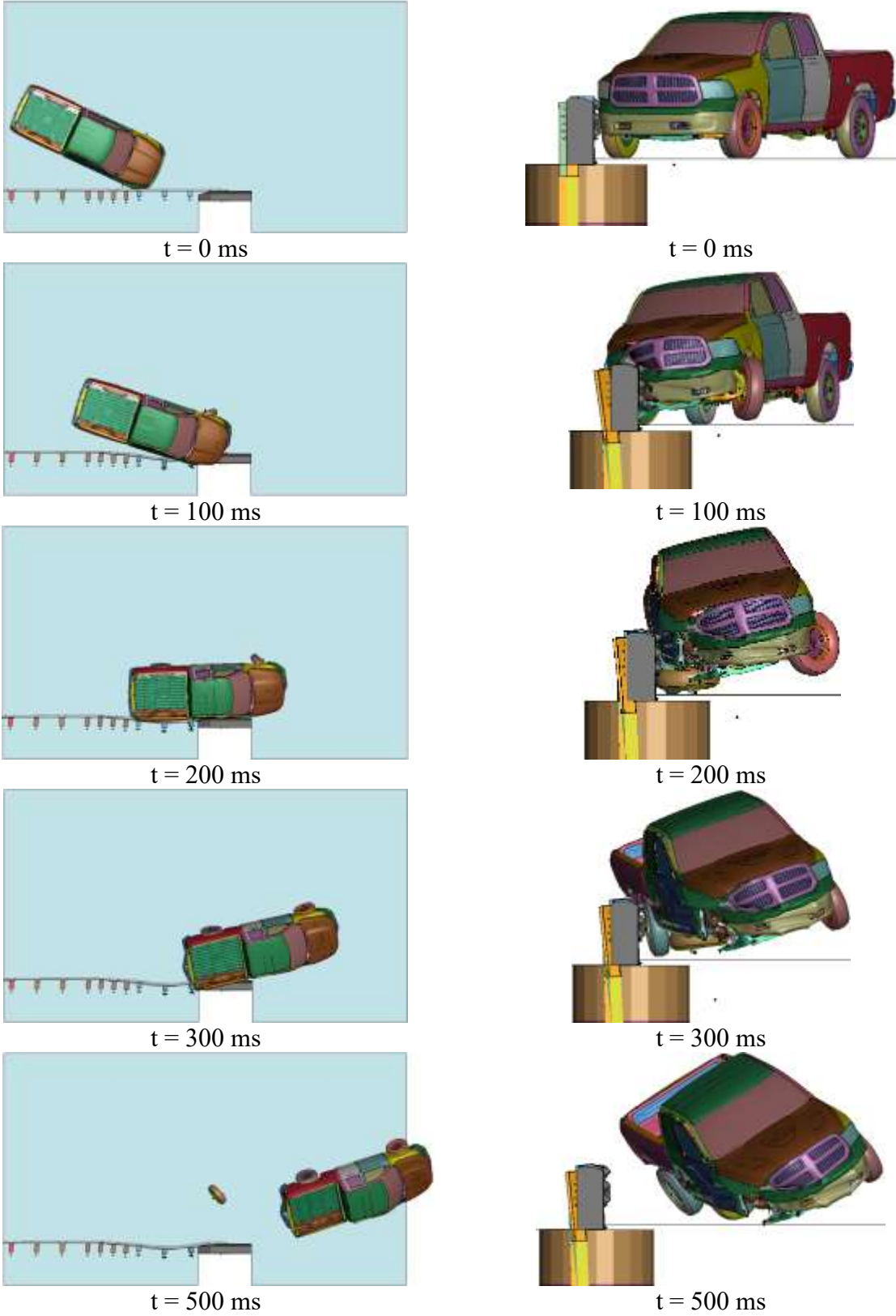
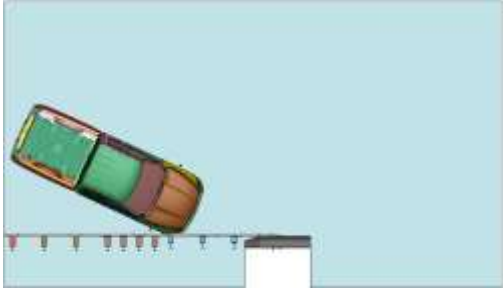
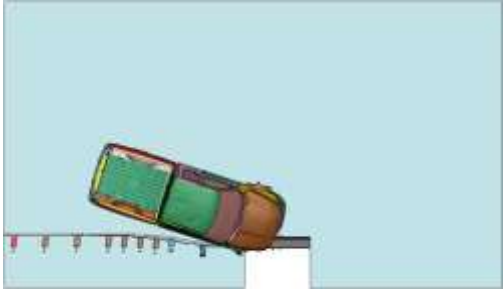


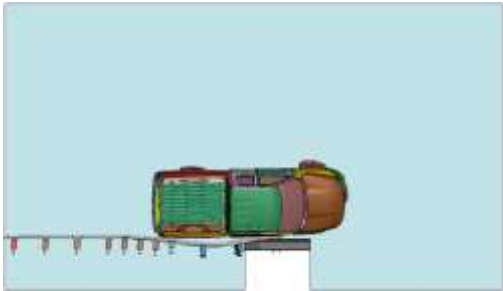
Figure 61. Sequential Images, Simulation No. B6-CP-5N-WD



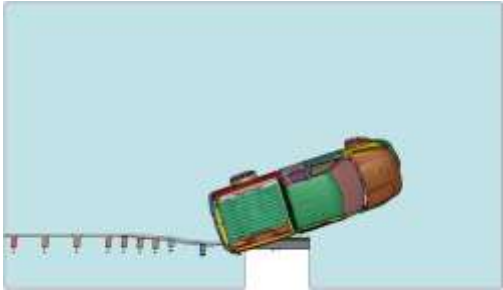
t = 0 ms



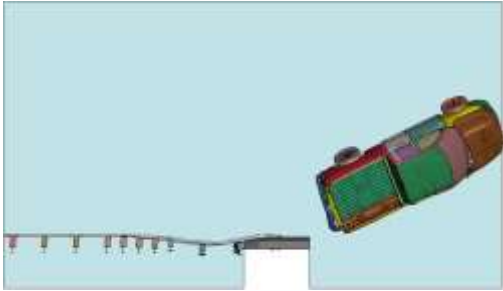
t = 100 ms



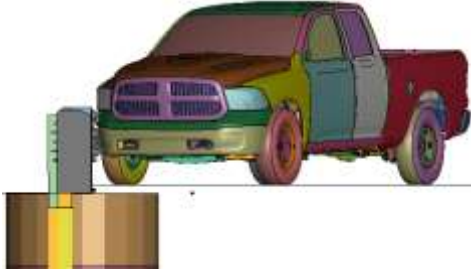
t = 200 ms



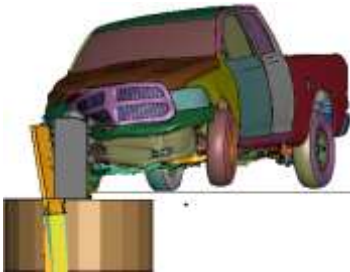
t = 300 ms



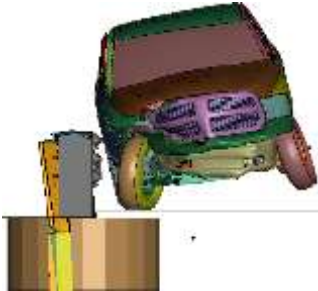
t = 500 ms



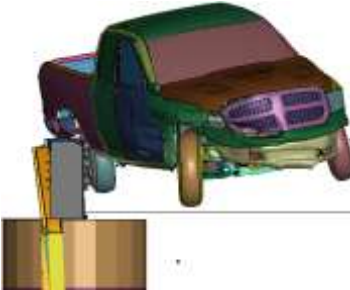
t = 0 ms



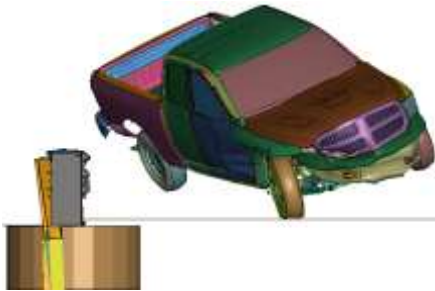
t = 100 ms



t = 200 ms



t = 300 ms



t = 500 ms

Figure 62. Sequential Images, Simulation No. B6-CP-3N-WA

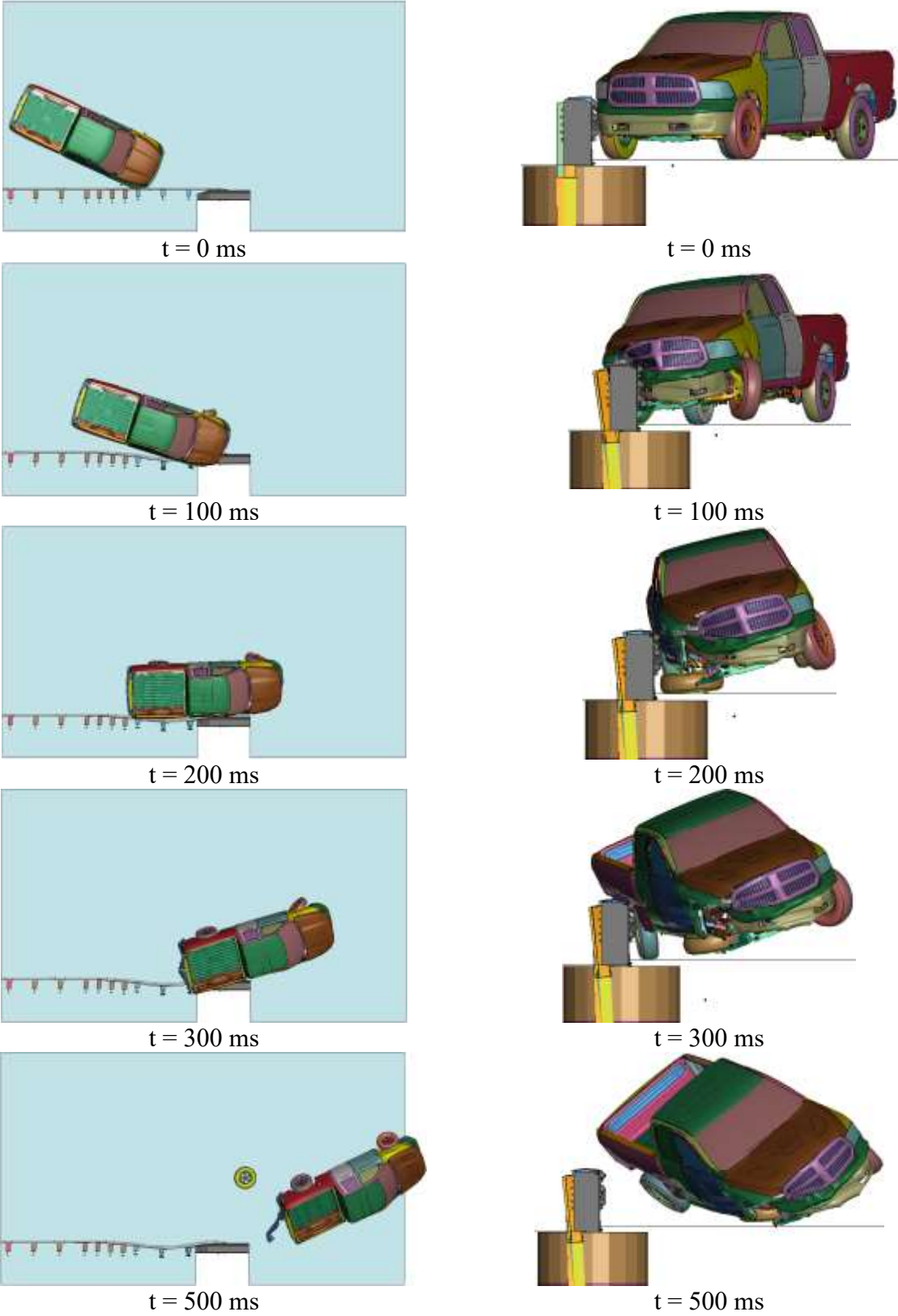


Figure 63. Sequential Images, Simulation No. B6-CP-3N-WD

The lateral overlap of the impacting tires across the upstream face of the concrete buttress are listed in Table 11 and shown in Figure 64. Simulations allowing wheel disengagement resulted in higher lateral overlap between the tire and concrete buttress compared to the simulations where the wheel remained attached. Additionally, differences in overlap distances observed in simulations with 5-nut anchorages vs. those with 3-nut anchorages were negligible. These results were very similar to those from simulations with Buttress 5.

Table 11. Tire-Buttress Overlap, Buttress 6

Simulation No.		Overlap (in.)
Wheel Remained Attached	B6-CP-5N-WA	7.0
	B6-CP-3N-WA	6.9
Wheel Disengaged	B6-CP-5N-WD	8.5
	B6-CP-3N-WD	8.4

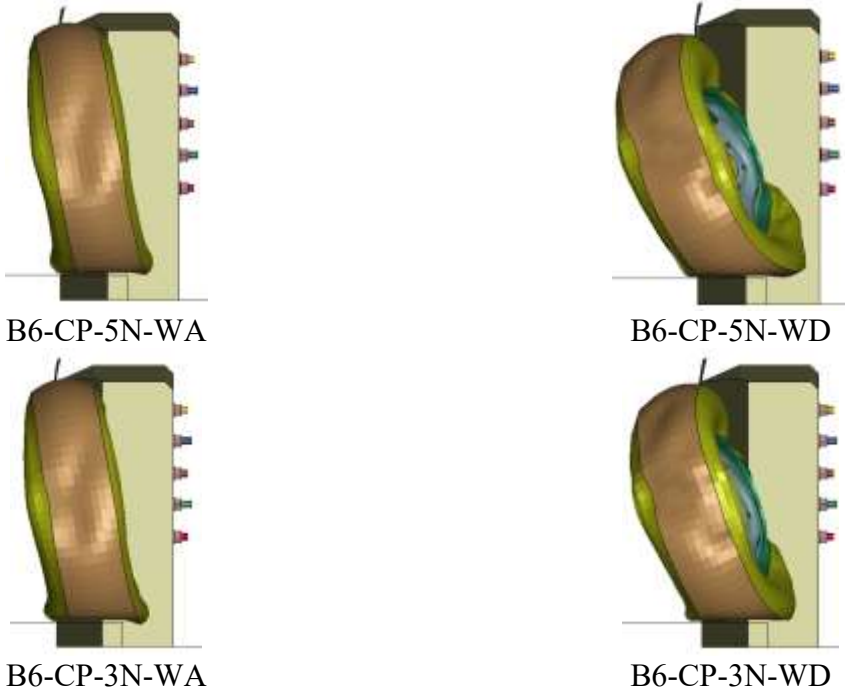
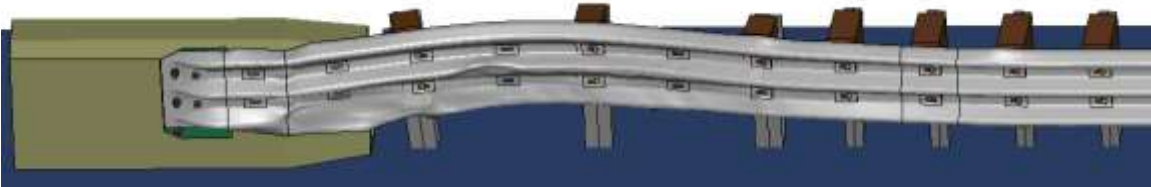


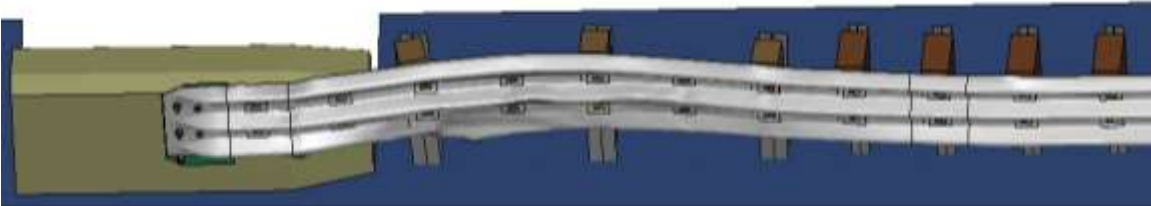
Figure 64. Tire-Buttress Overlap, Buttress 6

6.3.2 Barrier Damage

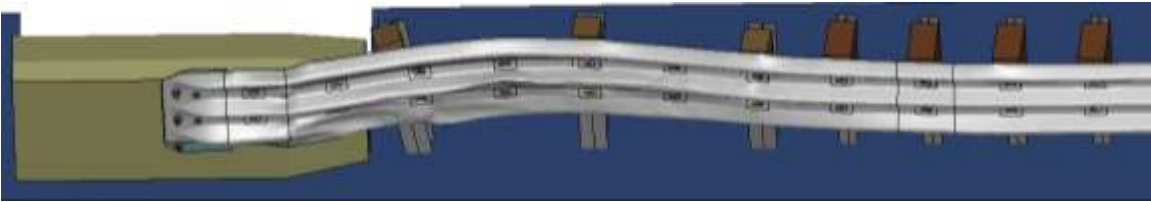
Barrier damage consisted of rail and post deformations, as shown in Figure 65. These deformations were consistent with those observed in physical crash testing and those observed in the simulations with Buttress 5. Maximum dynamic deflections were observed at the mid-span between post nos. 17 and 18 and are presented in Table 12. Deflections were slightly higher for the simulations in which the wheel remained attached to the vehicle, as observed previously. The simulated rail deflections were similar to those measured in the validation simulations, so they were not considered to be an issue.



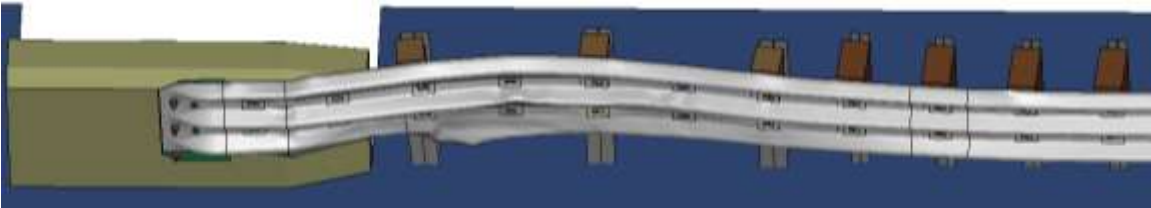
B6-CP-5N-WA



B6-CP-5N-WD



B6-CP-3N-WA



B6-CP-3N-WD

Figure 65. System Damage, Buttress 6

6.3.3 Occupant Risk

The calculated OIVs and ORAs in both the longitudinal and lateral directions are shown in Table 12. These occupant risk values compared well with the results from previous physical testing and the simulation results with Buttress 5. All simulations resulted in occupant risk values that satisfied MASH limits. Similar to the vehicle behaviors and system deflections, there were negligible differences in occupant risk values between the 5-nut and 3-nut anchorages.

Table 12. Summary of OIV, ORA, and Lateral Deflection, Buttress 6

Evaluation Criteria		Simulation				MASH Limits
		B6-CP-5N-WA	B6-CP-5N-WD	B6-CP-3N-WA	B6-CP-3N-WD	
OIV (ft/s)	Longitudinal	-23.3	-23.2	-24.3	-23.1	±40
	Lateral	24.6	24.5	23.9	24.0	±40
ORA (g's)	Longitudinal	-16.2	-14.9	-18.9	-16.1	±20.49
	Lateral	11.9	14.8	16.9	13.7	±20.49
Max. post deflection (in.)	Post no. 17	10.4	9.1	10.2	9.2	N/A
	Post no. 18	9.5	8.3	9.3	8.5	N/A
Max. dynamic deflection (in.)		11.2	10.1	11.2	10.4	N/A

6.4 Buttress 8 Simulation Results

The simulation matrix for the evaluation of the retrofit AGT connections with Buttress 8 is shown in Table 13. Buttress 8 contained a cantilevered segment on its upstream end that exposed the buttress to wheel snag below the guardrail. Accordingly, simulations were conducted with each of the three options to prevent wheel snag to evaluate their effectiveness. Baseline simulations were also conducted with the AGT attached to Buttress 8 without any wheel snag retrofits to understand the severity of the wheel snag risk. Wheel behavior was again varied between the front wheel remaining attached and the wheel disengaging.

Simulations of the AGT attached to Buttresses 5 and 6 showed little to no differences between the 5-nut and 3-nut anchorage configurations. Subsequently, only the 3-nut anchorage configuration was conducted on these simulations with Buttress 8, and it was assumed the 5-nut configuration would perform similarly.

Table 13. Simulations on Retrofit AGT with Buttress 8

Simulation No.	MASH Test No.	Impact Conditions		Wheel Behavior	Anchorage Nuts	Wheel Snag Retrofit Option
		Speed (mph)	Angle (deg.)			
B8-CP-3N-WA	3-21	62	25	Remained Attached	3	N/A
B8-CP-3N-WD	3-21	62	25	Disengaged	3	
B8-CP+CF-3N-WA	3-21	62	25	Remained Attached	3	Concrete fill
B8-CP+CF-3N-WD	3-21	62	25	Disengaged	3	
B8-CP+SA-3N-WA	3-21	62	25	Remained Attached	3	Steel Assembly
B8-CP+SA-3N-WD	3-21	62	25	Disengaged	3	
B8-CP+CB-3N-WA	3-21	62	25	Remained Attached	3	Curb
B8-CP+CB-3N-WD	3-21	62	25	Disengaged	3	

6.4.1 Vehicle Behavior

Sequential images of the eight simulations are shown in Figures 66 through 73. In these simulations, the 2270P pickup model impacted the AGT 89 in. upstream from Buttress 8 at a speed of 62 mph and an angle of 25 degrees. The vehicle was contained and smoothly redirected by the AGT installations. The vehicle remained stable throughout the impact events.

All maximum angular displacements of the vehicle were below MASH limits, as listed in Table 14. Simulations allowing wheel disengagement from the vehicle continued to show higher roll and pitch values, as the loss of the wheel reduced the ability of the vehicle to right itself. The angular displacements were similar in magnitude to those observed in the simulations with Buttresses 5 and 6.

Damage to the vehicle models was concentrated on the right-front corner and right side of the vehicle where the impact occurred. The right side of the front bumpers were typically crushed inward and back. Occupant compartment crushing was observed to the right-side front panel and the toe pan. The magnitude of the deformations tended to be higher for the simulations allowing wheel disengagement, though none violated MASH limits. Additionally, higher deformations were observed in the baseline simulations without a wheel snag retrofit applied to the system. Thus, utilizing the wheel snag retrofits appeared to reduce the amount damage caused by wheel snag.

Table 14. Vehicle Angular Displacements Results, Buttress 8

Simulation No.	Maximum Angular Displacements (Deg.)		
	Roll	Pitch	Yaw
B8-CP-3N-WA	21.9	4.4	49.5
B8-CP-3N-WD	31.5	8.0	45.3
B8-CP+CF-3N-WA	19.2	5.6	48.9
B8-CP+CF-3N-WD	30.3	6.9	44.2
B8-CP+SA-3N-WA	20.4	5.7	50.9
B8-CP+SA-3N-WD	27.8	6.9	39.7
B8-CP+CB-3N-WA	25.1	5.0	48.3
B8-CP+CB-3N-WD	38.1	8.3	56.2
MASH Limits	±75	±75	N/A

N/A – Not applicable.

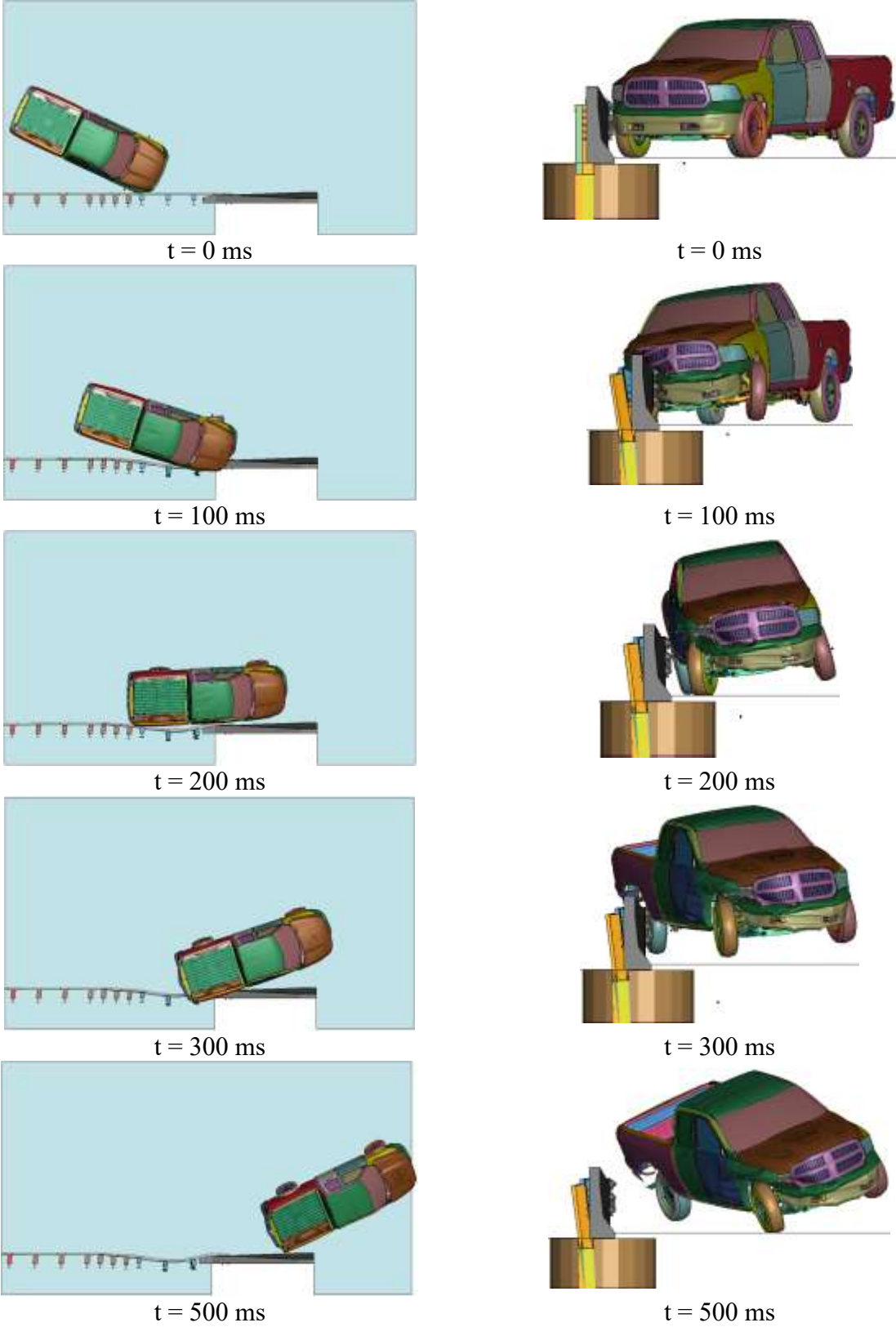
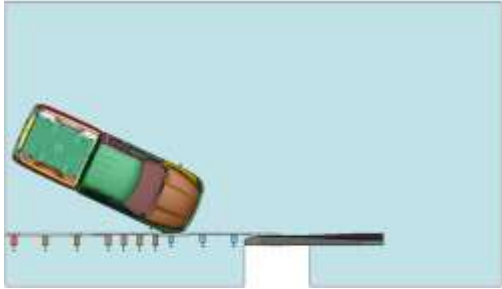
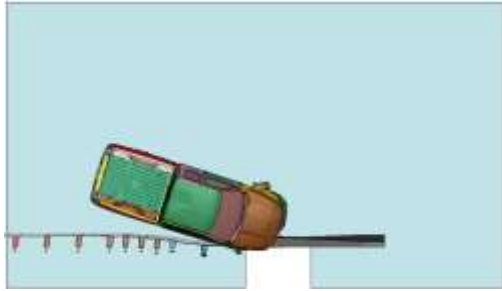


Figure 66. Sequential Images, Simulation No. B8-CP-3N-WA



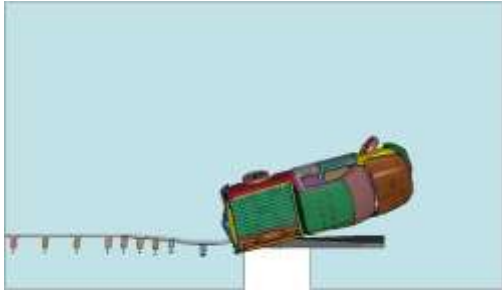
t = 0 ms



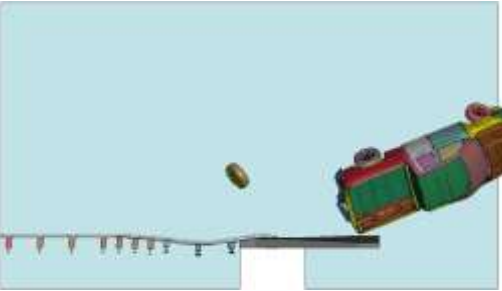
t = 100 ms



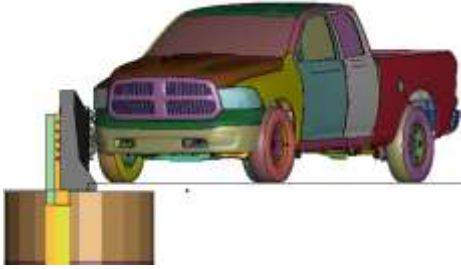
t = 200 ms



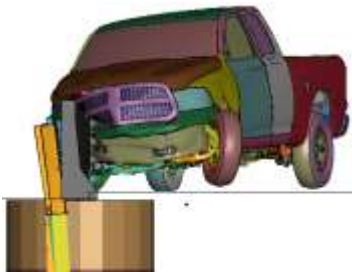
t = 300 ms



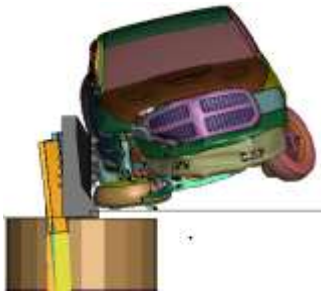
t = 500 ms



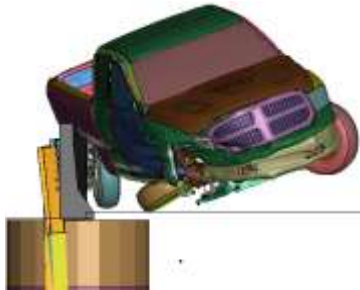
t = 0 ms



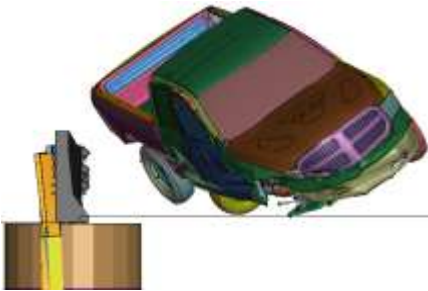
t = 100 ms



t = 200 ms



t = 300 ms



t = 500 ms

Figure 67. Sequential Images, Simulation No. B8-CP-3N-WD

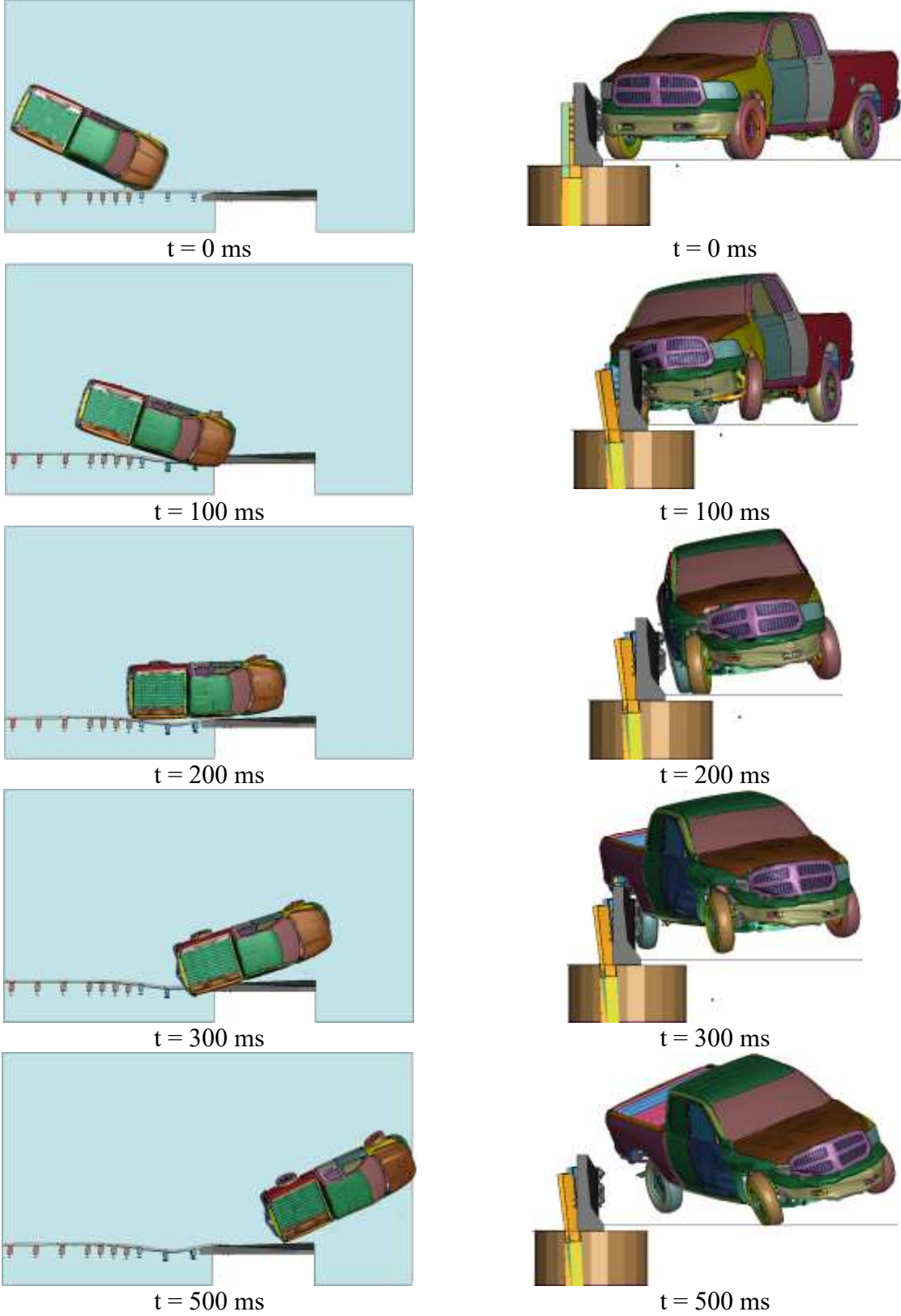


Figure 68. Sequential Images, Simulation No. B8-CP+CF-3N-WA

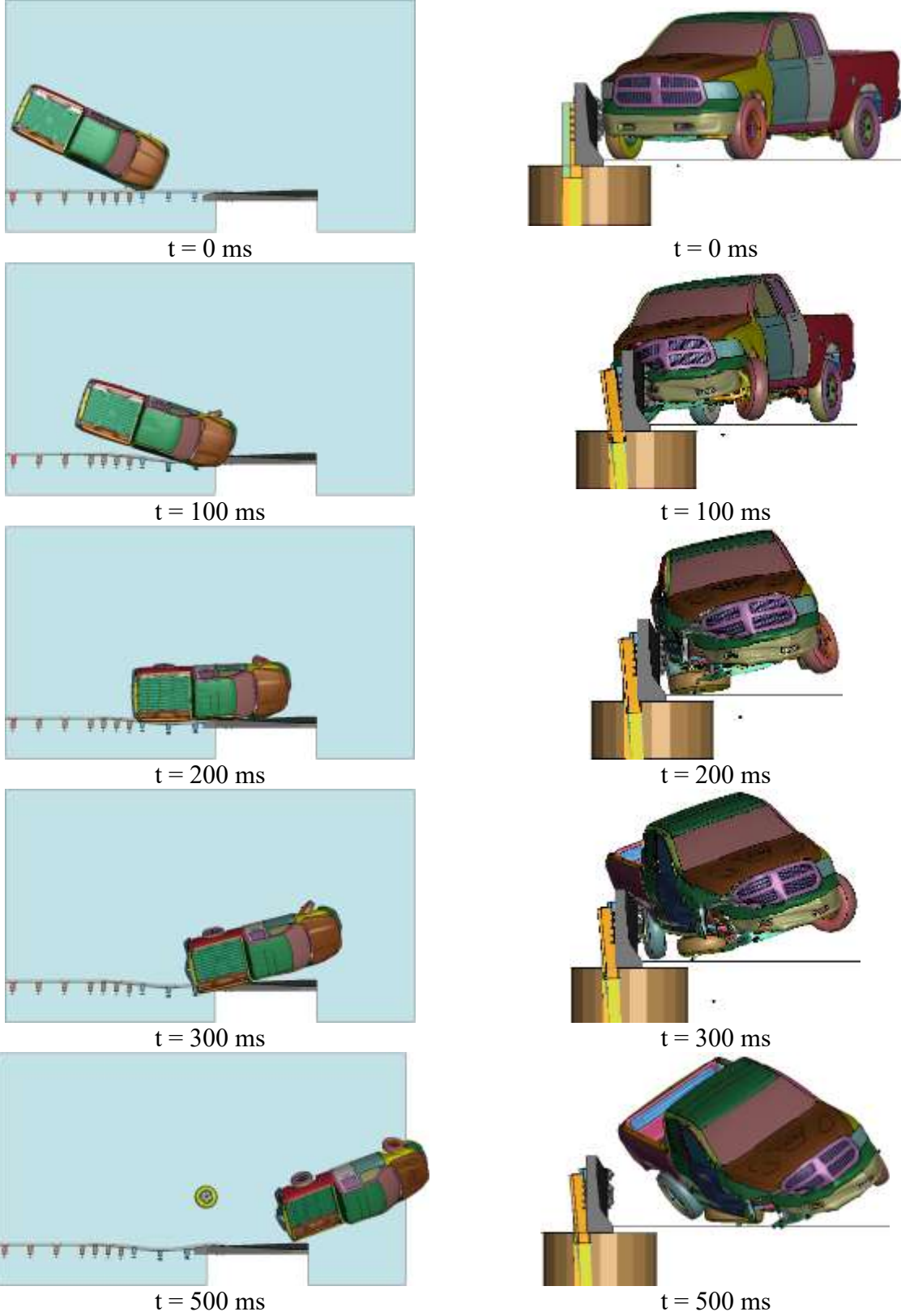


Figure 69. Sequential Images, Simulation No. B8-CP+CF-3N-WD

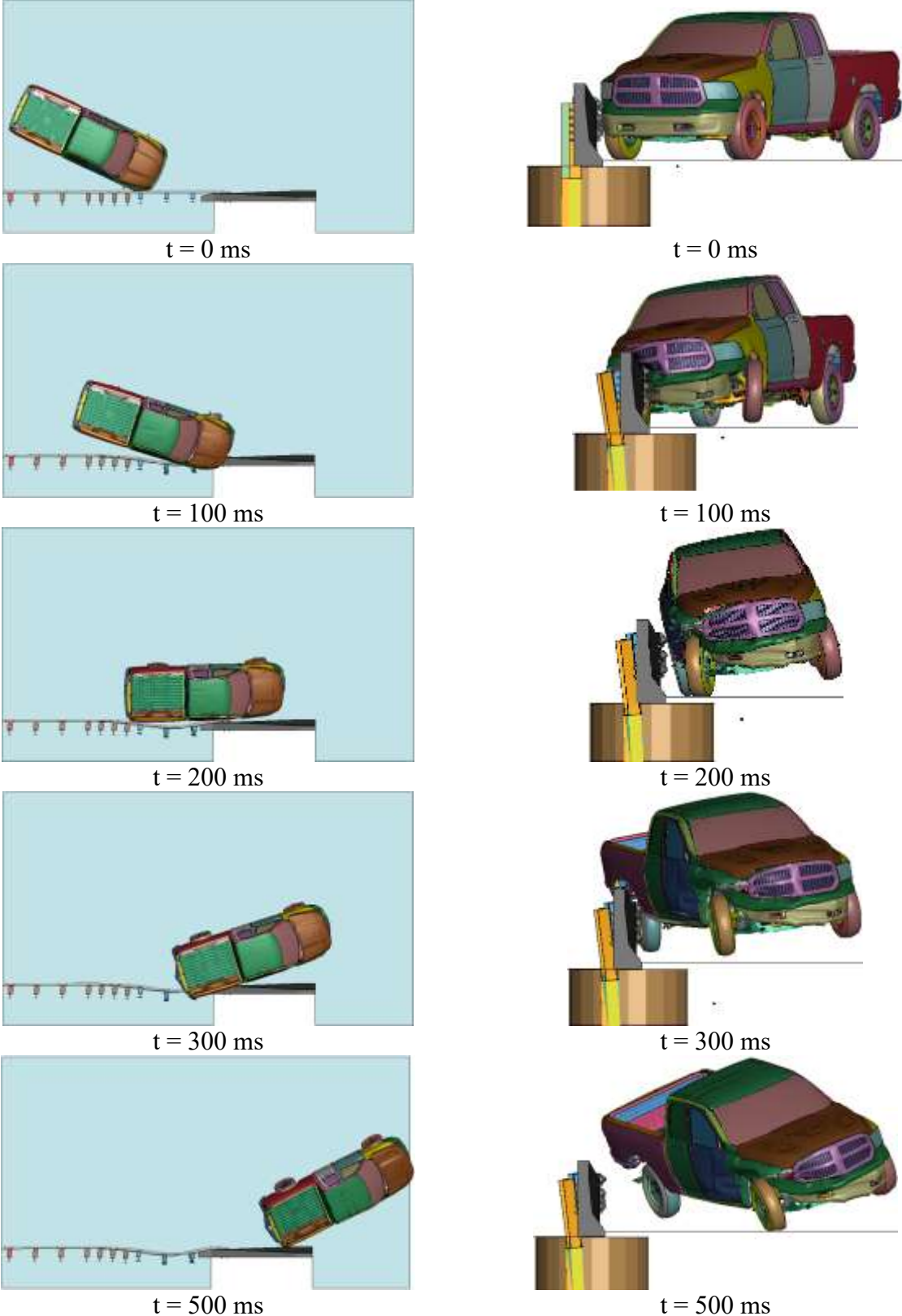


Figure 70. Sequential Images, Simulation No. B8-CP+SA-3N-WA

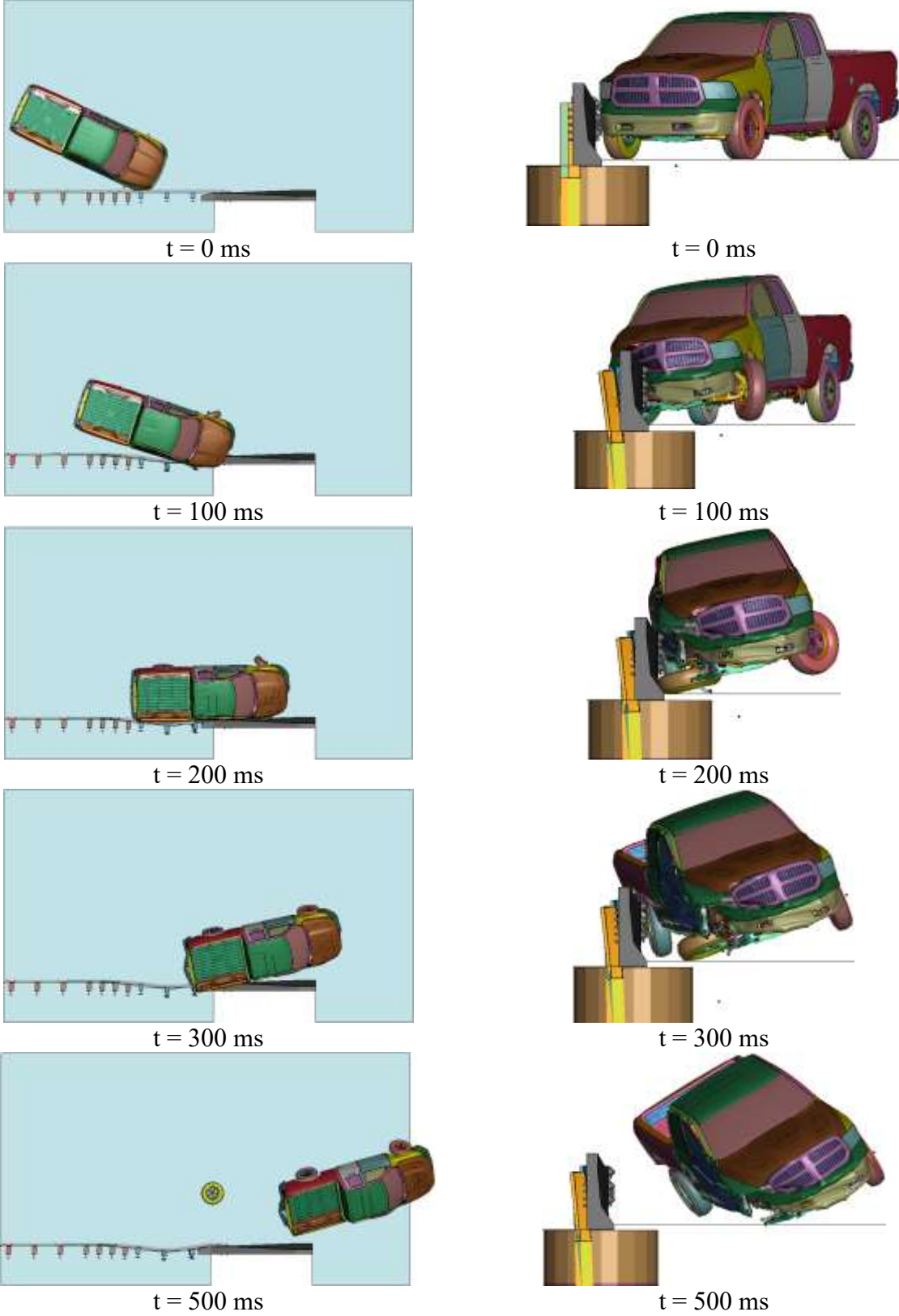


Figure 71. Sequential Images, Simulation No. B8-CP+SA-3N-WD

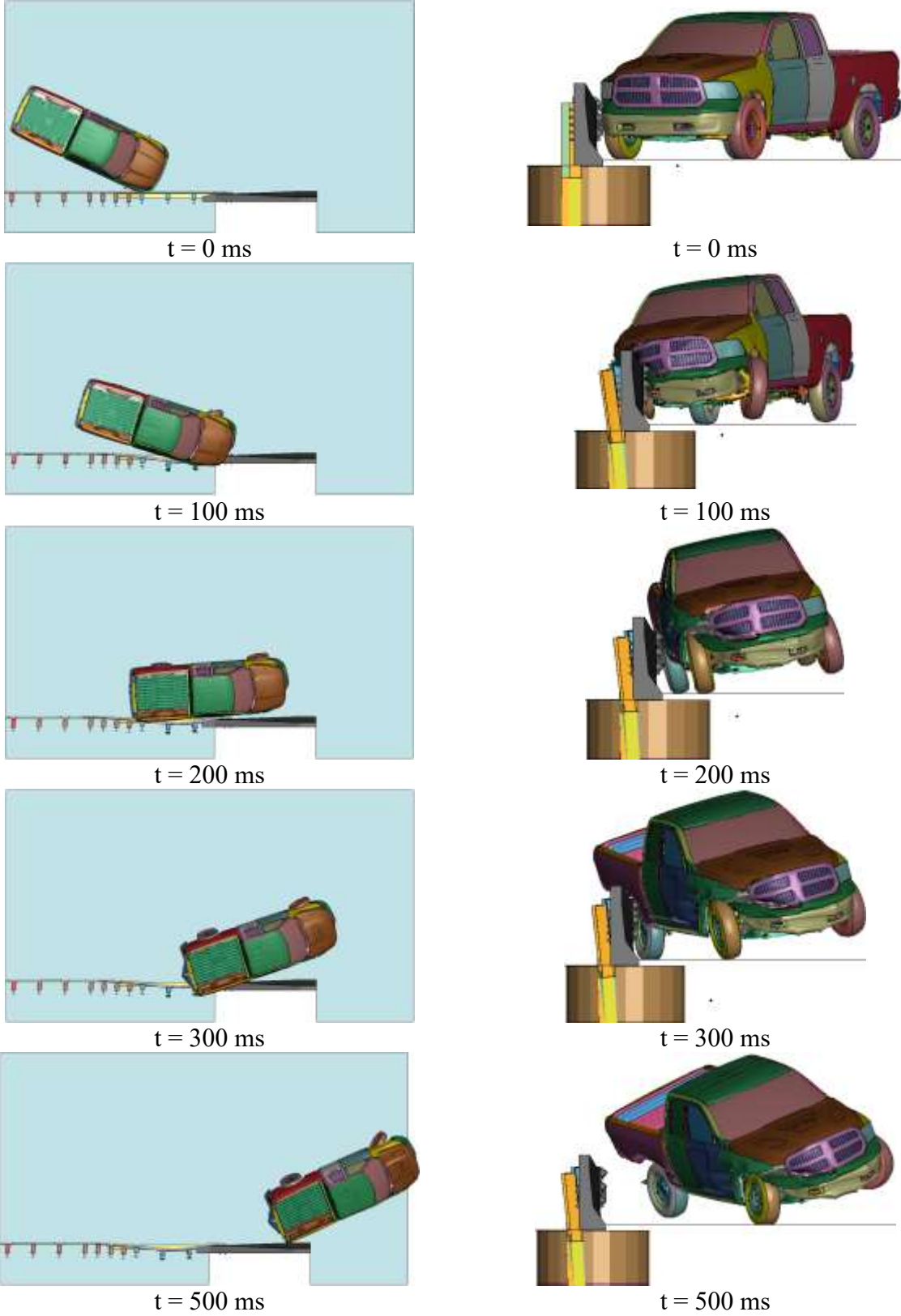


Figure 72. Sequential Images, Simulation No. B8-CP+CB-3N-WA

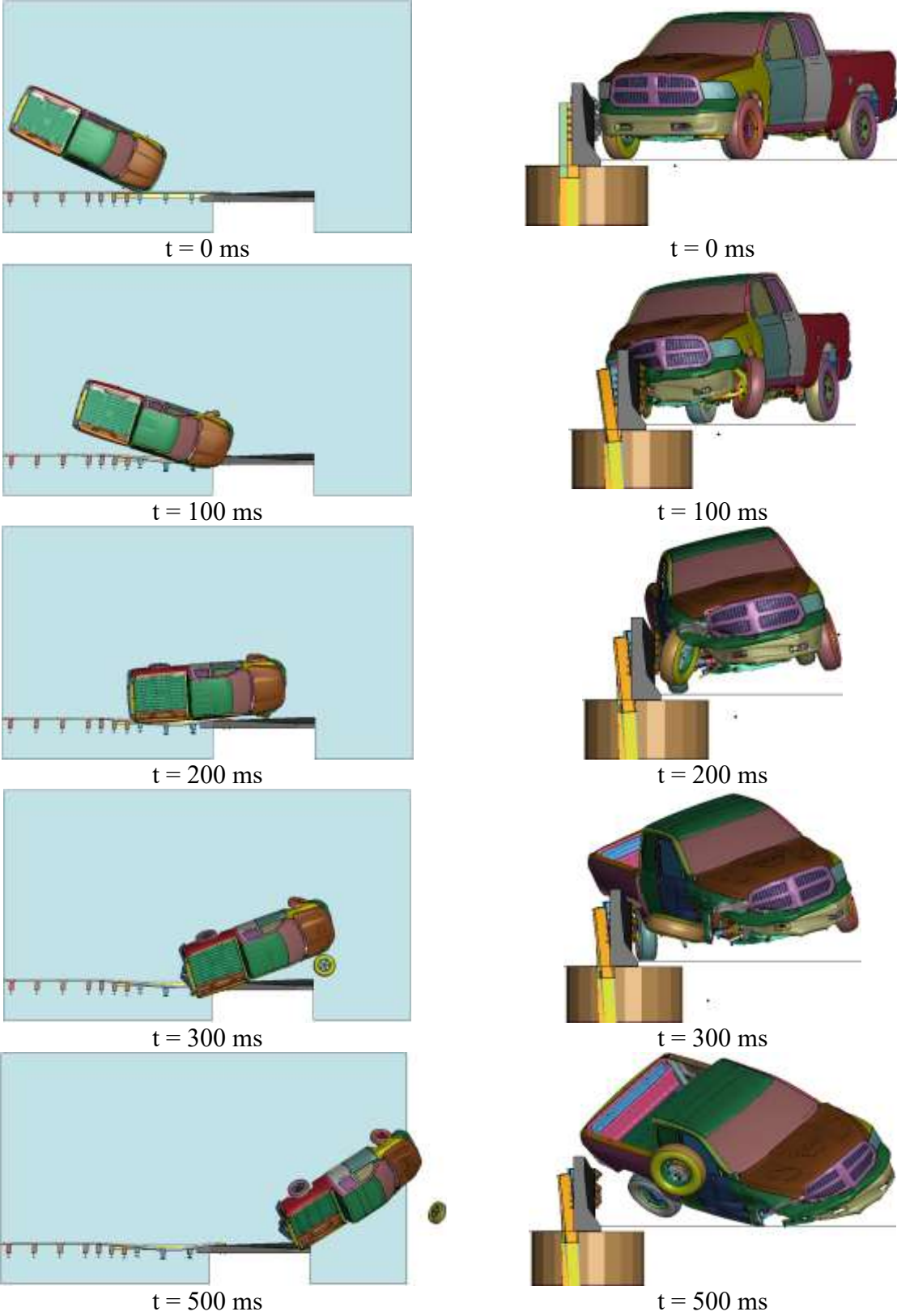


Figure 73. Sequential Images, Simulation No. B8-CP+CB-3N-WD

The lateral overlap of the impacting tires across the upstream face of the concrete buttress are listed in Table 15. Looking at the two simulations that did not involve any wheel snag retrofits, the maximum overlap numbers did not appear to be significantly different than those from the previous simulations on Buttresses 5 and 6. However, a difference was noted in the position of the wheel at the time of maximum overlap. Because of the large gap underneath the cantilevered segment, the wheel was allowed to remain at this lateral offset for a longer time, as shown in

Figure 74. Thus, the wheel impacted and severely snagged on the lower vertical face of the buttress, particularly for the simulation involving wheel disengagement.

The lateral overlap of the impacting tires for the simulations with the various wheel snag prevention retrofits are shown in Table 15 and

Figure 75. The amount of snag on the buttress was reduced for each of the wheel snag retrofit options. The concrete fill and steel assembly retrofits resulted in wheel overlap values and snag severities similar to those previously observed for the simulations with Buttresses 5 and 6. The addition of a curb below the guardrail reduced the amount of wheel overlap on the buttress even further, supporting the idea that curbs help prevent wheel snag below the rail of AGTs.

Table 15. Tire-Buttress Overlap, Buttress 8

Simulation No.		Overlap (in.)	
Front surface	Non-retrofit	B8-CP-5N-WA	7.0
		B8-CP-3N-WD	8.4
	Concrete fill	B8-CP+CF-3N-WA	6.8
		B8-CP+CF-3N-WD	8.4
	Steel assembly	B8-CP+SA-3N-WA	6.9
		B8-CP+SA-3N-WD	8.4
	Curb	B8-CP+CB-3N-WA	5.3
		B8-CP+CB-3N-WD	6.1



Figure 74. Tire-Buttress Overlap, Buttress 8 without Wheel Snag Retrofits

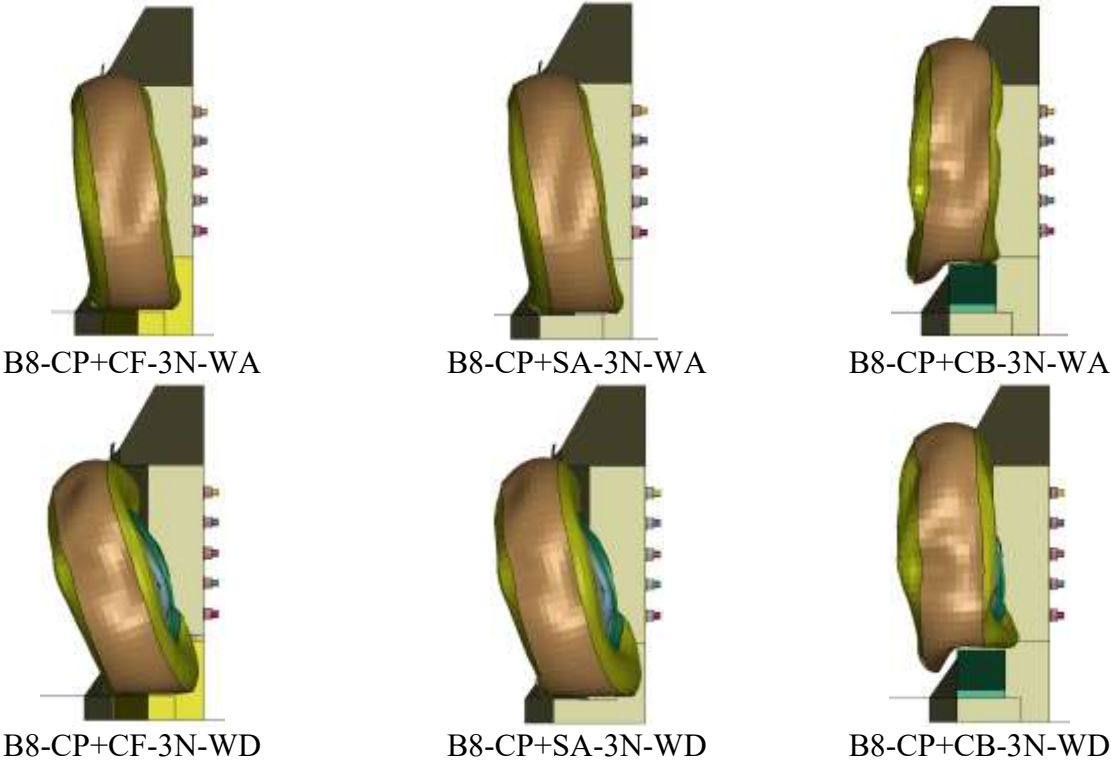


Figure 75. Tire-Buttress Overlap, Buttress 8 with Wheel Snag Retrofit Options

6.4.2 Barrier Damage

Damage to the barrier consisted of rail and post deformations, as shown in Figure 76. These deformations were consistent with those observed in physical crash testing and in the simulations with Buttresses 5 and 6. Maximum dynamic deflections were observed at the mid-span between post nos. 17 and 18 and are presented in Table 16. The simulated rail deflections were similar to those measured in the validation simulations, so they were not considered to be an issue.

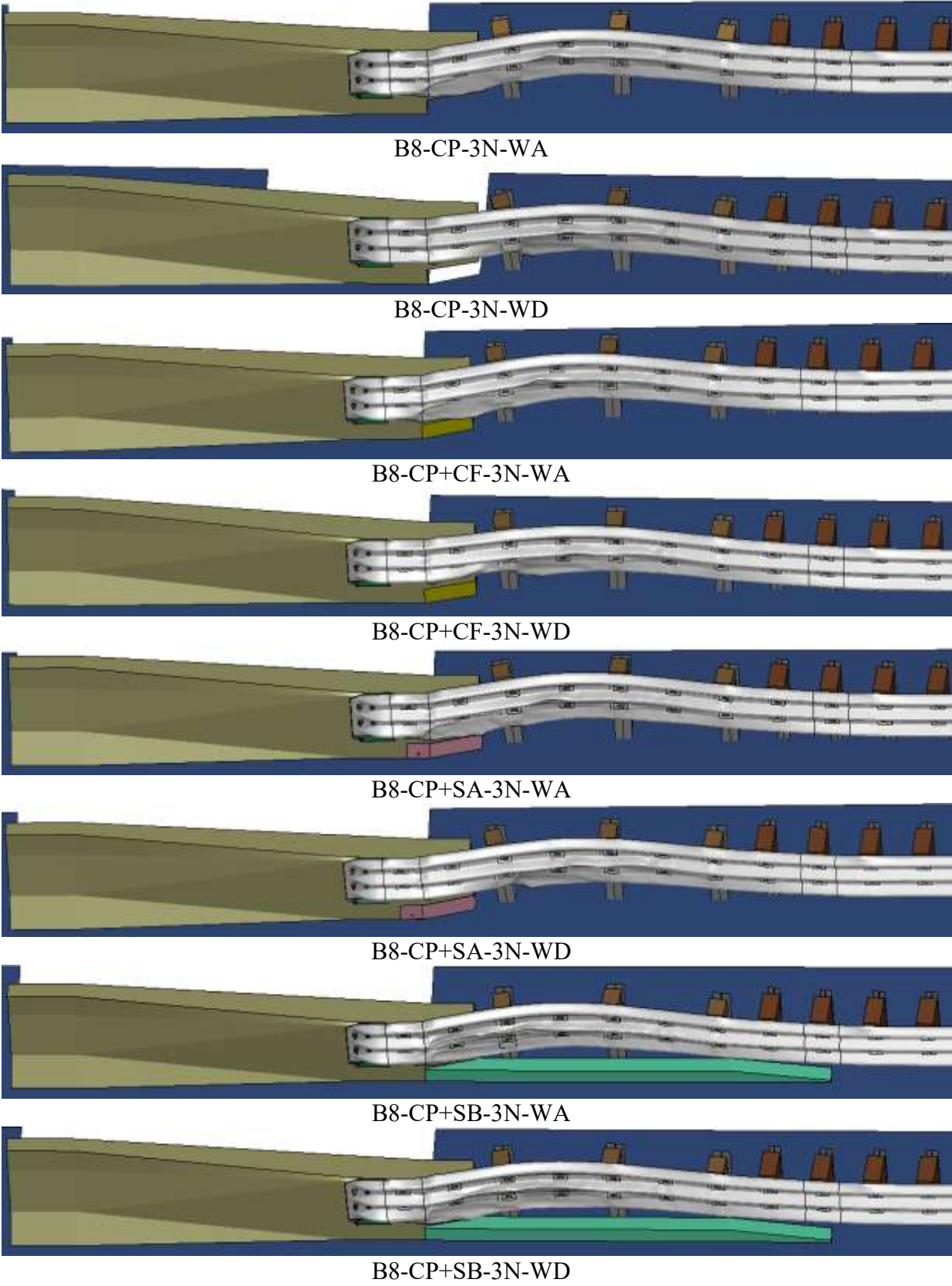


Figure 76. System Damage, Buttriss 8

6.4.3 Occupant Risk

The calculated OIVs and ORAs in both the longitudinal and lateral directions are shown in Table 16. These occupant risk values compared well with the results from previous physical testing as well as the simulation results with Buttress 5. All simulations resulted in occupant risk values that satisfied MASH limits. The three wheel-snap retrofit options had a minimal effect on the occupant risk values and did not negatively affect the safety performance of the system. After impact, the vehicle smoothly exited the AGT system and the vehicle trajectory did not violate the bounds of the exit box.

Table 16. Summary of OIV, ORA, and Lateral Deflection, Buttress 8

Evaluation Criteria		Simulation No.								MASH Limits
		B8-CP-3N-WA	B8-CP-3N-WD	B8-CP+CF-3N-WA	B8-CP+CF-3N-WD	B8-CP+SA-3N-WA	B8-CP+SA-3N-WD	B8-CP+SB-3N-WA	B8-CP+SB-3N-WD	
OIV (ft/s)	Long.	-22.8	-23.1	-23.0	-23.2	-23.1	-24.1	-22.4	-23.4	±40
	Lat.	24.9	24.1	25.0	24.4	25.0	24.6	25.6	24.7	±40
ORA (g's)	Long.	-14.8	-14.2	-17.0	-13.9	-18.4	-15.0	-12.7	-11.3	±20.49
	Lat.	13.1	15.2	11.9	14.3	16.5	13.5	9.4	11.5	±20.49
Max. post deflection (in.)	Post 17	10.3	9.5	10.4	9.3	10.3	9.4	9.4	8.6	N/A
	Post 18	9.5	8.4	9.2	8.1	9.3	8.4	8.1	8.2	N/A
Max. dynamic deflection (in.)		11.2	10.2	11.1	10.0	11.2	10.2	10.4	10.2	N/A

6.4.4 MASH Test 3-20 Evaluation

To ensure that the addition of the wheel snag prevention options did not negatively affect the safety performance of the AGT, simulations were also conducted in accordance with MASH Test 3-20 with the 1100C small car. The impact conditions for this test were 62 mph and 25 degrees. The critical impact point was 63 in. upstream of the concrete buttress, as shown in Figure 77, which was determined using the plots in Chapter 3 of MASH.

Previous crash testing with AGTs with a 6-in. curb below the guardrail has proven to be MASH crashworthy and prevents small car wheel contact with the buttress. Additionally, the simulations in Section 6.4.1 showed that the addition of a curb greatly reduced wheel snag for the 2270P vehicle. Thus, the addition of a curb was not considered critical to the performance with a small car. Concrete fill and the steel assembly options were considered to be equivalent, so for simplicity, only evaluation of the concrete fill was deemed necessary. Thus, simulations according to MASH Test 3-20 were conducted on Buttress 8 (as-is) and with the concrete fill retrofit, as shown in Table 17.

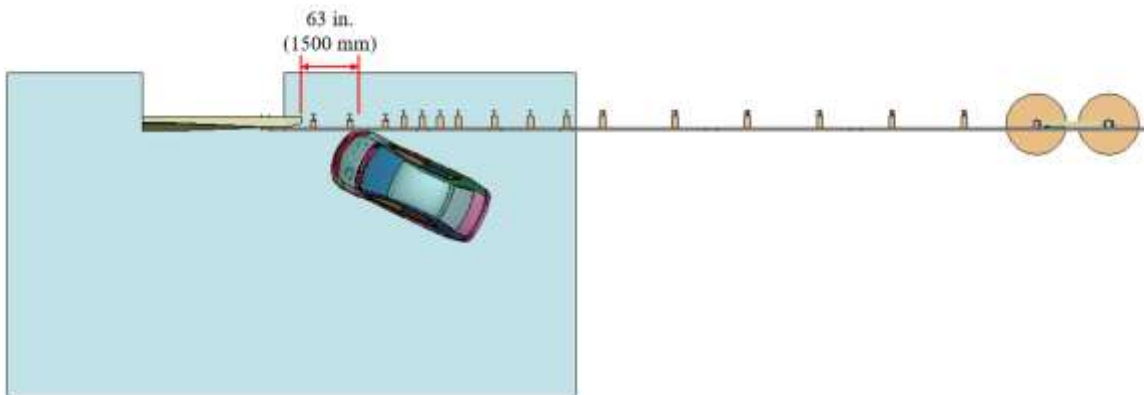


Figure 77. 1100C Vehicle Impact Point

Table 17. MASH 3-20 Simulations on AGT with Buttress 8

Simulation No.	MASH Test No.	Test Vehicle	Impact Conditions		Nuts	Retrofit option
			Speed (mph)	Angle (deg.)		
B8-CP-3N-3-20	3-20	1100C	62	25	3	N/A
B8-CP+CF-3N-3-20	3-20	1100C	62	25	3	Concrete fill

The 1100C small car was captured and smoothly redirected in both simulations, as shown in Figure 78 and Table 18. The maximum angular displacements of the small car vehicle were very similar between the two configurations, as shown in Table 18. System damage and maximum deflections were also very similar, as shown in Figure 80. The concrete fill reduced the severity of the wheel snag on the buttress due to the wheel being more gradually pushed back toward the roadway. The calculated OIVs and longitudinal ORAs appeared unaffected by the addition of the concrete fill. There was an increase in lateral ORA with the concrete fill retrofit, but the lateral ORA was still well below the MASH limit. Thus, the addition of concrete fill, the steel assembly, or the 6-in. curb were all considered crashworthy alternatives to mitigate wheel snag on existing buttresses with a cantilevered upstream end segment.

Table 18. Vehicle Behavior Results under MASH Test 3-60 Impacts, Buttress 8

Simulation No.	Max. Angular Displacement		
	Roll (Degree)	Pitch (Degree)	Yaw (Degree)
B8-CP-3N-3-20	7.0	10.2	80.1
B8-CP+CF-3N-3-20	8.1	11.7	76.3
MASH Limits	±75	±75	N/A

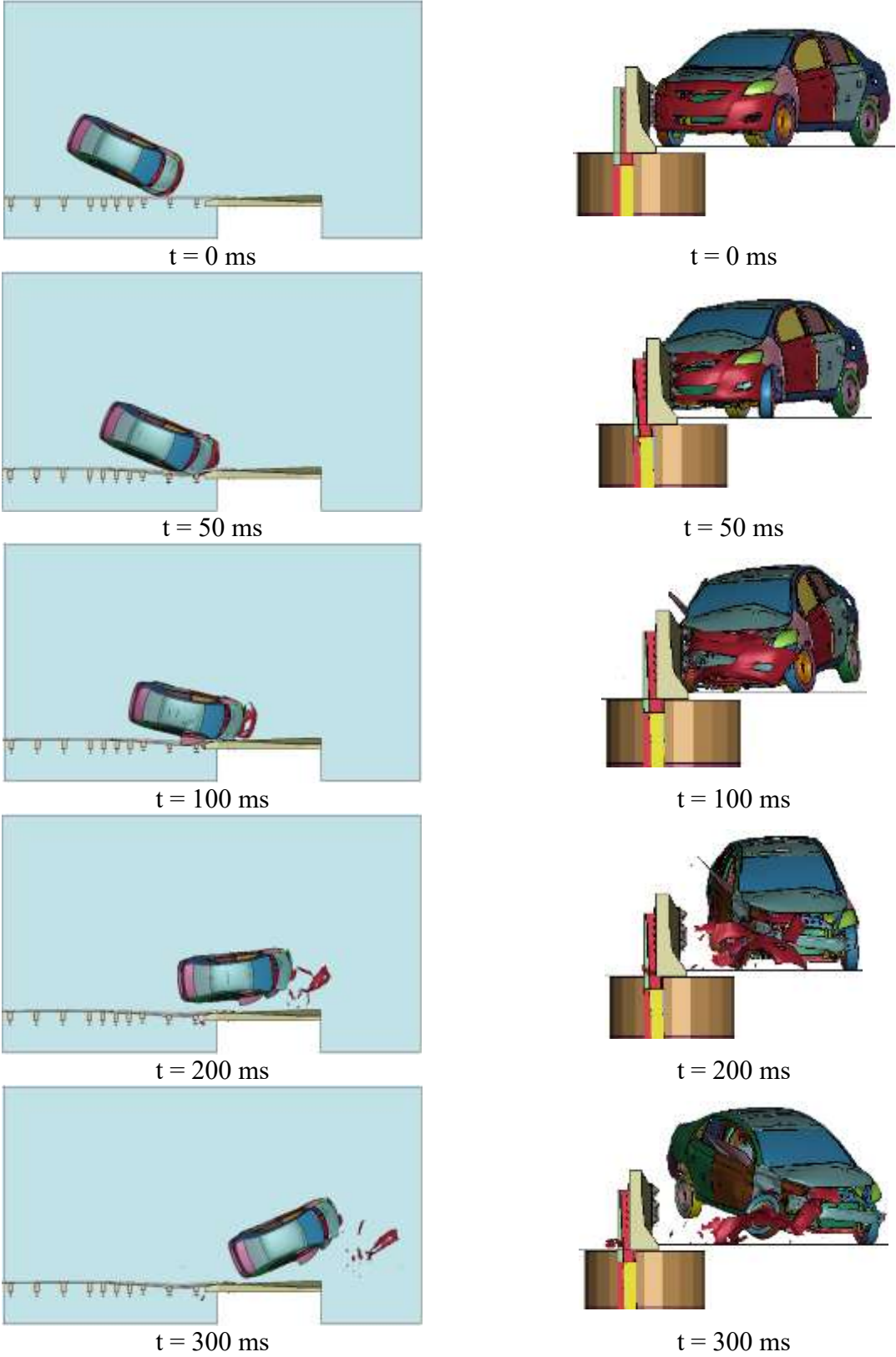


Figure 78. Sequential Images, Simulation No. B8-CP-3N-3-20

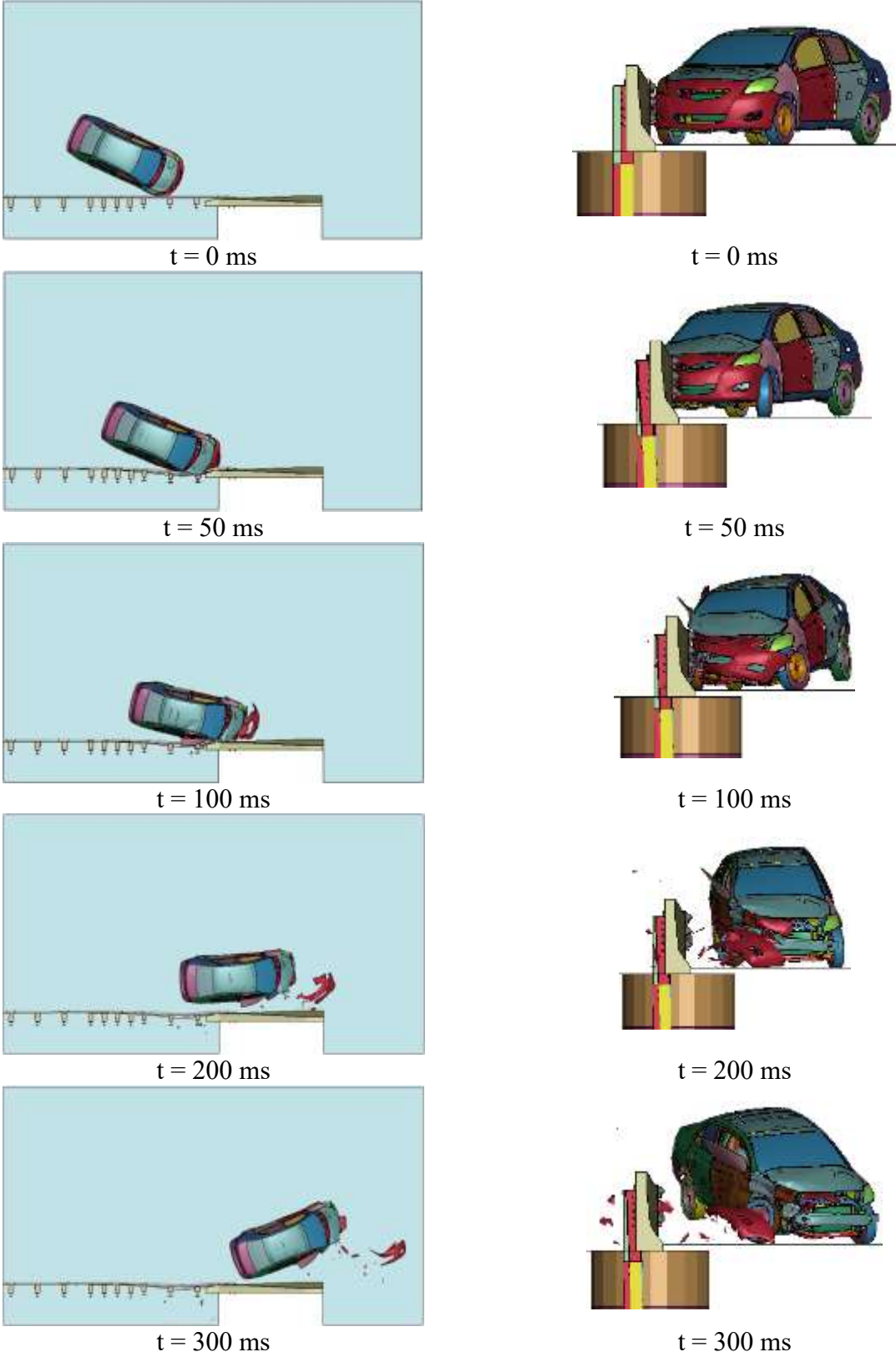
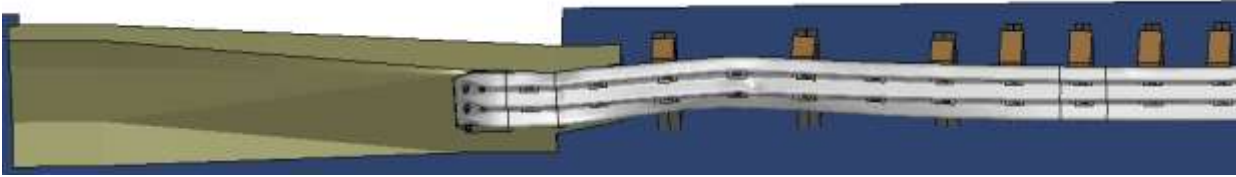
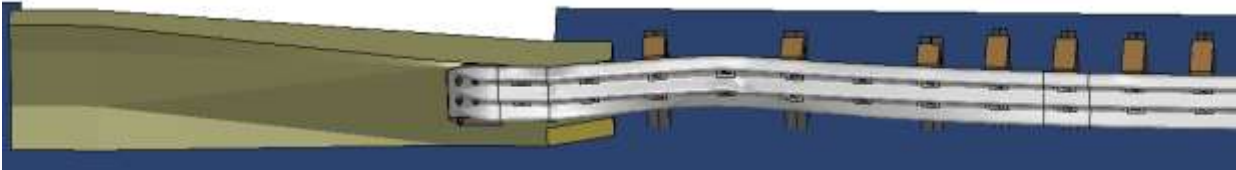


Figure 79. Sequential Images, Simulation No. B8-CP+CF-3N-3-20



B8-CP-3N-3-20



B8-CP+CF-3N-3-20

Figure 80. System Damage under MASH 3-20, Buttress 8

Table 19. Summary of OIV, ORA, and Lateral Deflection, Buttress 8 under MASH Test 3-20

Evaluation Criteria		B8-CP-3N-3-20	B8-CP+CF-3N-3-20	MASH Limits
OIV (ft/s)	Longitudinal	-31.1	-31.8	±40
	Lateral	34.9	34.5	±40
ORA (g's)	Longitudinal	-20.2	-23.8	±20.49
	Lateral	8.5	11.2	±20.49
Max. dynamic deflection (in.)		6.2	6.3	N/A

6.5 Buttress 10 Simulation Results

Buttress 10 was similar to Buttress 8 except that the vertical-to-New Jersey shape transition did not begin until further down the bridge rail. Thus, Buttress 10 held a constant 32-in. tall vertical shape through the transition region. To ensure that this shape difference did not cause issues, simulated impacts were conducted on the AGT attached to Buttress 10. All the simulated impacts were conducted using the 2270P pickup truck with concrete fill below the cantilevered segment and a 3-nut anchorage configuration. Both wheel behaviors, remaining attached and disengaging during impact, were evaluated. The simulation matrix of the AGT with Buttress 10 is shown in Table 20.

Table 20. Simulations on AGT with Buttress 10

Simulation No.	Test Designation No.	Test Vehicle	Impact Conditions		Wheel Behavior	Nuts	Retrofit option
			Speed (mph)	Angle (deg.)			
B10-CP+CF-3N-WA	3-21	2270P	62	25	WA	3	Concrete fill
B10-CP+CF-3N-WD	3-21	2270P	62	25	WD	3	

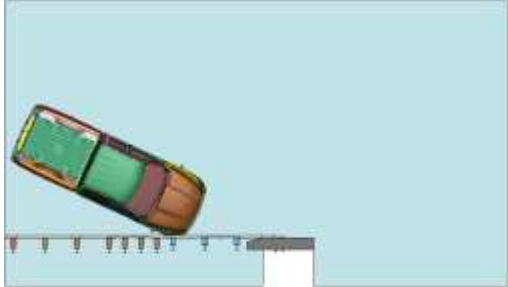
6.5.1 Vehicle Behavior

Sequential images of the two simulations are shown in Figures 81 and 82. The results were nearly identical to those for Buttress 8 with the concrete fill retrofit. The vehicle was contained and smoothly redirected, and remained stable throughout the impact events. Maximum roll and pitch angular displacements are listed in Table 21. The maximum wheel overlap, also shown in Table 21, closely matched those for Buttress 8. After the impact, the vehicle smoothly exited the AGT system, and the vehicle trajectory did not violate the bounds of the exit box.

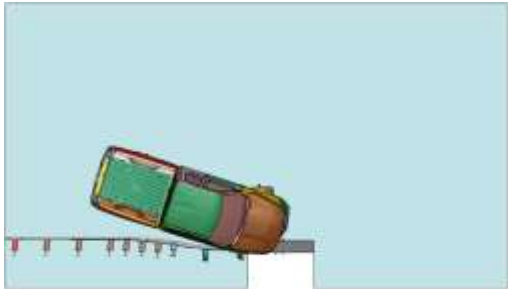
Table 21. Vehicle Behavior Results, Buttress 10

Buttress No.	Max. Angular Displacement	Roll (deg.)	Pitch (deg.)	Yaw (deg.)	Wheel Overlap (in.)
10	B10-CP+CF-3N-WA	21.3	4.8	50.4	6.8
	B10-CP+CF-3N-WD	25.8	7.0	42.3	8.4
MASH Limits		±75	±75	N/A	N/A

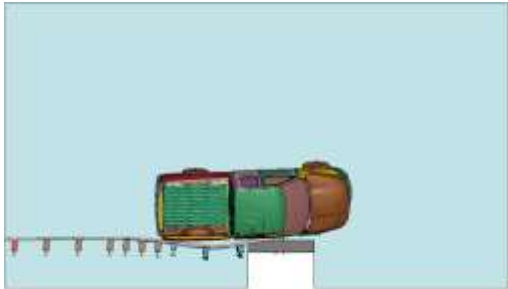
N/A – Not applicable.



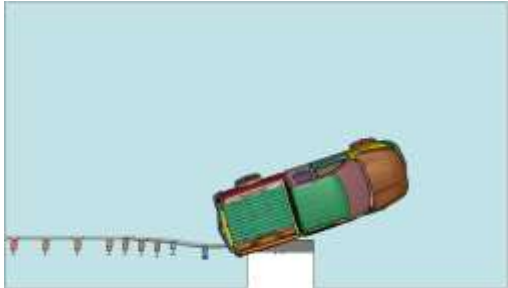
t = 0 ms



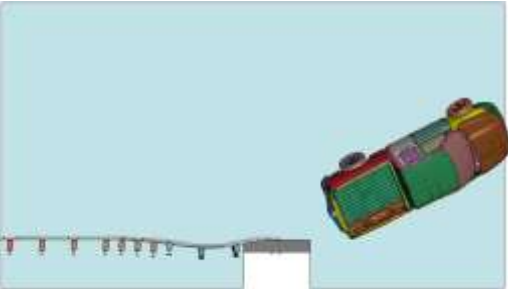
t = 100 ms



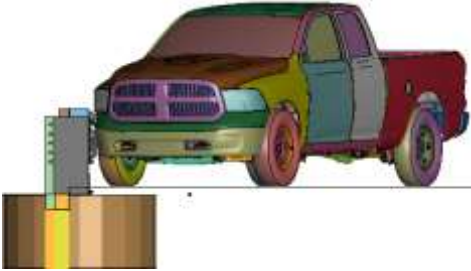
t = 200 ms



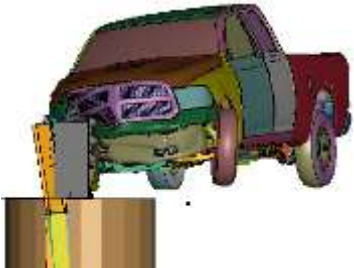
t = 300 ms



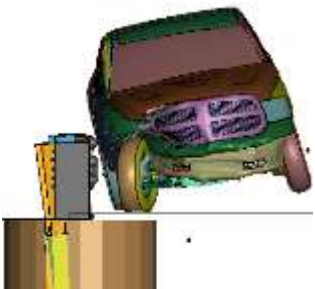
t = 500 ms



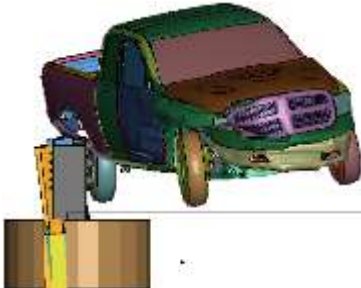
t = 0 ms



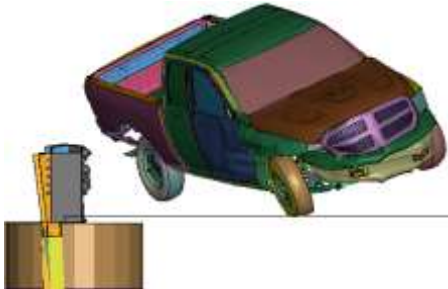
t = 100 ms



t = 200 ms



t = 300 ms



t = 500 ms

Figure 81. Sequential Images, Simulation No. B10-CP+CF-3N-WA

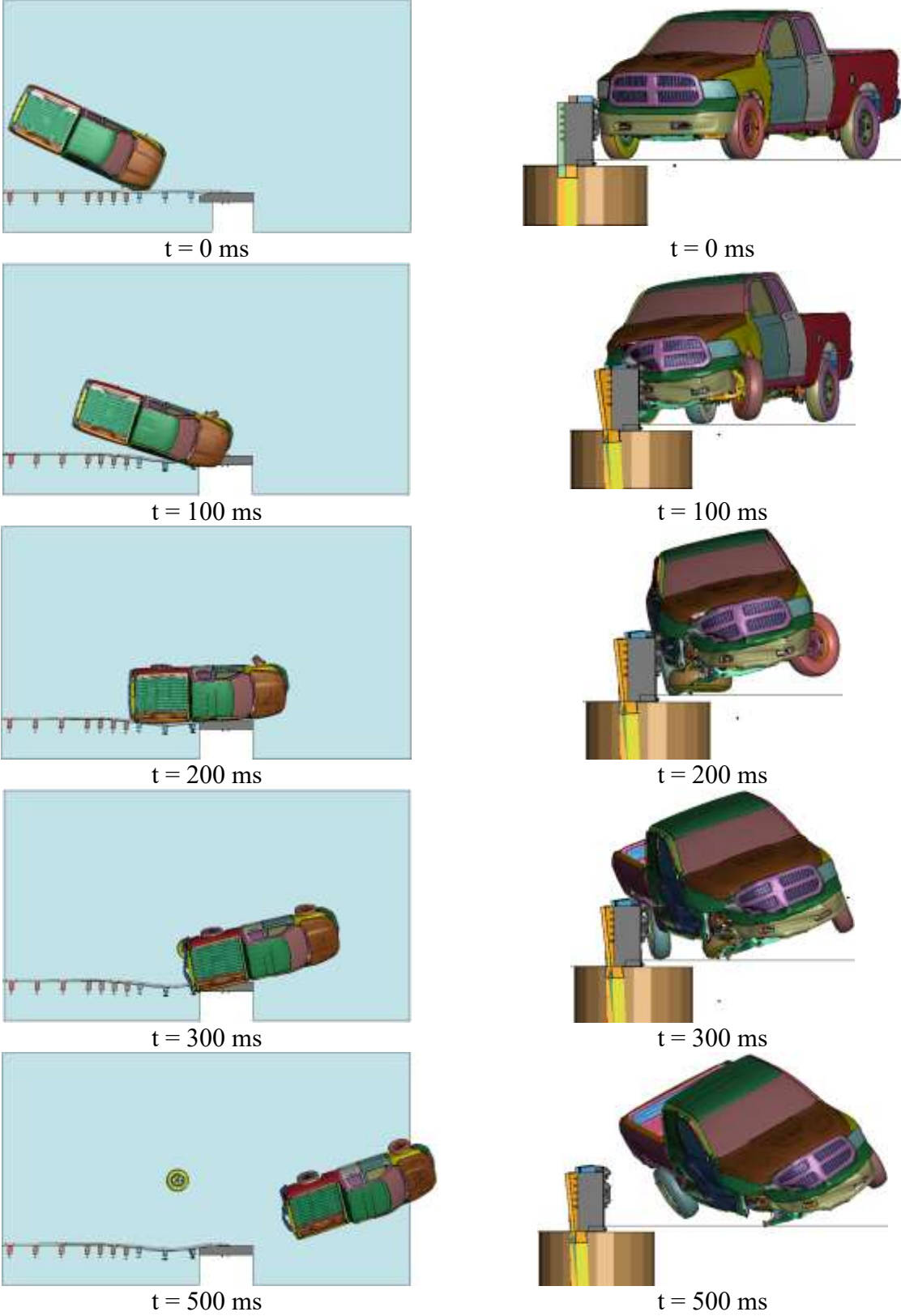
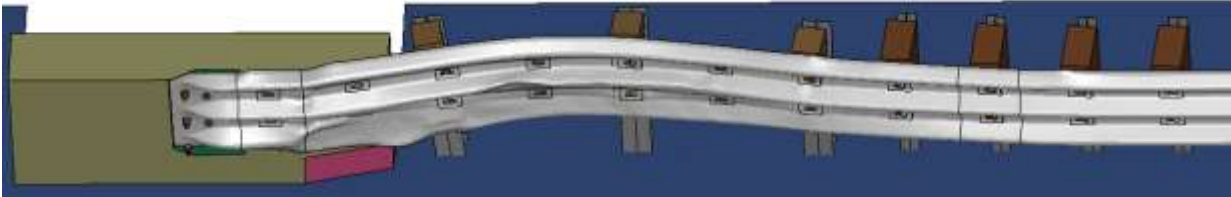


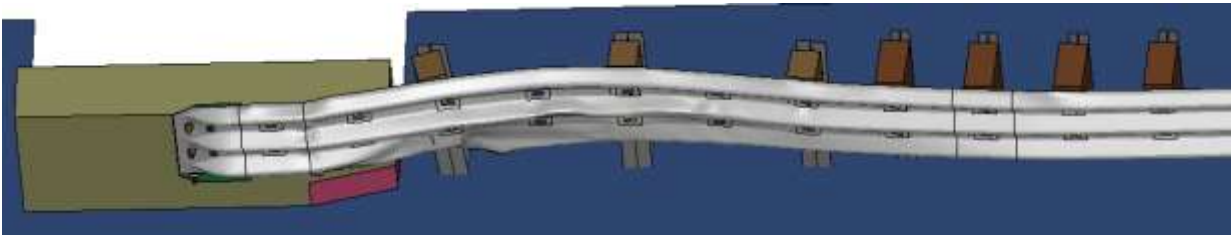
Figure 82. Sequential Images, Simulation No. B10-CP+CF-3N-WD

6.5.2 Barrier Damage

Barrier damage consisted of rail and post deformations, as shown in Figure 83. The maximum lateral dynamic deflection of the rail occurred at the mid-span between post nos. 17 and 18, and the magnitudes of 11.2 in. and 10.1 in. closely matched that of the deflections from the Buttress 8 simulations.



B10-CP+CF-3N-WA



B10-CP+CF-3N-WD

Figure 83. System Damage, Buttress 10

6.5.3 Occupant Risk

The calculated OIVs and ORAs in both the longitudinal and lateral directions are shown in Table 22. The OIVs and ORAs obtained from the simulations closely matched those from Buttress 8 simulations and were within MASH limits. Thus, there were no concerns about the AGT attached to Buttress 10 with any of the wheel snag mitigation retrofits.

Table 22. Summary of OIV, ORA, and Lateral Deflection, Buttress 10

Evaluation Criteria		B10-CP+CF-3N-WA	B10-CP+CF-3N-WD	MASH Limits
OIV (ft/s)	Longitudinal	-23.1	-24.0	±40
	Lateral	25.1	24.6	±40
ORA (g's)	Longitudinal	-15.5	-14.2	±20.49
	Lateral	12.9	16.7	±20.49
Max. post deflection (in.)	Post no. 17	10.3	9.2	N/A
	Post no. 18	9.3	8.3	N/A
Max. dynamic deflection (in.)		11.2	10.1	N/A

6.6 Buttress 2 Simulation Results

Buttress 2 had a few unique features to accommodate, including a 3½-in. wide guardrail connection blackout that created a significant snag hazard. To mitigate this snag hazard, a 3½-in. thick attachment spacer was placed behind the guardrail end terminal to bring the back of the guardrail flush with the face of the buttress/bridge rail. Note, the connection spacer was modeled as “rigid” but could be fabricated from timber or steel for real-world applications. Additionally, the connection blackout did not extend to the top of Buttress 2, so reverse direction snag on the guardrail and connection spacer could become an issue. Two retrofits for reverse direction snag on the guardrail and connection spacer were evaluated. The first involved using concrete to fill the void above the connection blackout, which created a constant width for the upper portion of Buttress 2. The second involved redesigning the downstream end of the connection spacer to slope down and meet the top of the connection blackout. These two retrofits are shown in Figures 84 and 85, respectively.

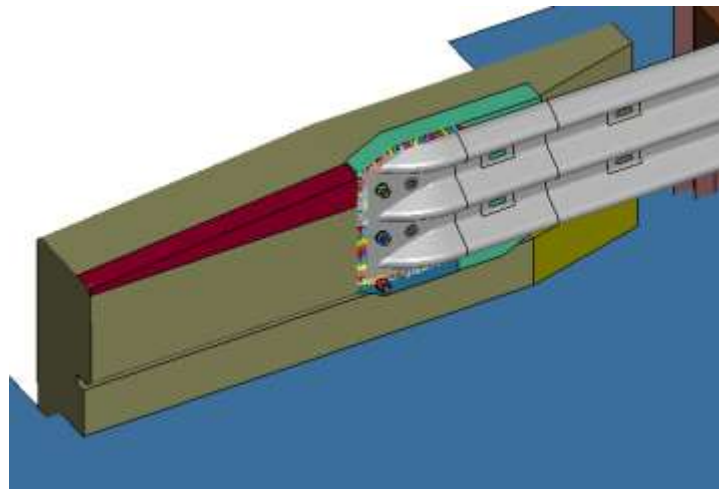


Figure 84. Concrete Fill (red) Placed above Connection Blockout, Buttress 2

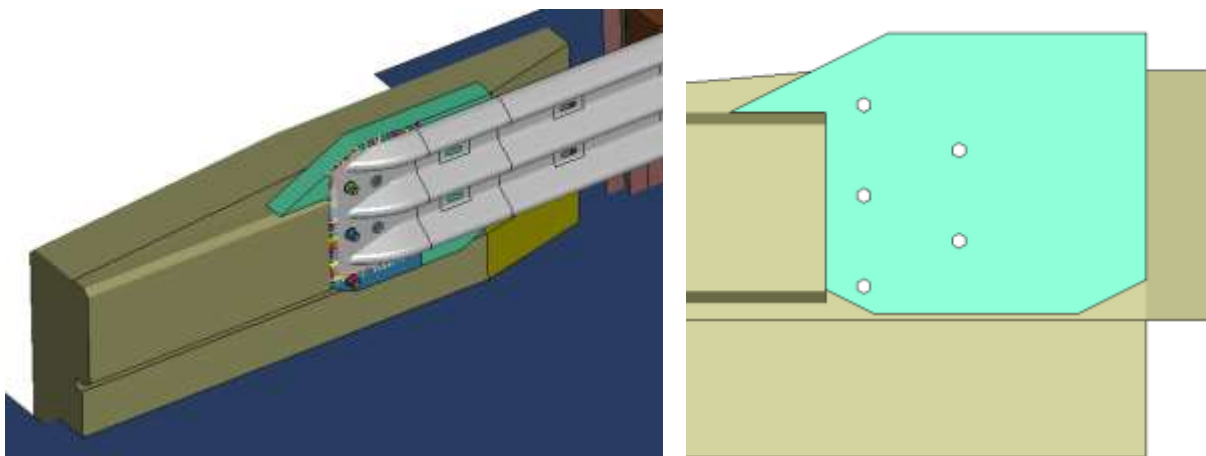


Figure 85. Redesigned Connection Spacer (teal), Buttress 2

Recall, Buttress 2 was originally designed for a 32-in. tall AGT, so the attachment bolts were located 1 in. higher than the other buttresses. However, it was desired to continue to use the same connector plate assembly as the previous AGT retrofits and avoid creating another specialty piece. Thus, after a 3-in. overlay, the retrofit AGT would be installed at a height of 32 in. This height fell within the 31 to 34-in. tall range of existing MASH AGTs, so it was not thought to create any problems.

All Buttress 2 simulations were conducted with a 3-nut anchorage pattern, since the 3-nut and 5-nut configurations had shown negligible differences in system performance. Additionally, previous simulation results had demonstrated the ability of all three wheel-sag retrofit options to perform safely. Thus, only concrete fill below the cantilevered portion of the buttress was used to evaluate the safety performance of retrofit AGT attached to Buttress 2. The simulation matrix for the evaluation of the retrofit AGT with Buttress 2 is shown in Table 23.

Table 23. Normal-Direction Simulations on Retrofit AGT with Buttress 2

Simulation No.	MASH Test No.	Impact Conditions		Wheel Behavior	Retrofit for Reverse Snag
		Speed, mph	Angle, deg.		
B2-CP+CF-3N-WA-CFA	3-21	62	25	WA	Concrete fill
B2-CP+CF-3N-WD- CFA	3-21	62	25	WD	Concrete fill
B2-CP+CF-3N-WA-RBA	3-21	62	25	WA	Redesigned block
B2-CP+CF-3N-WD-RBA	3-21	62	25	WD	Redesigned block

6.6.1 Vehicle Behavior

Sequential images of the four normal-direction simulations are shown in Figures 86 through 89. In these simulations, the Ram pickup truck model impacted the AGT 89 in. upstream from Buttress 2 at a speed of 62 mph and an angle of 25 degrees. The vehicle was contained and smoothly redirected by the retrofit AGT installations. Damage to the vehicle was consistent with the damage results from previous simulations. The vehicle remained stable throughout the impact events with maximum roll and pitch angular displacements within the MASH limit, as shown in Table 24.

Table 24. Vehicle Angular Displacements Results, Buttress 2

Simulation No.	Maximum Angular Displacements (Degrees)		
	Roll	Pitch	Yaw
B2-CP+CF-3N-WA-CFA	20.2	4.7	49.7
B2-CP+CF-3N-WD- CFA	28.7	-5.2	42.0
B2-CP+CF-3N-WA-RBA	17.6	4.7	48.1
B2-CP+CF-3N-WD-RBA	28.1	7.3	42.2
MASH Limits	±75	±75	N/A

N/A – Not applicable.

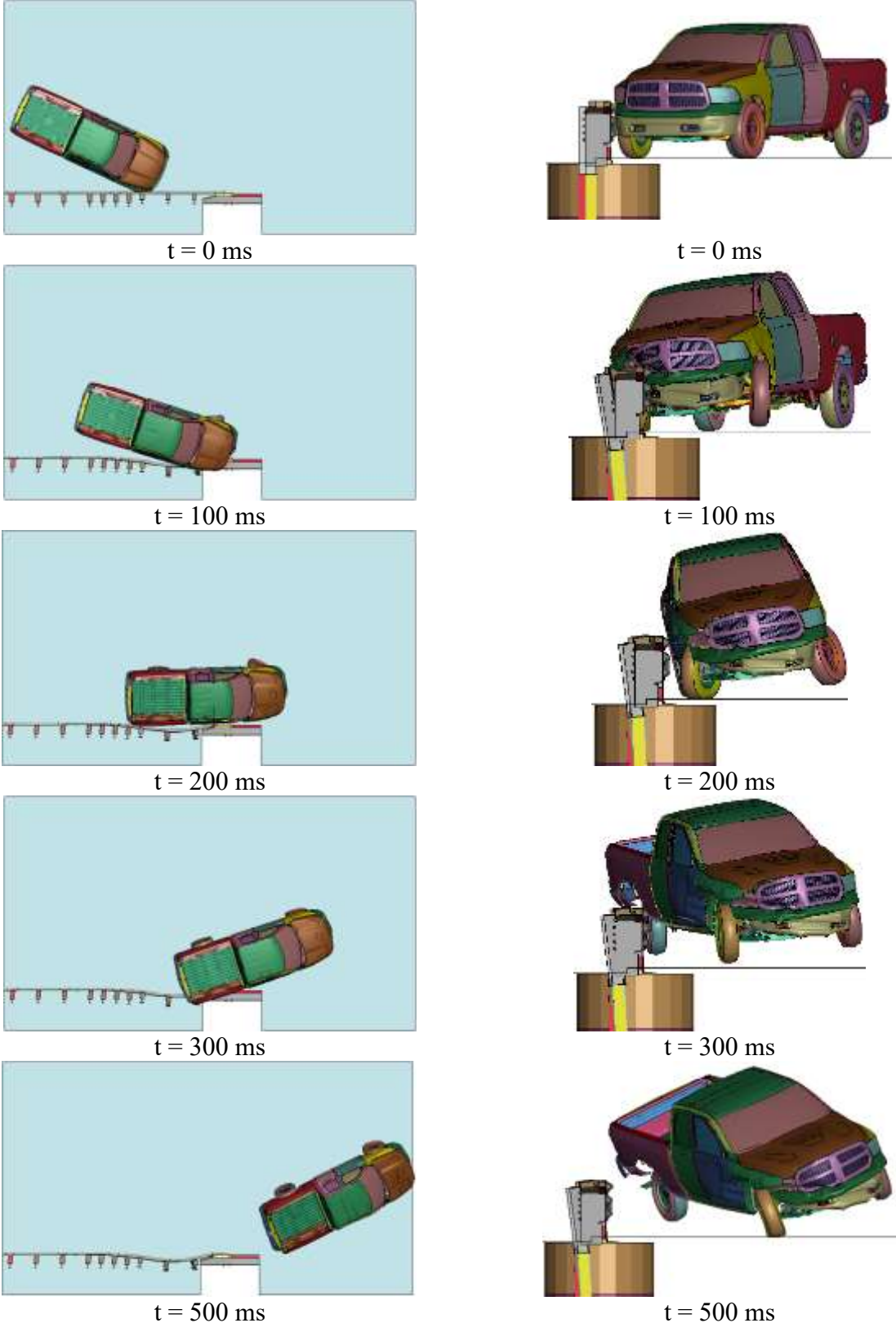


Figure 86. Sequential Images, Simulation No. B2-CP+CF-3N-WA-CFA

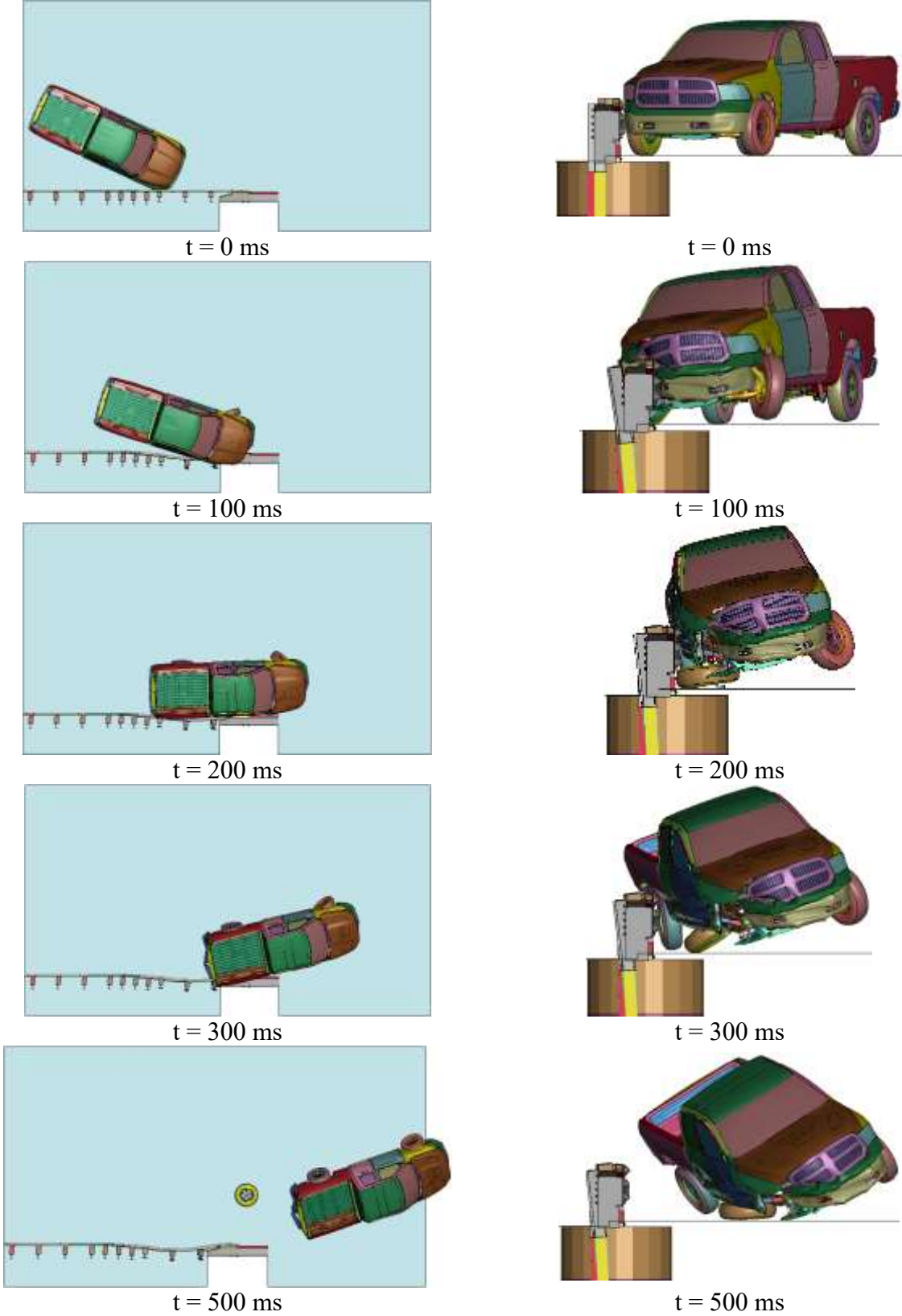


Figure 87. Sequential Images, Simulation No. B2-CP+CF-3N-WD-CFA

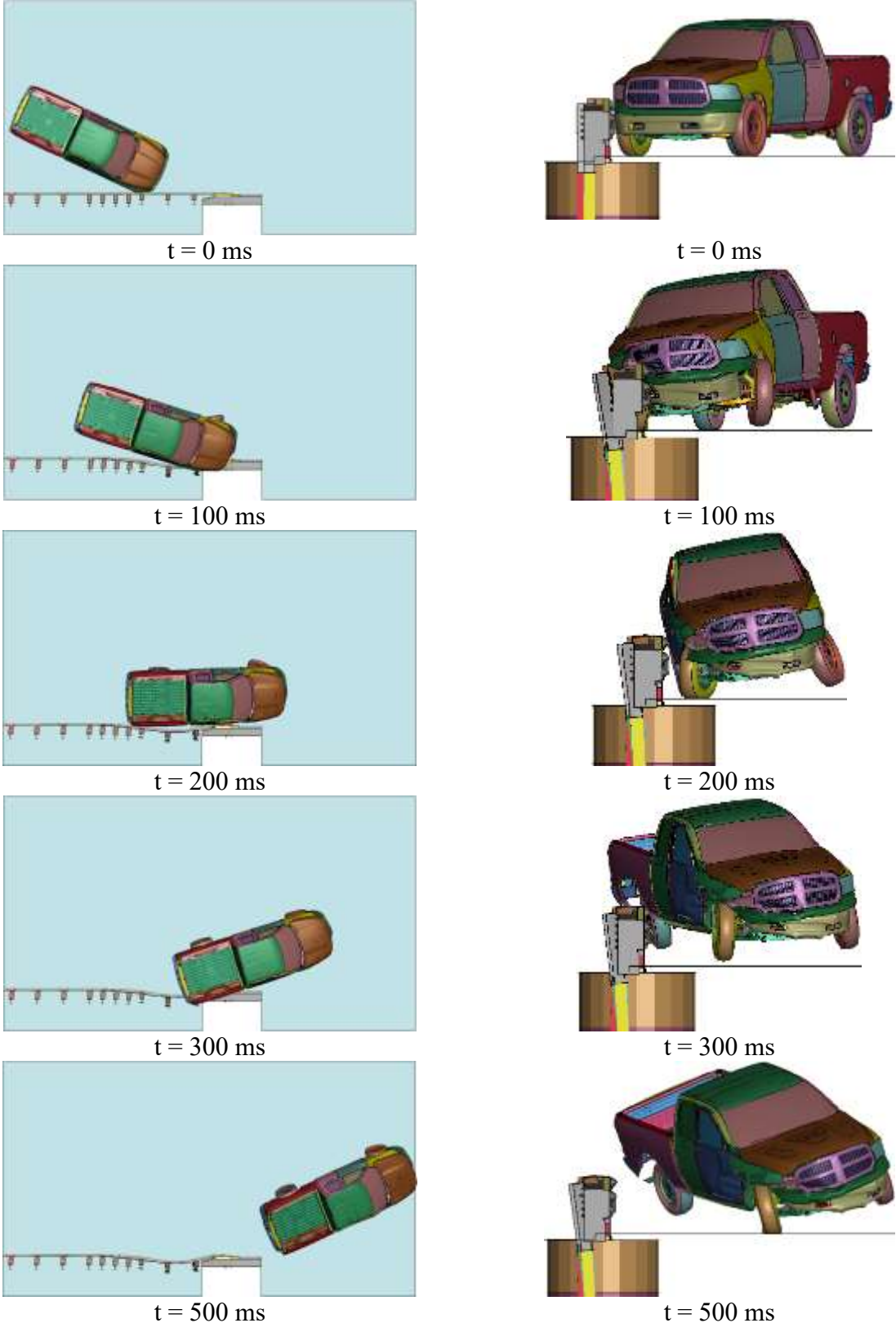


Figure 88. Sequential Images, Simulation No. B2-CP+CF-3N-WA-RBA

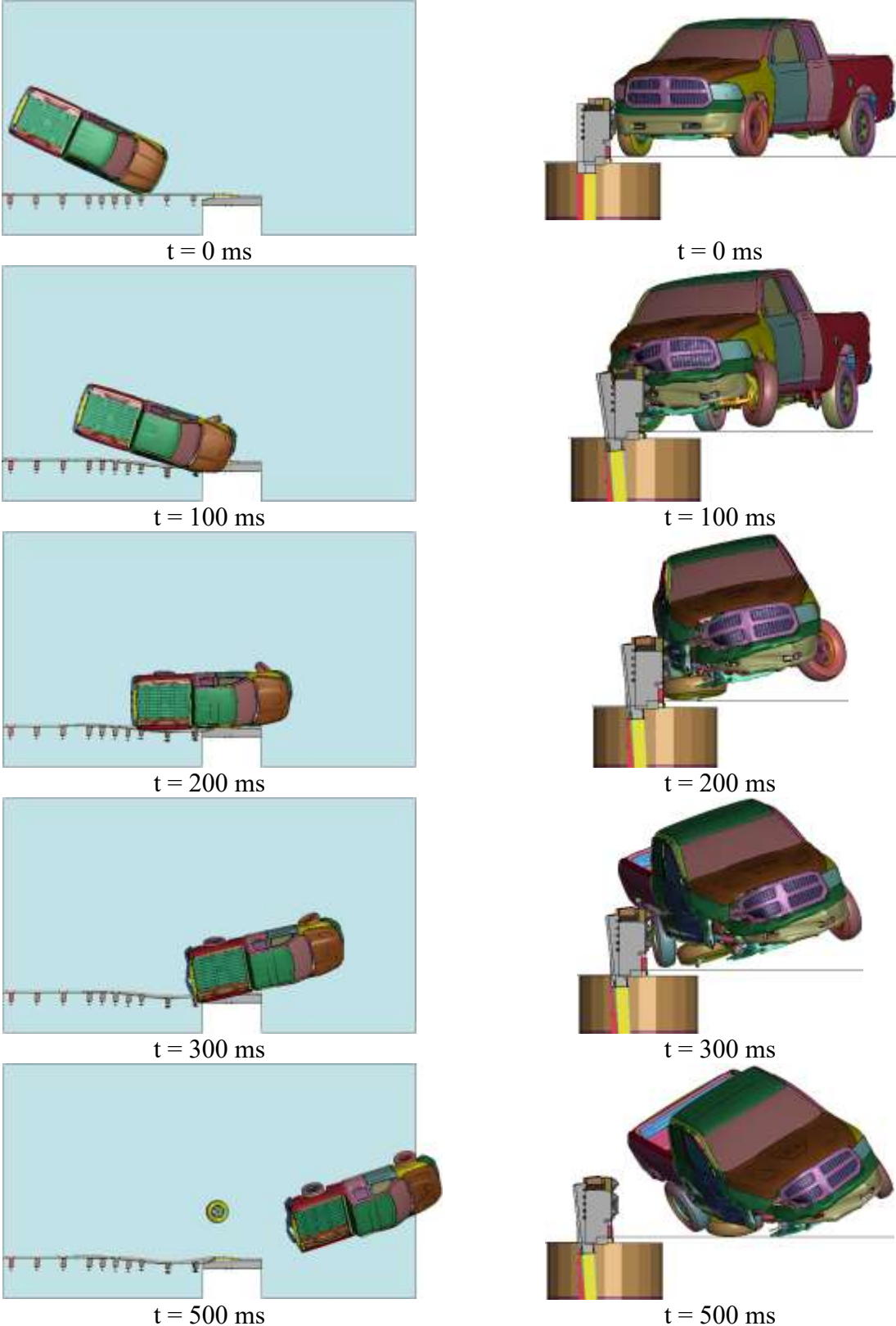


Figure 89. Sequential Images, Simulation No. B2-CP+CF-3N-WD-RBA

6.6.2 Barrier Damage

Damage to the barrier consisted of rail and post deformations, as shown in

Figure 90. System deflections, presented in Table 25, were consistent with the previous retrofit AGT simulations, so they were of no concern.

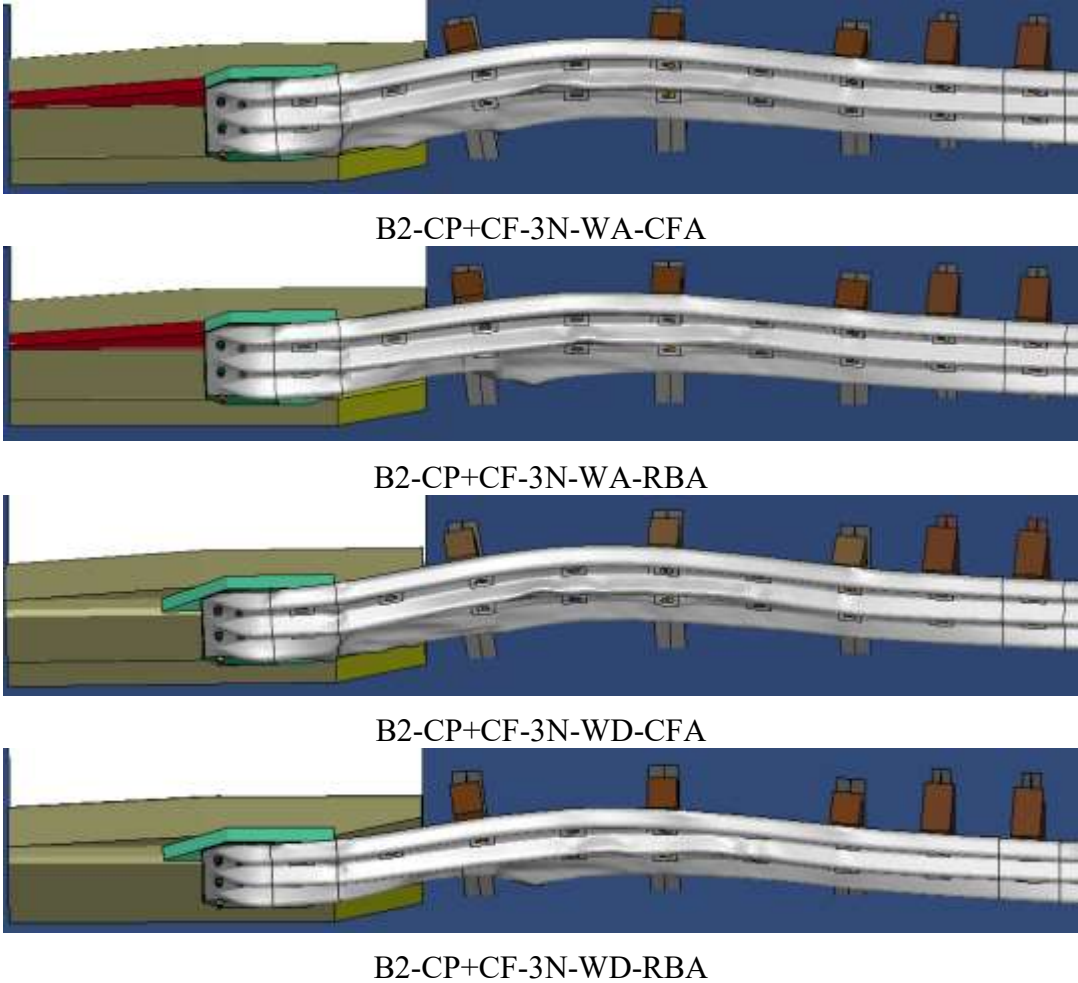


Figure 90. System Damage, Buttress 2

6.6.3 Occupant Risk

The calculated OIVs and ORAs in both the longitudinal and lateral directions are shown in Table 25. These occupant risk values compared well with the results from previous physical testing as well as previous simulation results. All of the simulations resulted in occupant risk values that satisfied MASH limits. The addition of the connection spacer successfully mitigated the vehicle snag on the connection blockout of Buttress 2. Further, the addition of the concrete fill or the modified connection spacer did not negatively affect the safety performance of the retrofit AGT.

Table 25. Summary of OIV, ORA, and Lateral Deflection, Buttress 2

Evaluation Criteria		B2-CP+CF-3N-WA-CFA	B2-CP+CF-3N-WD-CFA	B2-CP+CF-3N-WA-RBA	B2-CP+CF-3N-WD-RBA	MASH Limits
OIV (ft/s)	Longitudinal	-22.7	-22.8	-22.5	-23.6	±40
	Lateral	24.7	23.7	24.8	24.9	±40
ORA (g's)	Longitudinal	-19.3	-14.8	-17.2	-13.2	±20.49
	Lateral	13.1	11.9	11.8	12.5	±20.49
Max. post deflection (in.)	Post 17	10.4	9.2	10.6	9.1	N/A
	Post 18	10.2	8.7	10.3	8.8	N/A
Max. dynamic deflection (in.)		11.2	10.3	11.5	10.1	N/A

6.6.4 Reverse Impact Evaluation

Numerical simulations were conducted with the pickup impacting the system in the reverse direction to evaluate snag on the retrofit AGT components for Buttress 2. All four of the simulation configurations listed in Table 23 were rerun with the impacting the system from the other direction (i.e., traveling from the bridge rail toward the AGT). The impact conditions remained at 62 mph and 25 degrees, in accordance with MASH TL-3. The initial impact location was 4.3 ft from the end of the concrete buttress.

Sequential images of the four reverse-direction simulations are shown in Figures 91 through 94. In all reverse-direction simulations, the vehicle was contained and smoothly redirected by the retrofit AGT installations. The vehicle remained stable during the simulations, though there

was more vehicle roll during these tests than was observed for the normal-direction impacts. However, all angular displacements were within MASH limits, as shown in Table 26.

Because the impact was concentrated on the concrete buttress, system damage was minimal, as shown in

Figure 95. Only minor rail deformations and displacements occurred. The calculated OIVs and ORAs in both the longitudinal and lateral directions, as shown Table 27, were within MASH limits. Both the concrete fill and the modified connection spacer options successfully mitigated vehicle snag during reverse direction impacts.

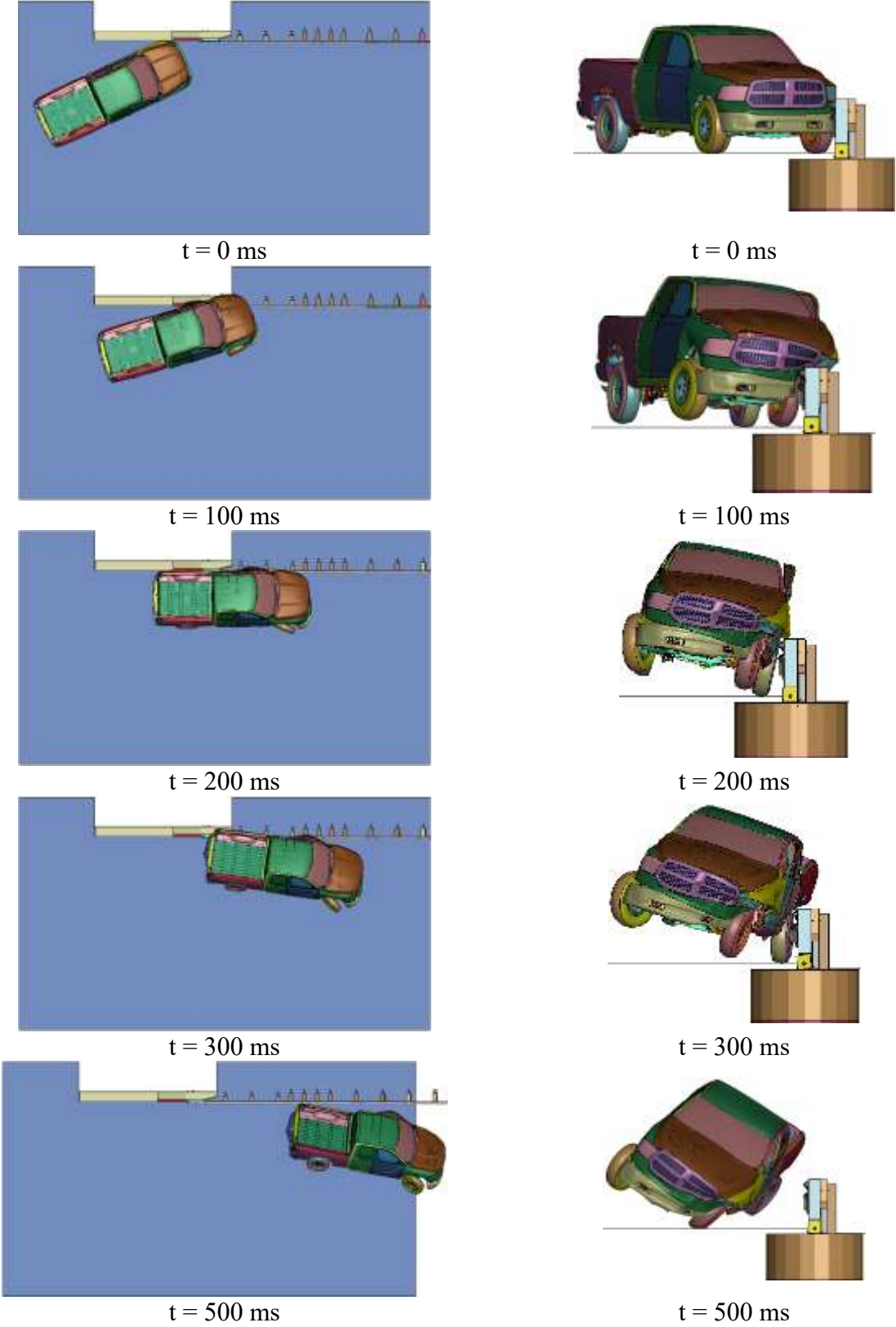


Figure 91. Sequential Images, Simulation No. B2-CP+CF-3N-WA-CFA-REV

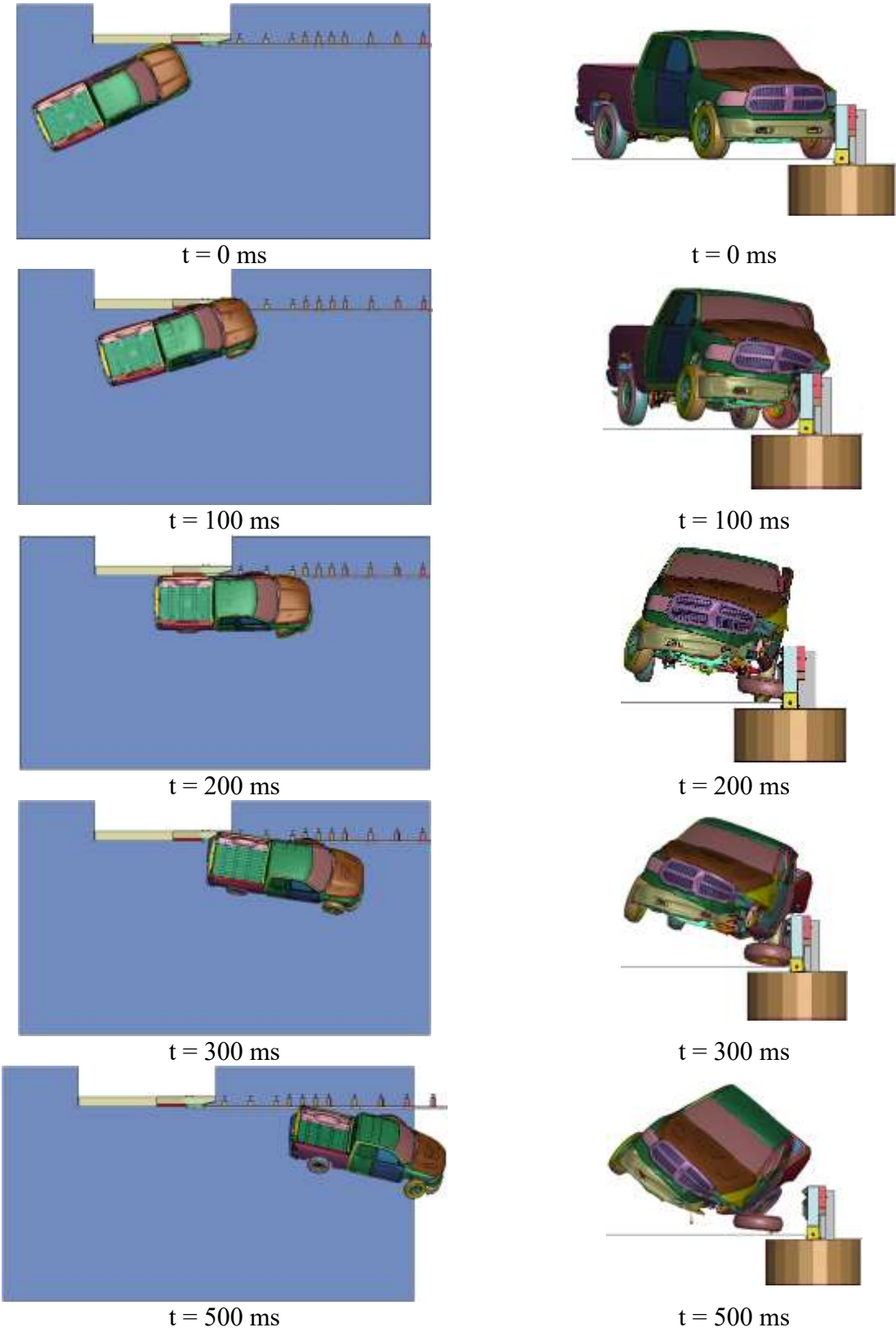


Figure 92. Sequential Images, Simulation No. B2-CP+CF-3N-WD-CFA-REV

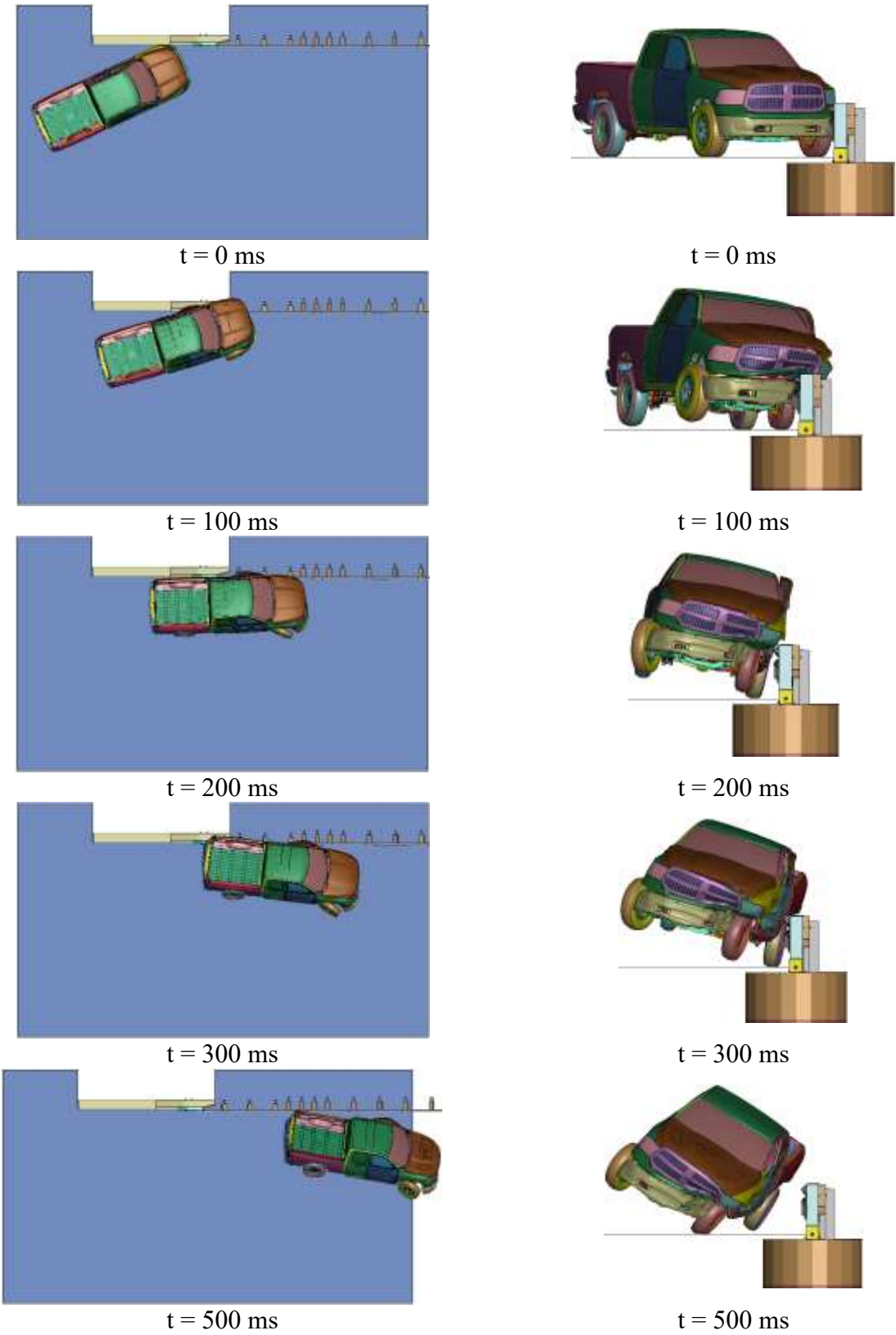


Figure 93. Sequential Images, Simulation No. B2-CP+CF-3N-WA- RBA-REV

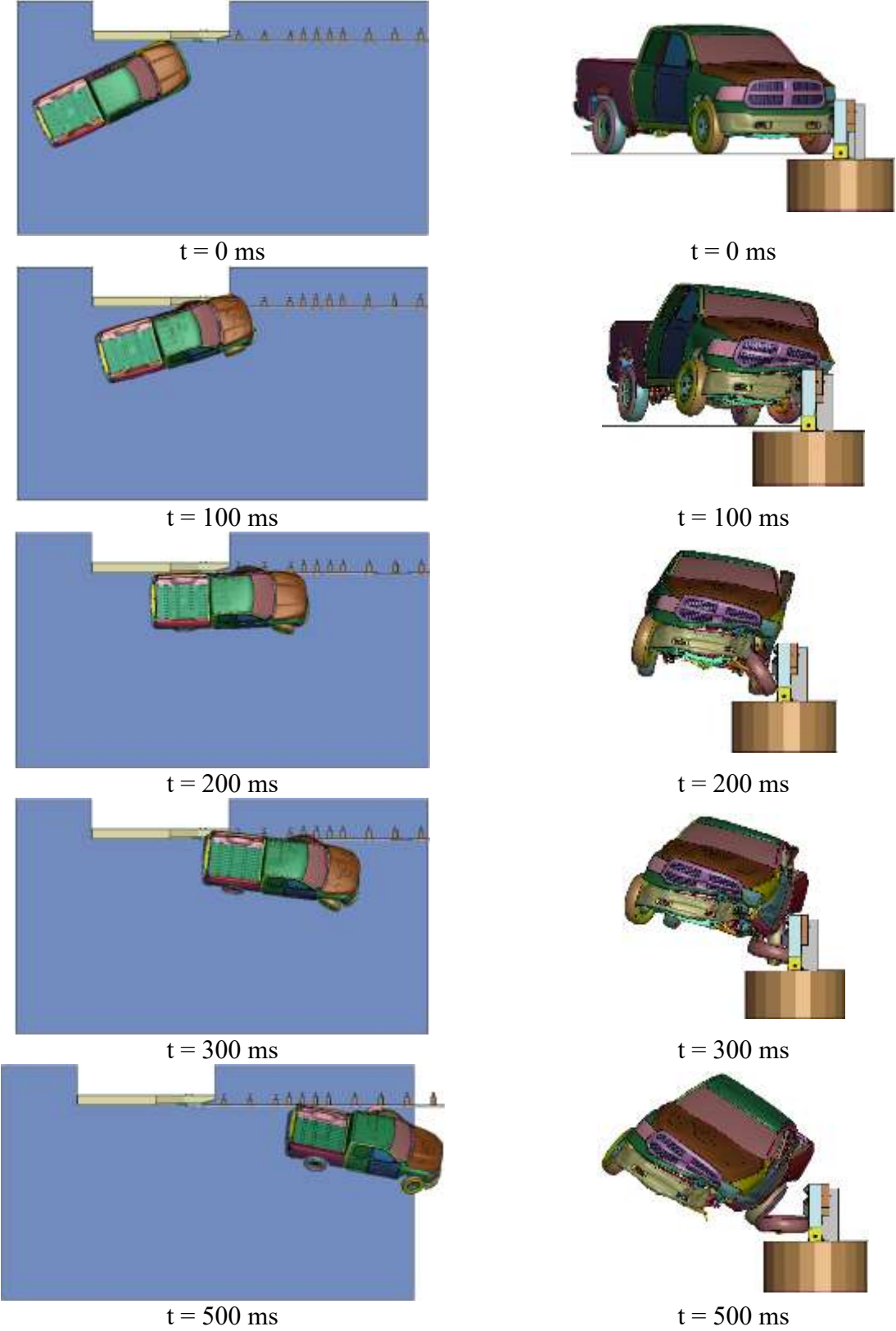


Figure 94. Sequential Images, Simulation No. B2-CP+CF-3N-WD- RBA-REV

Table 26. Vehicle Angular Displacements for Reverse-Direction Impacts, Buttress 2

Simulation No.	Max. Angular Displacement (deg.)		
	Roll	Pitch	Yaw
B2-CP+CF-3N-WA-CFA-REV	-31.5	8.9	-35.8
B2-CP+CF-3N-WD- CFA-REV	-36.5	5.2	-37.4
B2-CP+CF-3N-WA-RBA-REV	-32.0	6.5	-35.2
B2-CP+CF-3N-WD-RBA-REV	-33.5	4.8	-36.7
MASH Limits	±75	±75	N/A

N/A – Not applicable.

Table 27. Summary of OIV and ORA for Reverse-Direction Impacts, Buttress 2

Evaluation Criteria		B2-CP+CF-3N-WA-CFA-REV	B2-CP+CF-3N-WD-CFA-REV	B2-CP+CF-3N-WA-RBA-REV	B2-CP+CF-3N-WD-RBA-REV	MASH Limits
OIV (ft/s)	Longitudinal	27.0	-25.8	-27.9	-26.2	±40
	Lateral	29.2	-28.0	-30.4	-29.6	±40
ORA (g's)	Longitudinal	-15.2	-10.3	-12.3	-13.2	±20.49
	Lateral	9.3	-6.9	9.1	10.5	±20.49

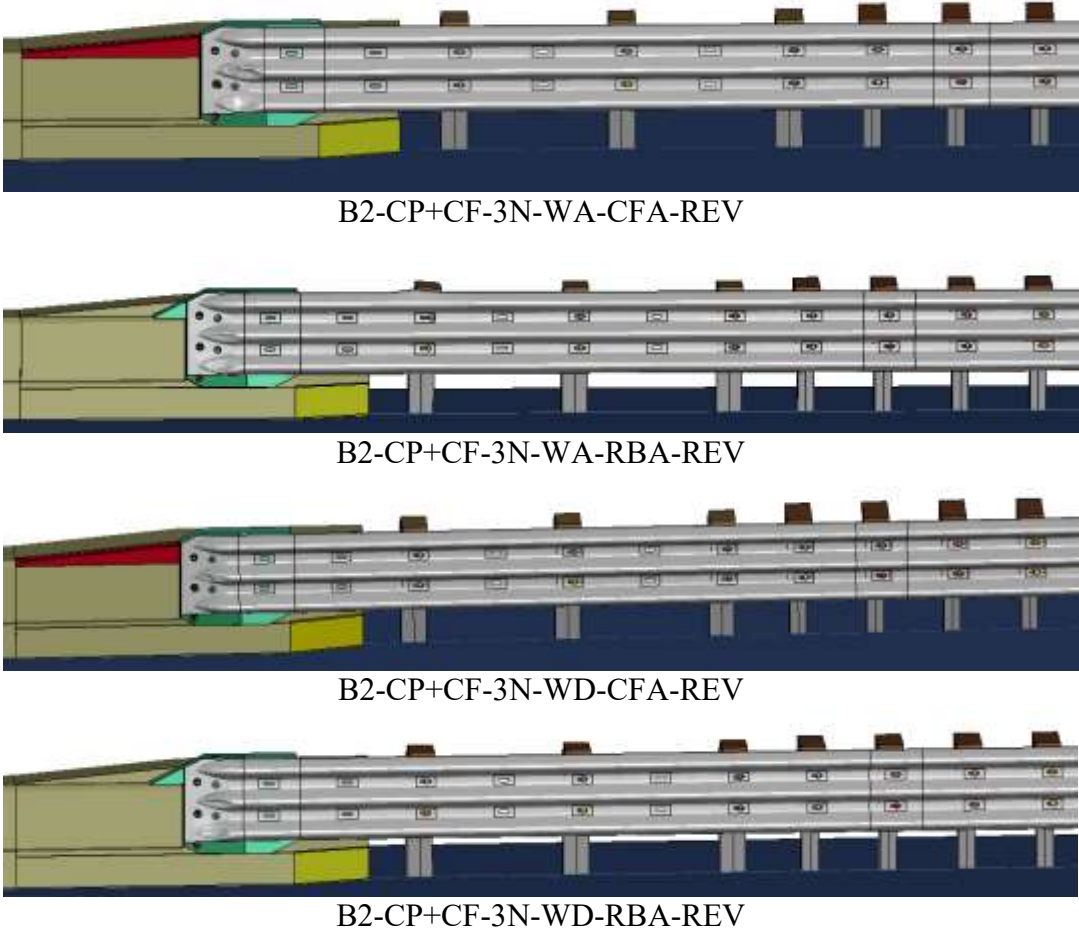


Figure 95. System Damage for Reverse-Direction Impacts, Buttruss 2

7 SUMMARY, CONCLUSIONS, AND RECOMMENDATIONS

The objective of this project was to develop retrofit options for the attachment of 31-in. tall thrie beam AGT systems to existing NDOT bridge rails and buttresses following a 3-in. thick roadway overlay. The existing concrete structures were not to be modified, and new connection hardware was to be developed to connect the AGT to the existing structure and create a MASH TL-3 crashworthy system. Ideally, the same anchorage bolts could be used as the original AGT connection.

The project began with a review of existing concrete bridge rails and end buttresses on NDOT roadways. Ten different bridge railings and buttress were submitted for review by NDOT personnel, and these buttresses were numbered 1 through 10 based on the order in which they were submitted. Buttress 7 was specifically designed for use with a 34-in tall AGT designed to be crashworthy after 3-in. roadway overlays, so that buttress was removed from consideration.

A review of the remaining nine buttresses identified five issues that occurred among many buttresses: (1) the vertical location of the original attachment bolts was too low for a 31-in. tall AGT after the overlay (34-in. tall relative to the original surface); (2) the original attachment bolts were located too close to the end of the buttress, creating an increased unsupported span length and increasing the risk of excessive deflections, pocketing, and snag; (3) cantilevered segments extending from the upstream end of the buttresses that could allow wheel snag on the buttresses below the cantilevered segment; (4) guardrail connection blockouts that created vehicle snag hazards immediately downstream from the guardrail terminal connector; and (5) vehicle snag concerns on the new AGT components during reverse direction impacts.

These issues were noted for each buttress, and the buttresses were then sorted by increasing complexity (i.e., fewer and simpler issues to more and complex issues), as shown previously in Table 2 in Section 3.6. Working within the limited project budget, retrofit designs were developed starting with the simpler buttresses and working toward the more complex buttresses, or left to right in Table 2, with the hope of using the same components in as many retrofit designs as possible. Note, all of the AGT retrofits utilized NDOT's 34-in. tall AGT, shown in Figure 96, which was effectively 31-in. tall after the 3-in. roadway overlay.

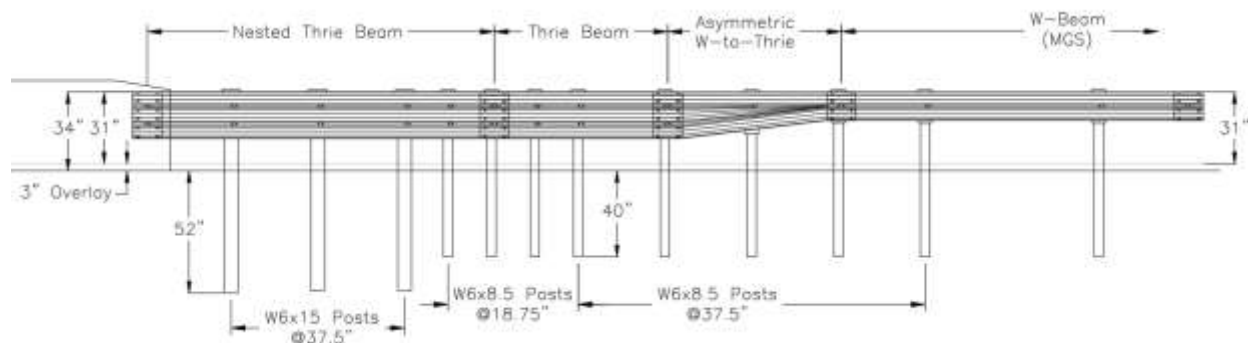


Figure 96. NDOT's 34-in. Tall AGT Shown with 3-in. Overlay

All the AGT connection retrofits were to be evaluated using LS-DYNA computer simulations. Thus, models of all ten submitted buttress configurations and NDOT's 34-in. tall AGT were assembled. The buttresses were modeled as rigid, creating a worst-case scenario for vehicle snag. The AGT model was modeled with appropriate steel and timber material properties and validated against previous MASH crash testing [2].

Through the design process described herein, a connector plate assembly was developed. The connector plate assembly was comprised of a $\frac{3}{16}$ -in. thick steel plate welded to the back of a standard 10-ga. thrie beam terminal connector. Holes were placed in the connector plate assembly that allowed the new component to be attached to the buttresses using their original anchors. Nuts were welded to the inside surface of the plate and underneath the lower and middle corrugation of the thrie beam so that the upstream two anchor bolts could be installed from the back side of the buttress. The downstream end was trimmed so that it would fit on multiple buttresses and the edges were chamfered to mitigate vehicle snag during reverse direction impacts. Design details for the connector plate assembly are shown in Figures 97 through 100.

The connector plate assembly was designed to be compatible with six of the buttresses submitted by NDOT: Buttresses 5, 6, 8, 10, 2, and 4. Simulated MASH TL-3 crash tests were used to evaluate the connector plate assembly as it connected the 34-in. tall AGT to these buttresses, and the simulated impacts showed good safety performance for each buttress. Note, simulations were not conducted with Buttress 4, but Buttress 4 was included due to its similar shape to Buttress 2. The only difference was the thickness of the connection spacer, which would not affect the performance of the retrofit AGT. Thus, Buttress 4 was listed as the sixth buttress to be compatible with the new connector assembly plate.

The shape of the connector plate assembly allows for the connection of a MASH crashworthy AGT to the six buttresses noted above without making any alterations to the buttresses. In most cases, the original attachment bolts could be reused. For attachment to Buttresses 2 and 4, longer bolts will be necessary to extend through the connection spacers placed behind the guardrail. If the original anchors were cast into the buttress, then nuts should not be welded to the connector plate assembly, and the guardrail will be attached using only three nuts on the downstream end of the connection. The existing anchor studs will still extend through the upstream holes in the back plate and provide shear strength for the connection.

For AGT attachments to Buttresses 2 and 4, a connection spacer block is required to bring the connector plate assembly flush with the face of the buttress and mitigate snag. Dimensions for the connection spacer are shown in Figure 101. Note, the thickness of the connection spacer is dependent upon the buttress; $3\frac{1}{2}$ in. thick for Buttress 2 and 2 in. thick for Buttress 4. The connection spacer may be made from wood or steel, or any other material that will not compress or fracture under impact loads.

Buttress 2 was unique as the top edge of the buttress could allow vehicle snag on the guardrail and connection spacer during reverse direction impacts. To mitigate this reverse direction snag, the connection spacer either needs to be tapered down on the downstream or a concrete fill needs to fill the void along the upper edge of the buttress, as shown in Figures 84 and 85. Both of these retrofits were shown to be viable options through reverse direction impact simulations in Section 6.6.4.

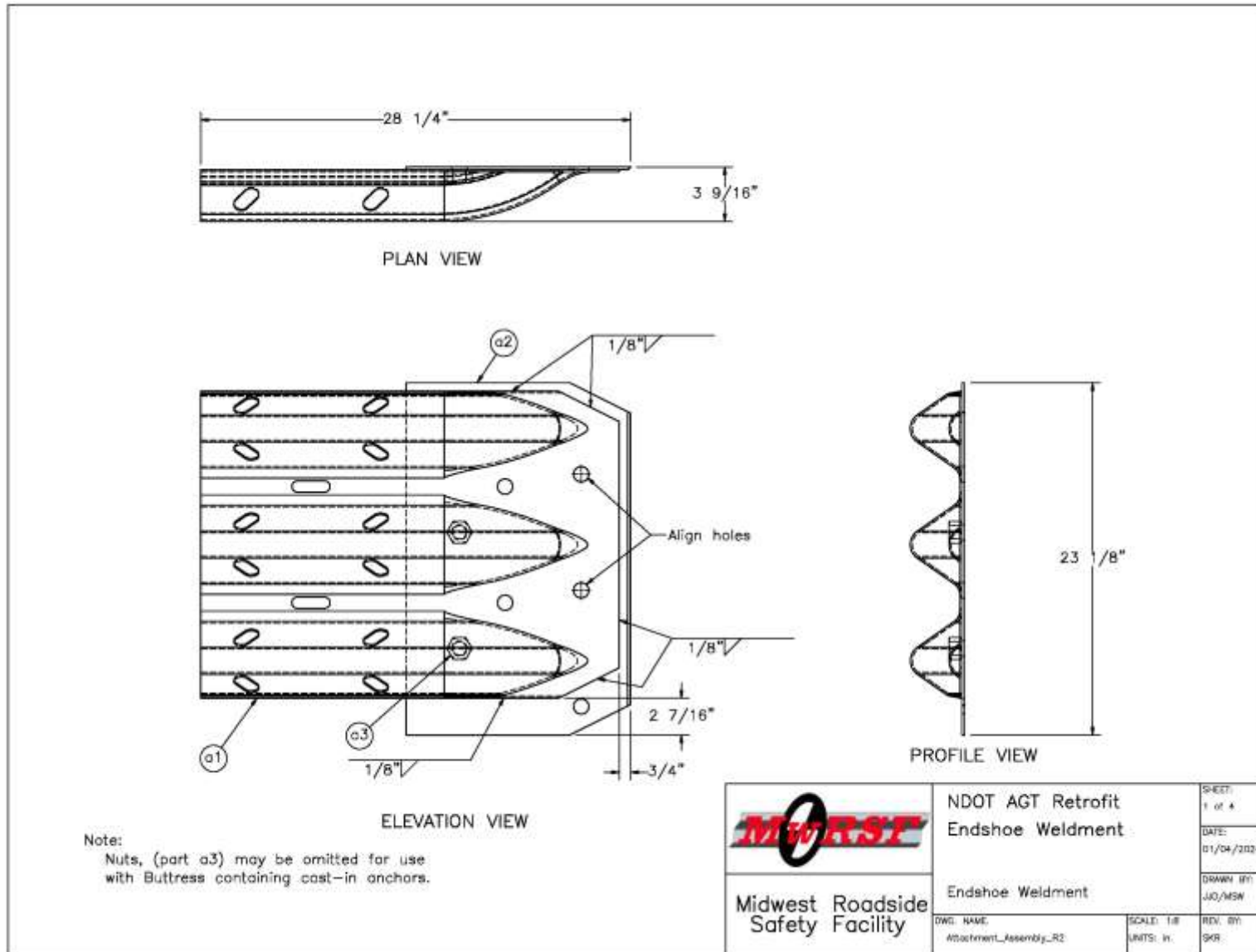


Figure 97. Connector Plate Assembly, Design Details

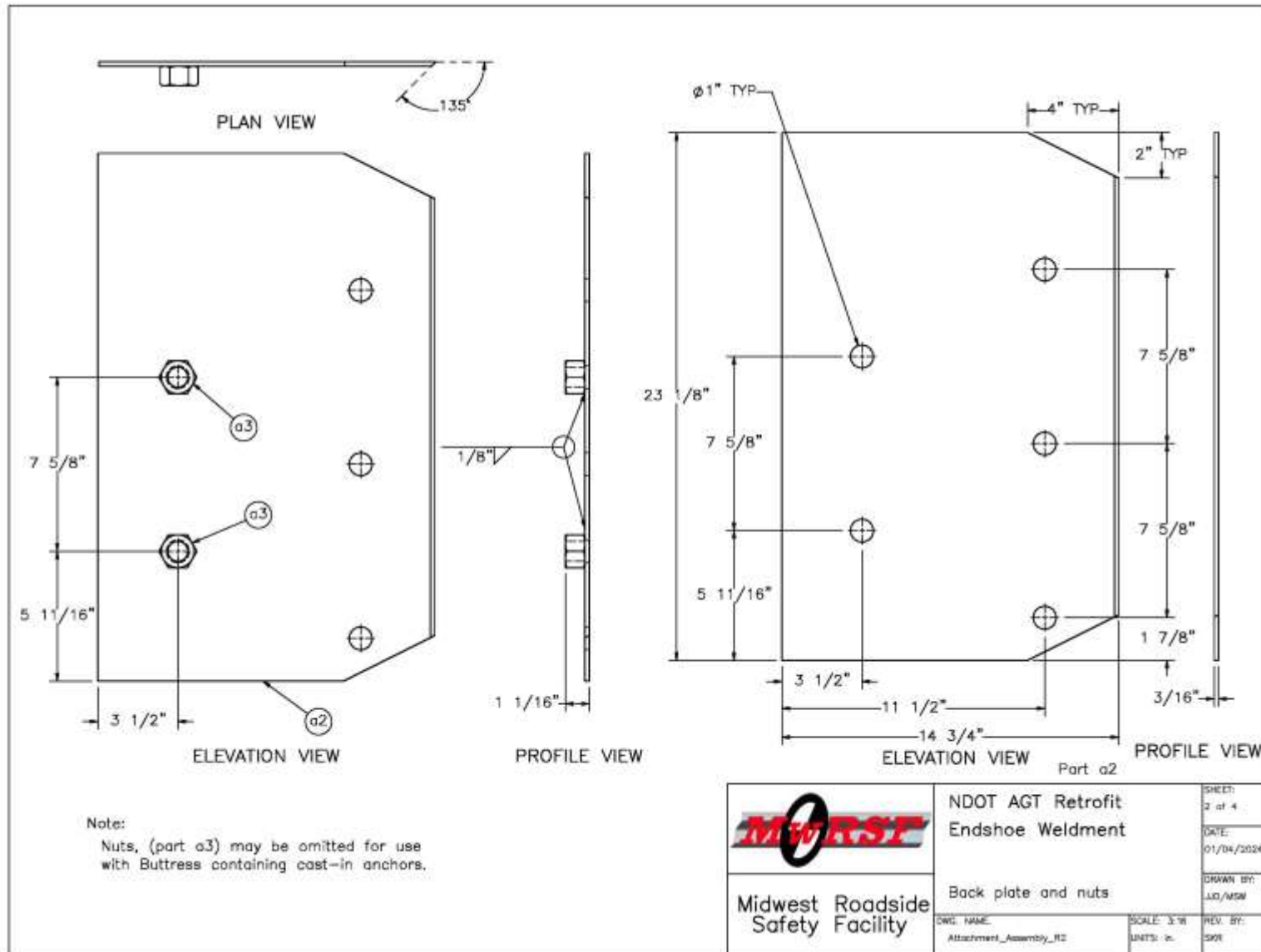


Figure 98. Connector Plate Assembly, Back Plate Design Details

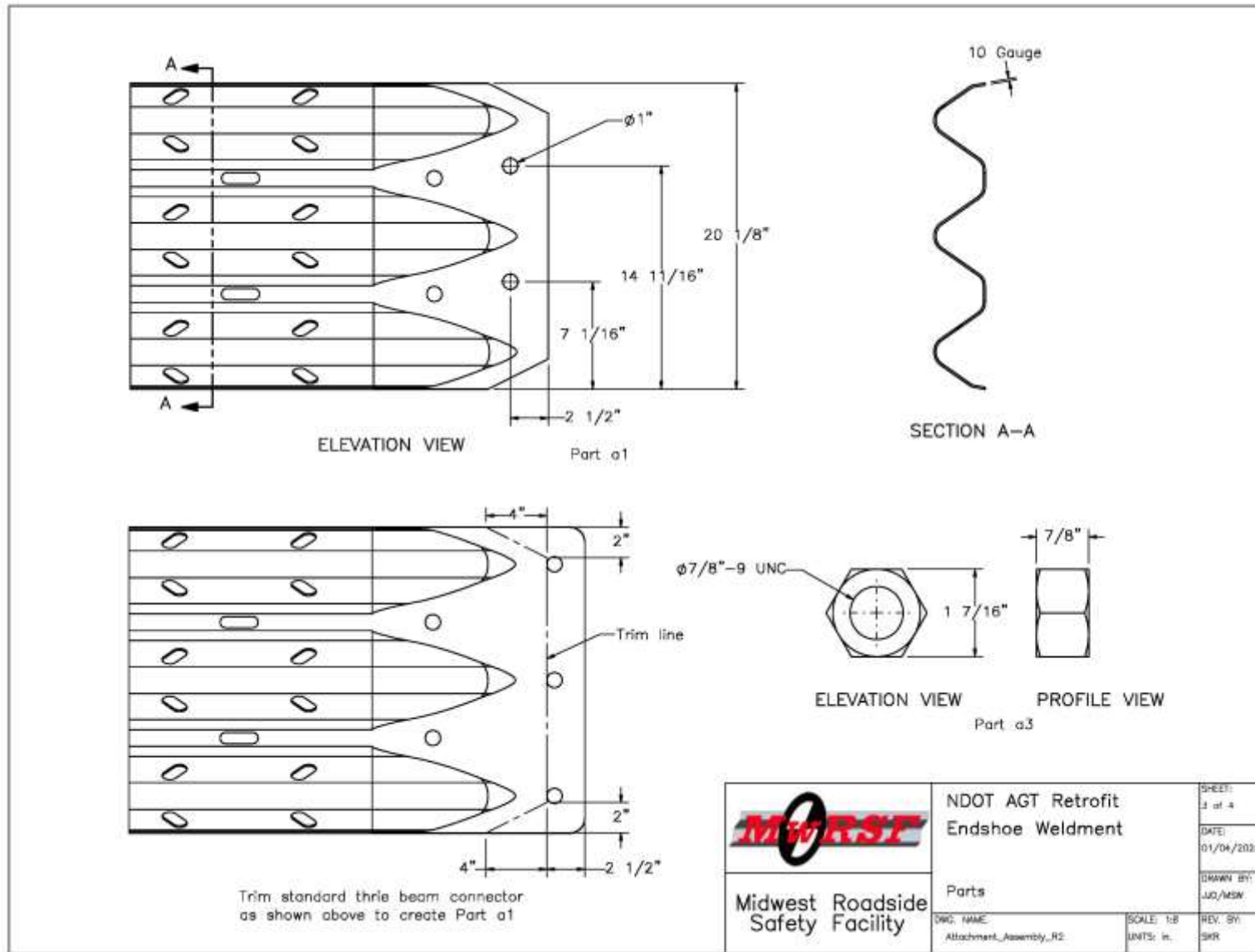



Figure 99. Connector Plate Assembly, Trim Lines for Thrie Beam Terminal Connector

 Midwest Roadside Safety Facility	NDOT AGT Retrofit Endshoe Weldment	SHEET: 3 of 4 DATE: 01/04/2024 DRAWN BY: JJD/MSW
	Parts DWG. NAME: Attachment_Assembly_R2	SCALE: 1:8 UNITS: in.

Item No.	QTY.	Description	Material Specification	Treatment Specification	Hardware Guide
a1	1	10-gauge [3.4] Thrie Beam End Shoe Section	AASHTO M180	ASTM A653	RTE01b
a2	1	Plate Base 14 3/4" x 23 1/8" x 10 gauge	ASTM A36	-	-
a3	2	7/8" [22] Dia. UNC Heavy Hex Nut	ASTM A563 DH		-


	NDOT AGT Retrofit Endshoe Weldment	SHEET: 4 of 4
	Description of View	DATE: 01/04/2024
MIDWEST Roadside Safety Facility	Dwg. NAME: Attachment_Assembly_R2	SCALE: 1/8" UNITS: in
		DRAWN BY: JJO/MSW
		REV. BY: SKR

Figure 100. Connector Plate Assembly, Bill of Materials

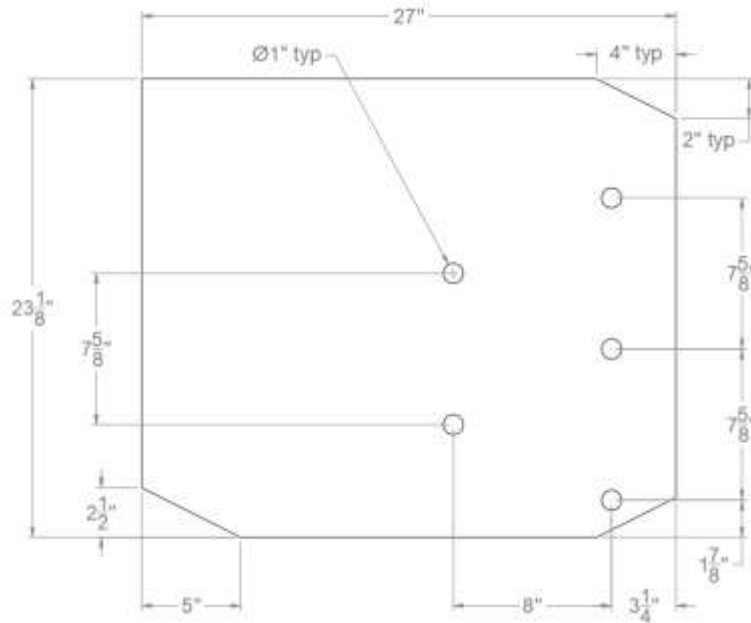


Figure 101. Connection Spacer Dimensions

Buttresses 2, 4, 8, and 10 included a cantilever segment that tapered back laterally to prevent vehicle snag. However, since this segment was not full-height, the upstream face of the buttresses below the rail and cantilevered segment was exposed and created a wheel snag hazard. Three options were explored to retrofit these buttresses and prevent wheel snag: (1) filling the void below the cantilever segment with concrete to create a full-height tapered segment, (2) bolting on a steel assembly below the cantilever segment to create a full-height cross section for the buttress, and (3) installing a 6-in. tall curb under the guardrail and adjacent to the buttress. All three wheel snag retrofit options were evaluated through simulated MASH crash tests, and all three were successful in mitigating the snag risk, as detailed in Section 6.4. Note, the curb should be terminated over a 3 ft distance prior to extending underneath the W-to-thrie transition segment due to vehicle snag concerns below the guardrail.

7.1 Retrofit AGT Recommendations

This section contains a list of the retrofit components necessary to attach a MASH crashworthy AGT to each of the existing buttresses evaluated herein. It is assumed that installers will reuse the existing attachment bolts, so bolts and nuts are not listed. However, new attachment hardware may be necessary if the original hardware is damaged or rusted. Also, installers will need to assess individual buttresses to determine if the original anchors were embedded within the buttress, thus requiring the use of the connector plate assembly option without the welded nuts and a 3-nut attachment.

Note, the structural integrity of the buttresses was not evaluated as part of this study, and the buttresses were modeled as rigid objects within the crash simulations. Thus, these retrofit AGT attachments should only be used on existing bridge rail and buttresses that have remained in good condition and are structurally capable of withstanding MASH TL-3 impact loads.

Finally, the retrofit attachments developed herein were designed specifically for use on existing buttresses conforming to the details provided by NDOT. They should not be applied to other bridge rails and/or buttresses without further evaluation, and they should not be used for new construction sites. New construction locations where a future overlay is anticipated should utilize the 34-in. tall AGT in combination with Buttress 7, as it was designed specifically for that use.

BUTTRESS 2: retrofit AGT components

- 34-in. tall AGT (guardrail, posts, and blockouts)
- Connector plate assembly
- Connection spacer
- Concrete fill along top edge of buttress (or use of modified connection spacer)
- Wheel snag mitigation option (1 of 3)
 - Concrete fill below cantilever segment
 - Steel assembly
 - 6-in. tall curb below thrie beam

BUTTRESS 4: retrofit AGT components

- 34-in. tall AGT (guardrail, posts, and blockouts)
- Connector plate assembly
- Connection spacer
- Wheel snag mitigation option (1 of 3)
 - Concrete fill below cantilever segment
 - Steel assembly
 - 6-in. tall curb below thrie beam

BUTTRESS 5: retrofit AGT components

- 34-in. tall AGT (guardrail, posts, and blockouts)
- Connector plate assembly

BUTTRESS 6: retrofit AGT components

- 34-in. tall AGT (guardrail, posts, and blockouts)
- Connector plate assembly

BUTTRESS 8: retrofit AGT components

- 34-in. tall AGT (guardrail, posts, and blockouts)
- Connector plate assembly
- Wheel snag mitigation option (1 of 3)
 - Concrete fill below cantilever segment
 - Steel assembly
 - 6-in. tall curb below thrie beam

BUTTRESS 10: retrofit AGT components

- 34-in. tall AGT (guardrail, posts, and blockouts)
- Connector plate assembly
- Wheel snag mitigation option (1 of 3)
 - Concrete fill below cantilever segment
 - Steel assembly
 - 6-in. tall curb below thrie beam

7.2 Future Research

This project developed AGT retrofit recommendations for six different existing bridge railings and buttresses. Due to budget limitations, three other existing bridge railings and buttresses submitted by NDOT were not addressed herein. If AGT attachment solutions for these structures (Buttresses, 1, 3, and 9) is desired, further research and development under a new project would be required.

The development and evaluation of the retrofit attachment components designed herein was completed using numerical analysis and LS-DYNA computer simulations to represent MASH TL-3 impact conditions. The results of these modeling and simulation efforts showed great promise and may be considered as the best available practices for addressing AGTs to existing buttresses following overlays. However, to fully evaluate the AGT retrofit recommendations to MASH TL-3 performance criteria, physical crash testing would be necessary.

8 REFERENCES

1. Rosenbaugh, S.K., Faller, R.K., Asselin, N., and Hartwell, A.J., *Development of a Standardized Buttress for Approach Guardrail Transitions*, Report No. TRP-03-369-20, Midwest Roadside Safety Facility, University of Nebraska-Lincoln, Lincoln, Nebraska, September 9, 2020.
2. Rosenbaugh, S.K., Fallet, W.G., Faller, R.K., Bielenberg, R.W., and Schmidt, J.D., *34-in. Tall Thrie Beam Transition to Concrete Buttress*, Report No. TRP-03-367-19, Midwest Roadside Safety Facility, University of Nebraska-Lincoln, Lincoln, Nebraska, July 2, 2019.
3. *Manual for Assessing Safety Hardware (MASH)*, Second Edition, American Association of State Highway and Transportation Officials (AASHTO), Washington, D.C., 2016.
4. Eller, C.M., Polivka, K.A., Faller, R.K., Sicking, D.L., Rohde, J.R., Reid, J.D., Bielenberg, R.W., and Allison, E.M., *Development of the Midwest Guardrail System (MGS) W-Beam to Thrie Beam Transition Element*, Report No. TRP-03-167-07, Midwest Roadside Safety Facility, University of Nebraska-Lincoln, Lincoln, Nebraska, November 26, 2007.
5. Ross, H.E., Sicking, D.L., Zimmer, R.A., and Michie, J.D., *Recommended Procedures for the Safety Performance Evaluation of Highway Features*, National Cooperative Research Program (NCHRP) Report No. 350, Transportation Research Board, Washington, D.C., 1993.
6. Michie, J.D., *Recommended Procedures for the Safety Performance Evaluation of Highway Appurtenances*, National Cooperative Highway Research Program (NCHRP) Report 230, Transportation Research Board, Washington, D.C., March 1981.
7. Rosenbaugh, S.K., Hovde, S.E., Faller, R.K., and Urbank, E.L., *Crash Testing and Evaluation of the Hawaii Thrie Beam Approach Guardrail Transition: MASH Test Nos. 3-20 and 3-21*, Report No. TRP-03-425-20, Midwest Roadside Safety Facility, University of Nebraska-Lincoln, Lincoln, Nebraska, March 2020.
8. Yosef, T.Y., Steelman, J.S., Faller, R.K., and Urbank, E.L., *Crash Testing and Evaluation of HDOT's Thrie-Beam Approach Guardrail Transition Attached to 42-in. Tall, Solid Concrete Bridge Rail with Aesthetic, Recessed, Rounded Panels and 6-ft Wide Sidewalk: MASH Test Nos. 3-20 and 3-21*, Report No. TRP-03-472-22, Midwest Roadside Safety Facility, University of Nebraska-Lincoln, Lincoln, Nebraska, December 2022.
9. Rasmussen, J.D., Rosenbaugh, S.K., Faller, R.K., Alvarado, R., Mauricio, P., Bielenberg, R.W., Steelman, J.S., *Development of a MASH TL-3 Approach Guardrail Transition to a MASH TL-4 Steel Bridge Rail*, Report No. TRP-03-411-20, Midwest Roadside Safety Facility, University of Nebraska-Lincoln, Lincoln, Nebraska, December 2020.
10. *LS-DYNA Keyword User's Manual, Volume 1 R13.0* Livermore Software Technology Company (LSTC), Livermore, California, 2017.

11. *2018 Dodge Ram 1500 FE Detailed Mesh Model v3 Validation*, Center for Collision Safety and Analysis, George Mason University, Washington, D.C., model released May 2022. <https://www.ccsa.gmu.edu/wp-content/uploads/2022/05/2018-dodge-ram-detailed-validation-v3.pdf>
12. *2010 Toyota Yaris Coarse Finite Element Model*, Version 1I, Center for Collision Safety and Analysis, George Mason University, Washington, D.C., model released December 2016. <https://www.ccsa.gmu.edu/models/2010-toyota-yaris/>

9 APPENDICES

Appendix A. NDOT Standard Drawings for Bridge Railings and Buttresses

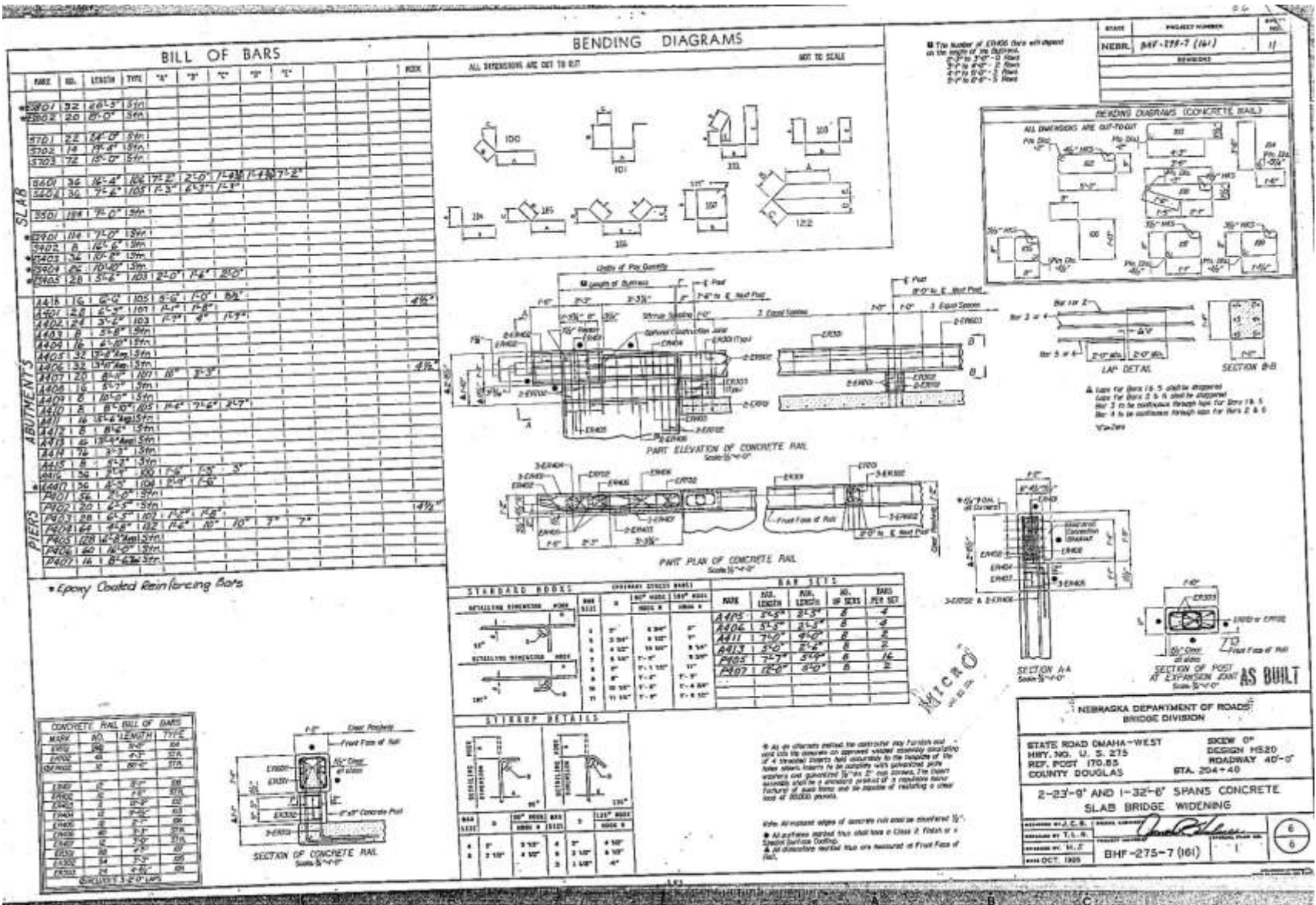


Figure A-2. NDOT Design Details, Buttruss 2

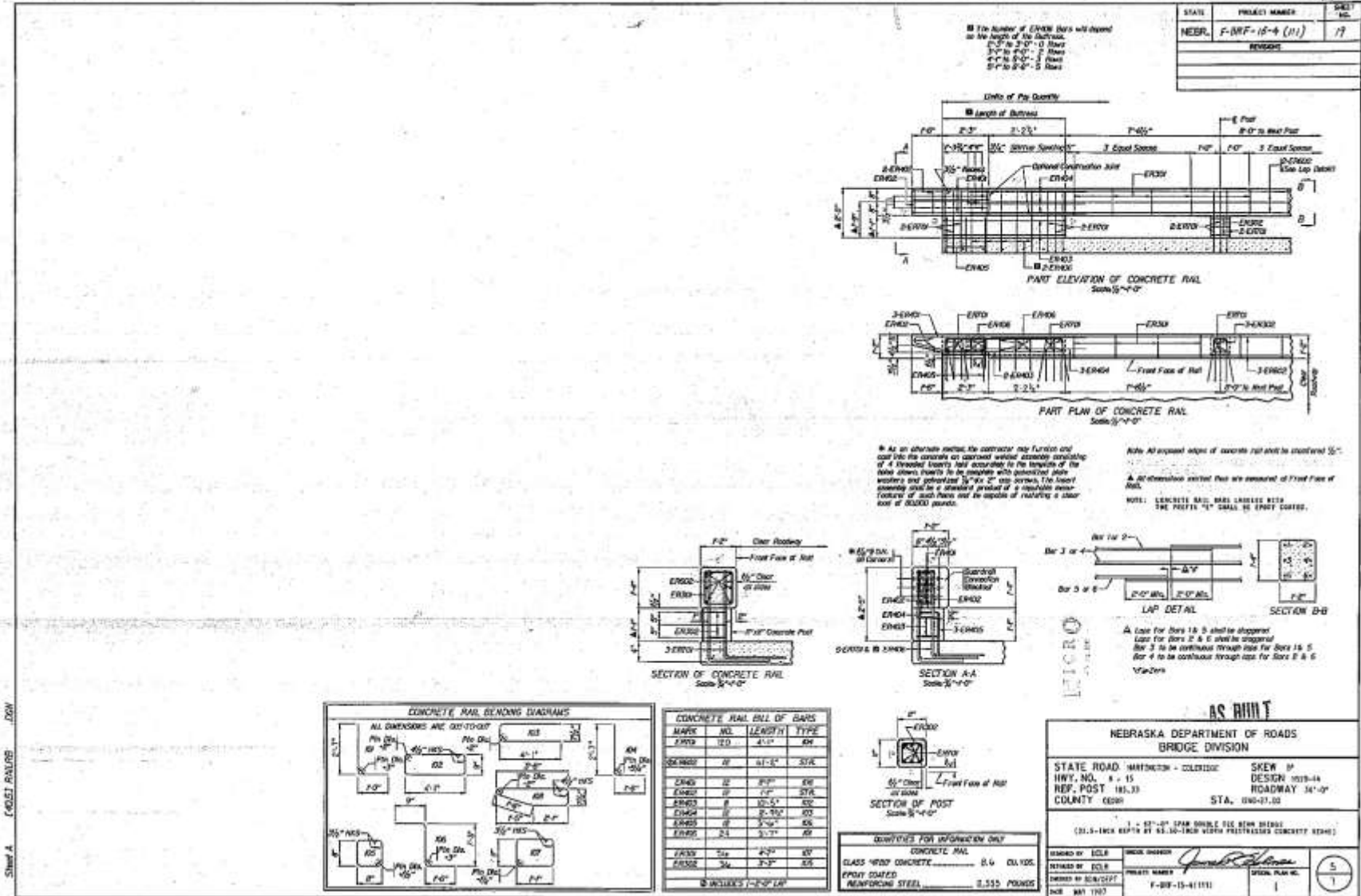


Figure A-3. NDOT Design Details, Buttrass 3

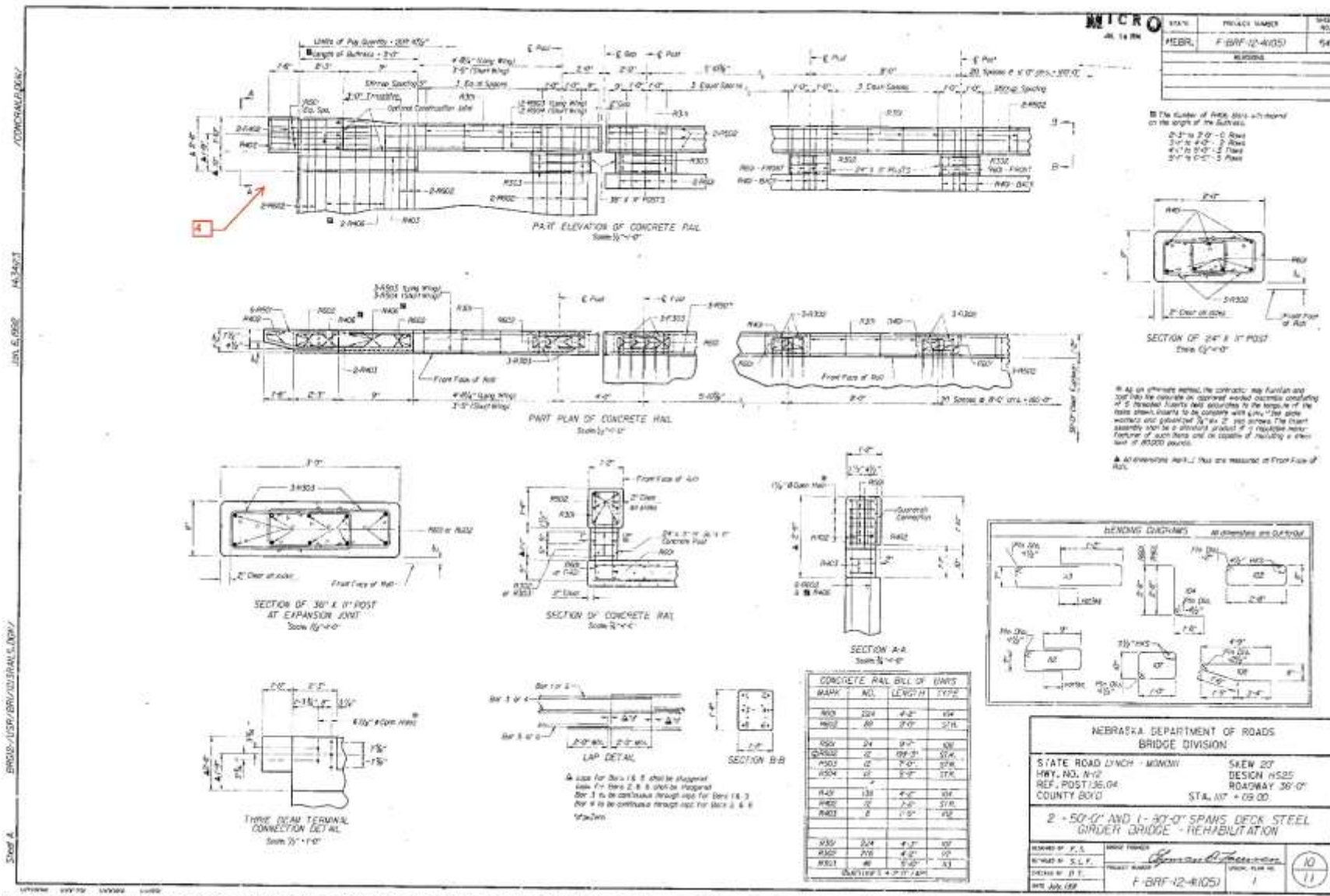


Figure A-4. NDOT Design Details, Buttress 4

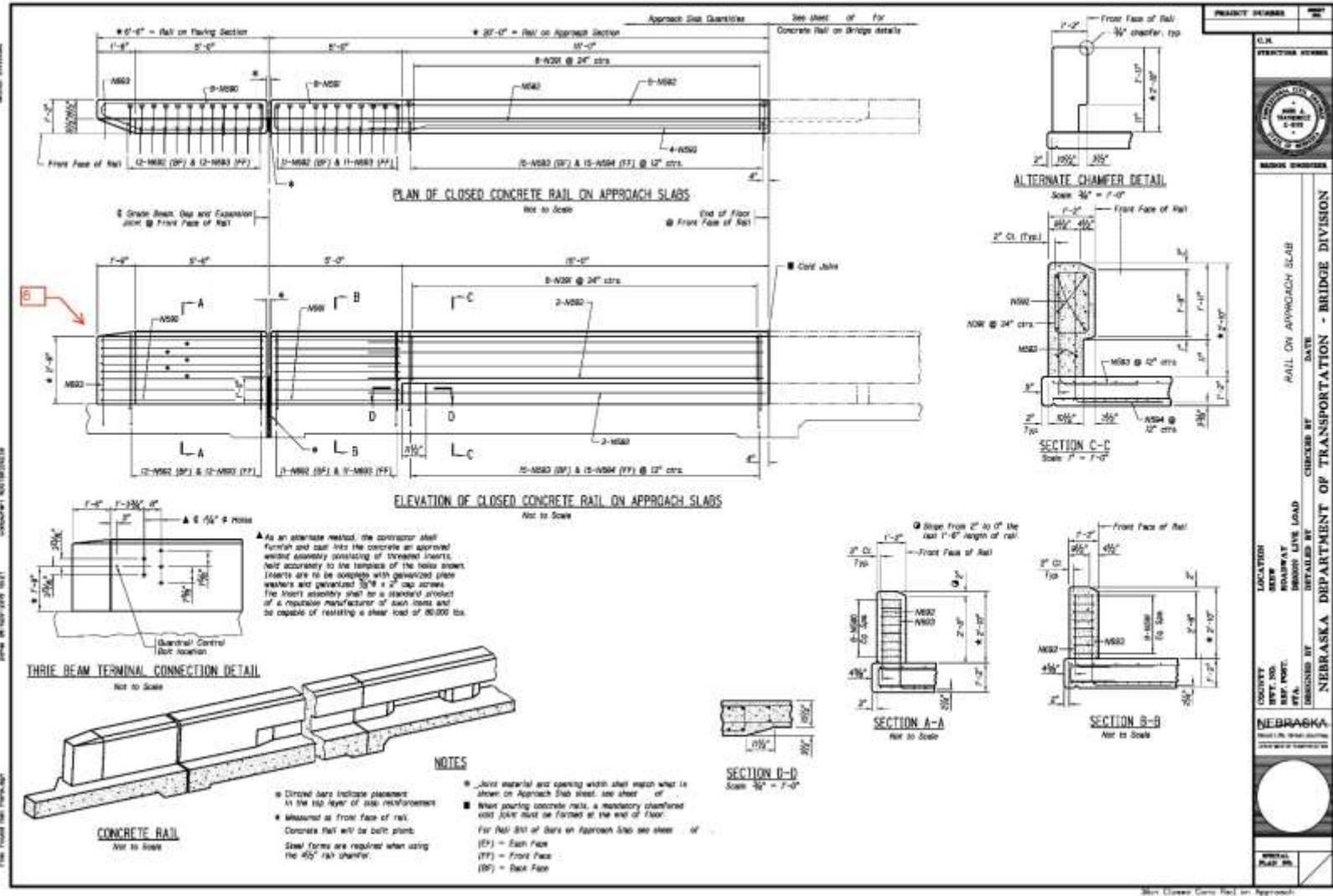


Figure A-6. NDOT Design Details, Buttruss 6

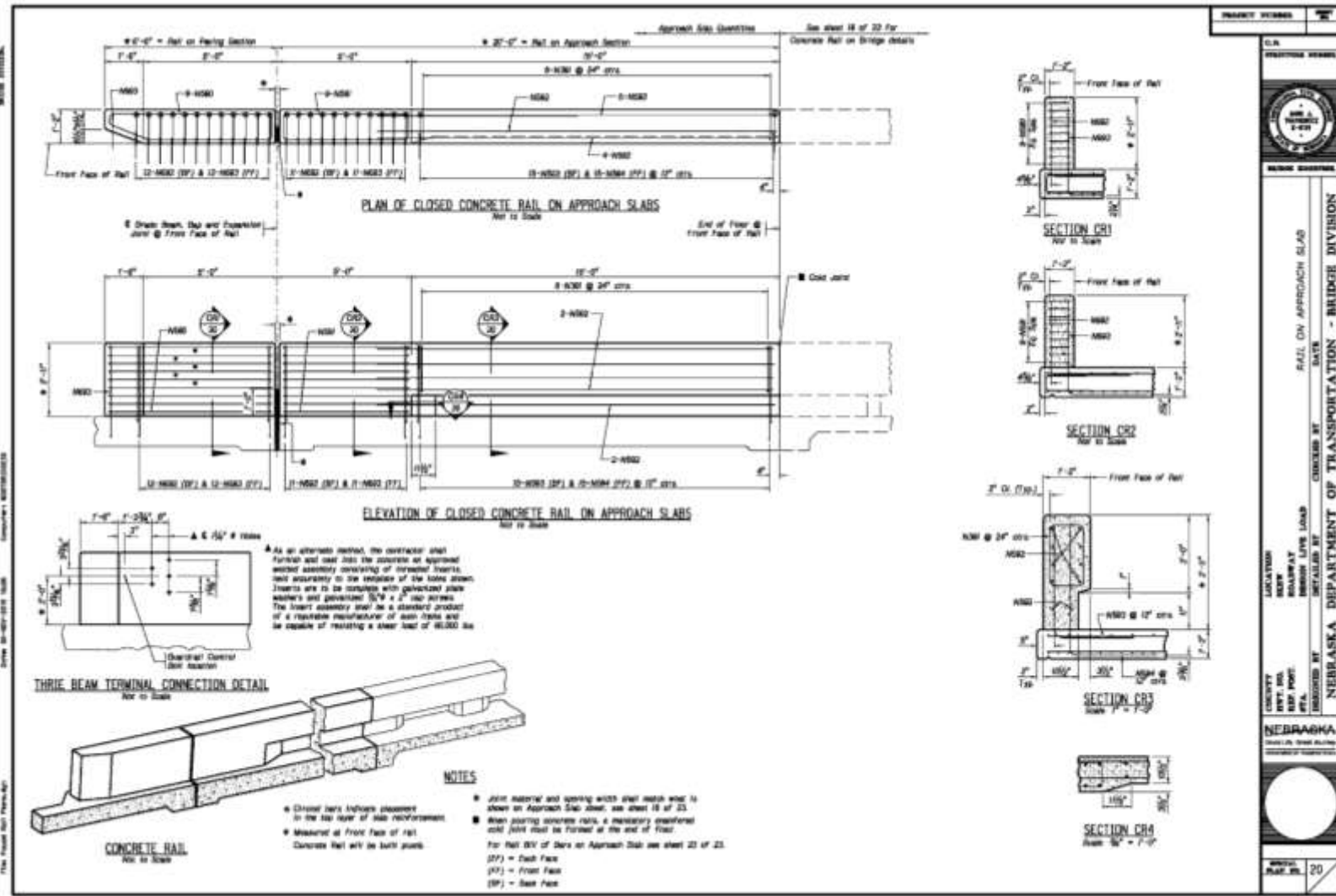


Figure A-7. NDOT Design Details, Buttress 7

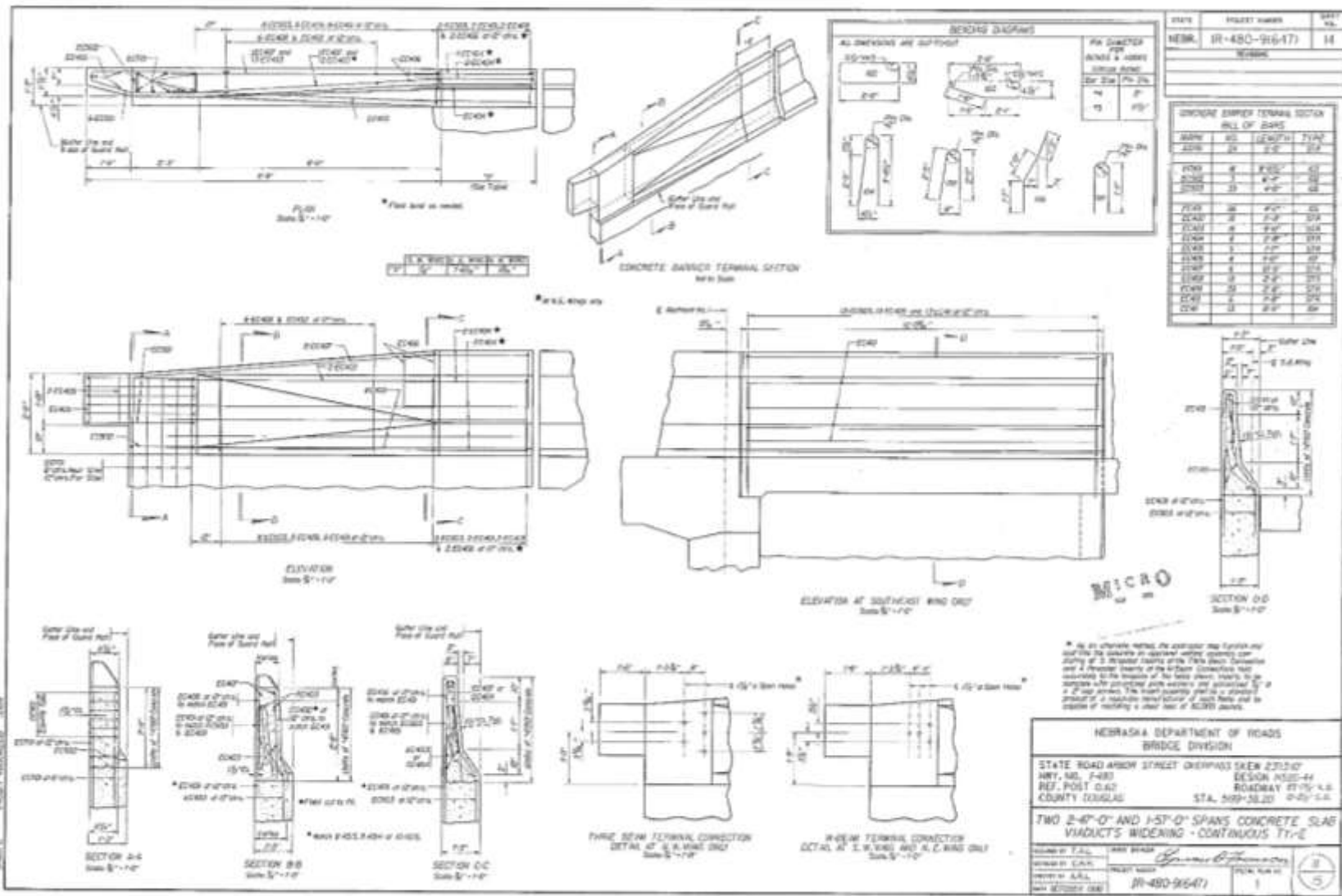


Figure A-8. NDOT Design Details, Buttress 8

END OF DOCUMENT